

2017

# Transcriptional Governance of Hair Follicle Stem Cell Quiescence and Niche Maintenance in Long-Term Tissue Regeneration

Kenneth Lay

Follow this and additional works at: [http://digitalcommons.rockefeller.edu/student\\_theses\\_and\\_dissertations](http://digitalcommons.rockefeller.edu/student_theses_and_dissertations)

 Part of the [Life Sciences Commons](#)

---

## Recommended Citation

Lay, Kenneth, "Transcriptional Governance of Hair Follicle Stem Cell Quiescence and Niche Maintenance in Long-Term Tissue Regeneration" (2017). *Student Theses and Dissertations*. 402.  
[http://digitalcommons.rockefeller.edu/student\\_theses\\_and\\_dissertations/402](http://digitalcommons.rockefeller.edu/student_theses_and_dissertations/402)

This Thesis is brought to you for free and open access by Digital Commons @ RU. It has been accepted for inclusion in Student Theses and Dissertations by an authorized administrator of Digital Commons @ RU. For more information, please contact [mcsweej@mail.rockefeller.edu](mailto:mcsweej@mail.rockefeller.edu).



TRANSCRIPTIONAL GOVERNANCE OF HAIR FOLLICLE  
STEM CELL QUIESCENCE AND NICHE MAINTENANCE  
IN LONG-TERM TISSUE REGENERATION

A Thesis Presented to the Faculty of  
The Rockefeller University  
in Partial Fulfillment of the Requirements for  
the degree of Doctor of Philosophy

by

Kenneth Lay

June 2017



# **TRANSCRIPTIONAL GOVERNANCE OF HAIR FOLLICLE STEM CELL QUIESCENCE AND NICHE MAINTENANCE IN LONG-TERM TISSUE REGENERATION**

Kenneth Lay, Ph.D.

The Rockefeller University 2017

Adult stem cells are endowed with the remarkable ability to maintain, regenerate and repair tissues throughout the lifetime of the organism. Whether parsimonious utilization of adult stem cells is necessary to preserve their long-term potential has not been fully explored. I investigated this issue using the adult murine hair follicle stem cell (HFSC) as my paradigm. HFSCs reside in their niche called the bulge, and mostly remain in a quiescent state, becoming mobilized only transiently to fuel cyclical bouts of hair follicle regeneration. By ablating a key HFSC transcription factor, Forkhead Box C1 (FOXC1), I discovered that hair follicles underwent more rounds of regeneration and yet were unable to result in a thickening of the animal's hair coat. Mechanistically, unlike WT HFSCs, FOXC1-deficient HFSCs failed to remain in prolonged durations of quiescence. Instead, they were primed to re-enter the cell cycle and launch new rounds of hair regeneration prematurely. After activation, they failed to re-establish quiescence promptly, and remained in a primed state to proliferate. In turn, their expression of cell adhesion proteins remained low. As new hairs grew, wild-type (WT) HFSCs that had returned to quiescence and restored their repertoire of adhesion-associated proteins were able to anchor their bulge niche and the older hairs in place. However, FOXC1-

deficient HFSCs were unable to do so, resulting in the gradual loss of their bulge and old hair coats. As the bulge is also a cellular source of HFSC-inhibitory factors, its loss exacerbated the inability of FOXC1-deficient HFSCs to maintain quiescence. Consequently, as these mutant mice aged, their hair coat appeared sparse. Indeed, their HFSC numbers and ability to regenerate new hairs upon stimulation had declined. Therefore, through FOXC1, HFSCs couple their quiescence to an adhesion-mediated niche maintenance to achieve long-term tissue homeostasis.

## **DEDICATION**

*I am dedicating this thesis to my grandfather. He was a wise and intelligent man. His favorite quotes were “to err is human, to forgive is divine” and “no man is an island”. The latter is a little easier to appreciate. Collaboration is key and integral to the advancement of science, and a conducive support network within and outside a laboratory is necessary to the success of every scientist. However, the former is harder to achieve, and I’m still learning, and slowly getting there. Throughout my childhood, he shared his life experiences with me, gave me history classes, and taught me how to be a good human being. He gave a lot to nurturing my brother and me. My father and uncle did not manage to attend college, so he had placed a lot of hope on my brother and me to do so, as he recognized the importance of a good degree to secure a better future. I went beyond his dream, and pursued a doctorate.*

*My grandfather passed away a few months after I completed my degree and returned home from London. He did not manage to attend my graduation ceremony in London, nor witness my brother graduate from college a few years later. Fortunately, he saw the photo of me in my graduation gown in the hospital bed, and while gasping for air, he still managed to heave a huge sigh of relief, contentment and pride.*

*Grandpa, I dedicate this thesis to you. I have not saved the day, nor found a wonder drug for a disease, but I have grown and matured as a scientist. The training I have gotten thus far will bring me far as I continue to pursue science. Please continue to have faith and confidence in me as I do my best to make a difference to the lives of others with my scientific pursuits.*

## ACKNOWLEDGMENTS

First and foremost, I would like to thank my mentor, Elaine Fuchs, for making this thesis possible. I joined Rockefeller's graduate program not knowing what to pursue for my PhD. After hearing Elaine's talk to the first year students, I became fascinated by how the hair follicle can be such a great model to study stem cell biology. Honestly, it was something I had not appreciated when reading the student prospectus before coming to Rockefeller. I approached her and asked if she would be willing to have me rotate in her laboratory. It was only a year or two later did I realize that students had to contact her months in advance in order to secure a rotation spot in her laboratory. I was indeed very fortunate! Elaine formally accepting me into her laboratory marked a memorable milestone in my research career. It was one of the happiest days of my life, as my hard work during my rotation paid off. For me, and everyone in her lab, she provided one of the best environments to do science. I dare say I have come a long way and matured greatly as a scientist. This would not have been possible without her mentorship. Thank you Elaine, for everything.

Of course, being the reputable scientist she is, Elaine is frequently out of town. During her absence, Ya-Chieh Hsu, a postdoc in the laboratory, was my go-to person. Ya-Chieh mentored me during my rotation, and continued to be pivotal throughout my stay in the laboratory in making me the scientist I am today. Her approaches towards science, her thoughtfulness, and even her attitude towards

life in general, influenced and shaped me greatly. I had learnt so much from her, and I cannot thank her enough for everything she has done for me.

All Fuchs lab members, past and present, had contributed to making my PhD experience a most fulfilling and enriching one. They supported me during my toughest times, and helped me get through them in any way they could. Scott Williams was also my rotation mentor, and together with Ya-Chieh, he taught me everything I needed to know to get my project started. I also enjoyed extensive in-depth discussions with Naoki Oshimori about science and everything in life. Wen-Hui Lien, Brice Keyes, Amma Asare, Evan Heller, and Irina Matos have also been integral throughout my stay in the lab, and I am very grateful for their friendships.

I would also like to thank my Singapore funding agency, A\*STAR, for giving me the invaluable funding opportunity to pursue my college and graduate studies in Imperial College and Rockefeller.

Last but not least, I would like to thank my family. My parents and grandmother are back home in Singapore, far away, yet I always feel their support and encouragement during our weekly or fortnightly Skype phone calls. Most importantly, I am very thankful to my fiancé, and my very best friend, Jinyue Liu. We had gone through the best and worst times as we pursued our PhD together. We bounced ideas off and discussed our works with each other everyday. We faltered often, but always plucked enough courage to continue our pursuits together. I look forward to more fruitful scientific discussions with her, indeed, for the rest of our academic careers.

# TABLE OF CONTENTS

<b>CHAPTER 1: INTRODUCTION .....</b>	<b>1</b>
1.1 Adult stem cells and their niche .....	1
1.2 The adult hair follicle and the hair cycle .....	1
1.3 The hair follicle stem cell and its niche .....	5
1.4 Hair follicle stem cell quiescence and activation .....	6
1.5 Purifying and profiling hair follicle stem cell gene expression signatures	8
1.6 Stem cells and aging .....	10
<b>CHAPTER 2: THE ROLE OF FOXC1 IN MAINTAINING HAIR FOLLICLE STEM CELL QUIESCENCE.....</b>	<b>13</b>
2.1 Introduction .....	13
2.2 Results .....	16
2.2.1 FOXC1 expression in adult mouse skin .....	16
2.2.1.1 Generating a FOXC1 antibody .....	16
2.2.1.2 Expression of FOXC1 and other HFSC genes in telogen .....	17
2.2.1.3 FOXC1 expression in anagen .....	20
2.2.1.4 FOXC1 expression in catagen.....	20
2.2.2 Depletion of FOXC1 results in faster hair cycling and impacts long term hair coat maintenance .....	23
2.2.3 FOXC1 is necessary to establish a multiple-bulge hair follicle architecture, and maintain HFSC numbers and function with age ...	27
2.2.4 FOXC1-deficient hair follicles can make a new bulge but fail to maintain the older one .....	31
2.2.5 Preservation of the old bulge contributes to HFSC quiescence .....	34
2.2.6 Loss of FOXC1 in the presence of the old bulge also shortens telogen.....	35
2.2.7 FOXC1 re-establishes and maintains quiescence of HFSCs after their activation .....	39
2.2.8 FOXC1 ensures anchorage of old bulge to prevent its loss during anagen .....	46

2.2.9	Proliferative Bu-HFSCs display reduced E-cadherin.....	52
2.2.10	Direct perturbation to cell-cell adhesion is sufficient for bulge loss.....	57
2.3	Discussion.....	59
2.3.1	Summary of results .....	59
2.3.2	Two is better than one: the role of the older bulge .....	60
2.3.3	A distinct hair loss mechanism .....	62
2.3.4	An aged phenotype not normally observed in WT .....	63
2.3.5	Intercellular adhesion, E-cadherin and stem cell biology .....	65
2.4	Materials and Methods.....	68
<b>CHAPTER 3: STEM CELL ADHESION AND ACTIVITY .....</b>		<b>76</b>
3.1	Introduction .....	76
3.1.1	Comparing <i>Foxc1</i> -cKO and <i>Cdh1</i> -cKO hair follicles .....	76
3.1.2	Cell-ECM and cell-cell adhesion .....	77
3.1.3	Adherens junctions and loss-of-function studies .....	78
3.2	Results .....	81
3.2.1	ECAD-cKO HFs exhibit an aberrant stem cell niche architecture ....	81
3.2.2	Bu-HFSCs proliferate precociously without contributing to new HF regeneration in the absence of ECAD .....	86
3.2.3	RNA-seq revealed enrichment of genes associated with inflammatory response following ECAD loss .....	88
3.3	Discussion and future directions .....	95
3.3.1	ECAD loss causes downstream ectopic proliferation of Bu-HFSCs, resulting in stem cell niche architectural disruption .....	95
3.3.2	An immune response was mounted in the absence of ECAD.....	98
3.3.3	Investigating the direct cause of Bu-HFSC proliferation upon ECAD loss .....	99
3.3.4	Implications for EMT and cancer biology .....	101
3.4	Materials and Methods.....	102
<b>CHAPTER 4: CONCLUSION.....</b>		<b>103</b>
<b>BIBLIOGRAPHY .....</b>		<b>106</b>

# LIST OF FIGURES

Figure 1. Schematic of the adult mouse hair follicle..... 2

Figure 2. The adult hair follicle cycles through telogen, anagen and catagen. .... 4

Figure 3. Expression of FOXC1 and other key HFSC transcription factors in telogen. .... 19

Figure 4. Expression of FOXC1 in anagen and catagen..... 22

Figure 5. Depletion of FOXC1 from HFs causes faster hair cycling, yielding a sparser hair coat with age. .... 25

Figure 6. ~~When reduced FOXC1, HFs fail to maintain multiple bulges and club hairs~~ <sup>display reduced FOXC1, HFs</sup>..... 29

Figure 7. FOXC1-deficient HFs can make a new bulge but fail to maintain the old one. .... 32

Figure 8. The old bulge contributes to HFSC quiescence..... 37

Figure 9. RNA-seq summary of up-regulated genes in *Foxc1*-cKO Bu-HFSCs. . 42

Figure 10. Governance of HFSC quiescence is necessary to maintain the old bulge. .... 44

Figure 11. RNA-seq summary of down-regulated genes in *Foxc1*-cKO Bu-HFSCs..... 48

Figure 12. FOXC1 functions to anchor the old bulge during hair growth. .... 50

Figure 13. Exploring cell-ECM and cell-cell adhesion properties of *Foxc1*-cKO Bu-HFSCs. .... 55

Figure 14. Reducing intercellular junctions between HFSCs contributes to the loss of the old bulge during new hair growth..... 58

Figure 15. Analyzing bulge architecture and expression of junctional complex proteins upon ECAD loss. .... 84

Figure 16. ECAD-cKO Bu-HFSCs proliferate precociously without regenerating new hairs. .... 87

Figure 17. ECAD-cKO Bu-HFSCs differ from WT in cell and colony morphology in vitro..... 91

Figure 18. Skin sagittal sections reveal recruitment of CD45+ immune cells  
around ECAD-cKO bulge. ....95

Figure 19. Proposed model for the role of FOXC1 and adhesion in HFSCs. .... 104

## LIST OF TABLES

Table 1. KEGG pathway analysis of genes down-regulated in ECAD-cKO Bu-HFSCs vs. Het.....	92
Table 2. KEGG pathway analysis of genes up-regulated in ECAD-cKO Bu-HFSCs vs. Het.....	93

## LIST OF ABBREVIATIONS

Ana	Anagen
BMP	Bone morphogenetic protein
Bu	Bulge
Cat	Catagen
DP	Dermal papilla
Epi	Epidermis
FACS	Fluorescence activated cell sorting
FGF	Fibroblast growth factor
FOXC1	Forkhead Box C1
HF	Hair follicle
HFSCs	Hair follicle stem cells
HG	Hair germ
Inf	Infundibulum
IRS	Inner root sheath
Isth	Isthmus
Mx	Matrix
NFATc1	Nuclear factor of activated T-cells c1
ORS	Outer root sheath
SG	Sebaceous gland
TACs	Transit amplifying cells
Tel	Telogen

# **CHAPTER 1: INTRODUCTION**

## **1.1 Adult stem cells and their niche**

Most, if not all, tissues of an adult organism contain a resident population of stem cells, defined by their ability to self-renew, potential to adopt one or more differentiated cell fates, and capacity to last long-term. These adult stem cells are tasked with the responsibility of maintaining the tissues they reside in, differentiating into one or more specialized cell type(s) to replace those turned over during homeostasis or lost through injury, while keeping their numbers constant through self-renewal so as to perform its functions throughout the lifetime of the organism.

Adult stem cells reside in specific locations within their tissues. Termed the “niche”, it refers to the local tissue microenvironment which maintains stem cells and influences their characteristics and behavior (Morrison and Spradling, 2008).

## **1.2 The adult hair follicle and the hair cycle**

The adult mouse skin and its appendages contain stem cell populations. The hair follicle is connected to the epidermis via its infundibulum. Appended to each hair follicle below the infundibulum is the sebaceous gland. The region of the hair follicle below the sebaceous gland is called the isthmus, which in turn lies above an anatomically defined region termed the bulge. The bulge consists of two layers

of cells. The inner layer of terminally differentiated keratinocytes expressing keratin 6 (K6) serve to anchor the club hair, which protrudes out of the skin to form the hair coat of the animal (Hsu et al., 2011). On the other hand, the outer layer comprises the long-term stem cells of the hair follicle, identified by pulse-chase label-retaining experiments (hereby termed bulge hair follicle stem cells, or Bu-HFSCs) (Cotsarelis et al., 1990; Tumber et al., 2004). Below the bulge lies the hair germ, which consists of shorter-lived stem cells (hereby termed hair germ hair follicle stem cells, or HG-HFSCs). The hair germ directly abuts the dermal papilla (DP), a condensed group of mesenchymal cells that represents the major source of activating signals for the hair follicle stem cells (HFSCs) (Figure 1).

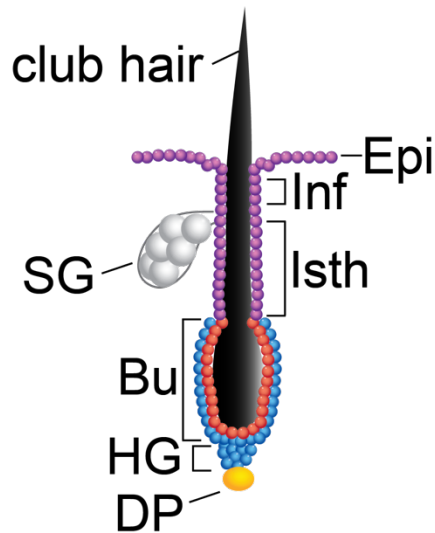


**Figure 1. Schematic of the adult mouse hair follicle.**

Epi, epidermis (skin). Inf, infundibulum. SG, sebaceous gland. Isth, isthmus. Bu, bulge. HG, hair germ. DP, dermal papilla.

By postnatal day 19 (P19), a full hair coat is formed on the surface of the animal. The hair follicle is a unique organ in that it undergoes periodic cycles of

regeneration. It can exist in three distinct stages, namely telogen, or rest; anagen, or regeneration; and catagen, or degeneration (Muller-Rover et al., 2001) (Figure 2). At P19, hair follicles are in their “first telogen” and consists of a single bulge anchoring a single club hair. Approximately two to three days later, they enter anagen substage I, during which the HG-HFSCs respond to the DP’s activating signals by proliferating (Greco et al., 2009). In anagen II, the hair germ enlarges while Bu-HFSCs now become proliferative. In anagen III, Bu-HFSC proliferation peaks, giving rise to the outermost layer of the growing hair follicle called the outer root sheath (ORS), while the expanded hair germ forms a pool of transit-amplifying cells (TACs) termed the matrix that now surrounds the DP (Hsu et al., 2014; Hsu et al., 2011). At this point, TACs begin to differentiate into seven concentric layers of keratinized cells, giving rise to a new hair shaft encased by the inner root sheath (IRS) and companion layer. In anagen IV, Bu-HFSC proliferation wanes, the hair follicle grows even deeper, and the hair shaft extends upwards towards the skin surface along with its differentiated layers. This continues in anagen V, and by anagen VI, the hair shaft protrudes out of the skin. Anagen VI persists to lengthen the hair shaft as the TACs continue to proliferate (Figure 2).

After a full-length hair shaft is achieved by around P35, hair follicles enter catagen, during which the TACs and the portion below the bulge degenerate via apoptosis, forming an epithelial strand. As the epithelial strand retracts upwards, some ORS cells survive and make a new bulge and hair germ. The surviving cells in the lower ORS will reconstitute the inner terminally differentiated K6+ layer of the new bulge; those in the mid-ORS will make the new hair germ; and finally, cells

in the upper ORS will form a new pool of Bu-HFSCs (Hsu et al., 2011). Completion of these processes marks the re-entry of the hair follicle into telogen (“second telogen”) by around P40. In the case of the pelage (back skin) hair follicle, it retains the older bulge and club hair alongside the newly formed bulge and club hair. As it undergoes more rounds of anagen, it can accumulate up to 4 bulges and club hairs (Figure 2).

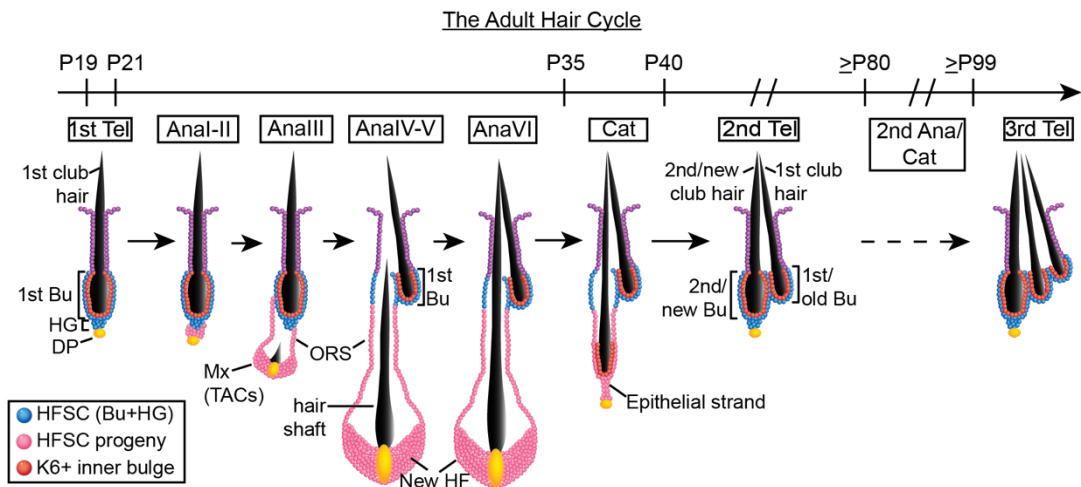


**Figure 2. The adult hair follicle cycles through telogen, anagen and catagen.** Schematic of the adult hair cycle. Hair follicles (HFs) undergo cycles of telogen (Tel, rest), anagen (Ana, regeneration) and catagen (Cat, degeneration) throughout the lifetime of the animal. Each HF generates a new bulge and new club hair with every anagen. Note that length of hair that protrudes out of the skin surface is not drawn to scale with that of hair follicle below the skin. Bu, bulge; HG, hair germ; DP, dermal papilla; ORS, outer root sheath; Mx, matrix; TACs, transit amplifying cells.

### 1.3 The hair follicle stem cell and its niche

The HFSC niche is a plexus of activating and inhibitory signaling networks contributed by diverse cell types. The surrounding dermis, comprising multiple cell types including fibroblasts and adipocytes, produces high levels of bone morphogenetic proteins (BMP), mainly BMP2 and BMP4, which inhibit HFSCs and keep them in a quiescent state (Plikus and Chuong, 2008). In contrast, the adipocyte precursor cells secrete platelet derived growth factor  $\alpha$  (PDGF $\alpha$ ) which stimulate HFSC activity via the DP (Festa et al., 2011). The DP is the major source of HFSC-activating cues that include transforming growth factor  $\beta$ 2 (TGF $\beta$ 2), noggin (which inhibits BMP), fibroblast growth factor 7 (FGF7) and FGF10 (Botchkarev et al., 2001; Greco et al., 2009; Oshimori and Fuchs, 2012; Rendl et al., 2005; Rosenquist and Martin, 1996; Woo et al., 2012). It has also been discovered that stem cell progeny can feedback to stem cells and influence their behavior. Within the bulge, the inner layer of Bu-HFSC-derived terminally differentiated cells also secrete high levels of BMP6 and fibroblast growth factor 18 (FGF18) that in turn strongly inhibit HFSCs (Hsu et al., 2011). The TACs, derived from the HG, which in turn originates from Bu-HFSCs in the mid-ORS, secrete sonic hedgehog (SHH), that acts long-range to induce proliferation in the Bu-HFSCs during anagen II and III (Hsu et al., 2014). In these ways, HFSC activity is tightly regulated by its niche to ensure that sufficient proliferation can occur without excessiveness to generate new tissue.

## 1.4 Hair follicle stem cell quiescence and activation

During telogen, several lines of evidence point to BMP signaling playing a significant role in maintaining HFSCs in a quiescent state. It has been hypothesized that cyclic BMP signaling in the surrounding dermis divides telogen into two phases: refractory telogen as characterized by high dermal BMP levels, and competent telogen as defined by lower dermal BMP signals. As these names suggest, HFSCs are unable to proliferate during refractory telogen, but are then able to exit their quiescent state during competent telogen when activating signals become strong enough to overcome the reduced dermal BMP levels (Plikus et al., 2008). Indeed, skin implantation of beads coated with the BMP inhibitor noggin stimulates HFSC proliferation, while conditional ablation of BMP receptor 1a (BMPR1A) from HFSCs to eliminate their BMP signaling response is sufficient to cause them to proliferate and launch them into anagen much earlier than their WT counterparts (Botchkarev et al., 2001; Genander et al., 2014; Kobiela et al., 2003; Kobiela et al., 2007; Zhang et al., 2006).

Besides a reduction in BMP signaling, stabilization and nuclear translocation of  $\beta$ -catenin, which is an effector and transcriptional co-factor of active Wnt signaling, is crucial for the transition of HFSCs from telogen to anagen. HFSCs made to express a constitutively stabilized form of  $\beta$ -catenin ( $\Delta N$   $\beta$ -catenin) proliferate to initiate anagen earlier than their WT counterparts, similar to BMPR1a-deficient HFSCs (Lo Celso et al., 2004; Lowry et al., 2005; Van Mater et al., 2003).

A two-step mode of activation has been established that governs the proliferation of HFSCs to fuel a new cycle of regeneration (Greco et al., 2009). With dermal BMP being reduced and further inhibited by DP-derived noggin, HG-HFSCs, being more primed and directly abutting the DP, will proliferate first in response to the DP-derived TGF $\beta$ 2, FGF7 and FGF10, marking the entry of telogen hair follicles into anagen I (Greco et al., 2009). TGF $\beta$  signaling in HG-HFSCs induces expression of TMEFF1, which acts to further restrict BMP signals within the HFSC niche (Oshimori and Fuchs, 2012). This reduction in the BMP threshold is then sufficient to induce proliferation of Bu-HFSCs in anagen II. At this point, the expanded HG starts to form the matrix and secrete SHH, which further increases and sustains the proliferation of both matrix TACs and Bu-HFSCs in anagen III (Hsu et al., 2014).

In contrast to the HG-HFSC-derived TACs which will proliferate throughout anagen, Bu-HFSCs will stop proliferating in anagen IV, when the hair follicle has grown to a certain depth such that the DP and SHH-producing matrix is now far away from the Bu-HFSCs, and inhibitory factors produced from the inner bulge layer now act to re-establish Bu-HFSC quiescence (Hsu et al., 2014).

In these ways, the extrinsic HFSC niche is instrumental in maintaining HFSC quiescence during telogen, tightly regulating their activation for only a short window of time during anagen I-III, and returning them to quiescence during anagen IV-VI. Are there intrinsic mechanisms in place within HFSCs to govern their properties and behavior? Indeed, the ability to purify HFSCs has allowed us to explore this question.

## **1.5 Purifying and profiling hair follicle stem cell gene expression signatures**

The existence of slow-cycling cells within the hair follicle was first identified in 1990 by Lavker and colleagues, who pulsed mice with a nucleotide analogue, 5-bromo-2'-deoxyuridine (BrdU), and observed its retention in the bulge after hair follicles had undergone a regeneration cycle, when all other cycling cells had diluted it out, thereby refuting a long-established belief that the matrix TACs are the HFSCs (Cotsarelis et al., 1990). In 2004, Fuchs and colleagues asked whether these label-retaining cells (LRCs) of the bulge are stem cells. They devised a different pulse-chase strategy to label these slow-cycling LRCs, this time by fluorescence. Mice were engineered to express a keratin 5 (K5) promoter-driven tet-repressor-VP16, that bound to a tetracycline-responsive regulatory element (TRE) and induced the expression of histone H2B-green fluorescent protein (H2B-GFP) specifically in the K5-expressing epidermis and hair follicles [pulse]. When these 4-week old mice undergoing the first adult hair cycle were fed with doxycycline, H2B-GFP expression began to shut down as tet-repressor-VP16 no longer bound to TRE. After a chase period of 4 weeks to 4 months, well after the completion of at least the first adult hair cycle, only cells within the bulge retained their original H2B-GFP label, confirming the findings by Lavker and colleagues (Tumbar et al., 2004). This paved the way for the purification of bulge LRCs by fluorescence-activated cell sorting (FACS) and profiling of their gene expression. Most importantly, they showed that in the normal hair cycle and in wound repair, these LRCs were utilized, documenting that they were indeed HFSCs (Morris et

al., 2004; Tumber et al., 2004). Exploiting the gene expression profile of label-retaining Bu-HFSCs, characteristic surface markers were then identified to facilitate the FACS-isolation of Bu-HFSCs without the need for K5-tet-VP16/TRE-H2BGFP transgenes. This had led to Bu-HFSC culture and grafting experiments to establish their long-term stemness and their versatility to make entire new hair follicles, epidermis and sebaceous glands when grafted back onto mice (Blanpain et al., 2004). These findings sealed the fate of bulge LRCs as bona fide stem cells of the hair follicle.

The ability to FACS-purify Bu-HFSCs resulted in a surge in efforts to characterize their defining genetic and molecular signatures. Transcription factors that are enriched in Bu-HFSCs relative to inter-follicular epidermal basal cells and matrix TACs have been uncovered to play key roles in establishing Bu-HFSC fate and behavior. During homeostasis, TCF3 [transcription factor 7 like 1, (T-cell specific, HMG box)] and TCF4 [transcription factor 7 like 2, (T-cell specific, HMG box)] maintain HFSCs in an undifferentiated state (Merrill et al., 2001; Nguyen et al., 2009; Nguyen et al., 2006), while SOX9 [SRY (sex-determining region Y)-box 9] and LHX2 (lim-homeobox protein 2) suppress epidermal and sebaceous gland fates respectively to maintain HFSC identity (Folgueras et al., 2013; Kadaja et al., 2014; Nowak et al., 2008; Vidal et al., 2005). NFATc1 (nuclear factor of activated T-cells c1) and LHX2 are critical to keep HFSCs in a quiescent state, as loss-of-function mouse models resulted in premature entry of their hair follicles into anagen (Folgueras et al., 2013; Horsley et al., 2008; Rhee et al., 2006). TBX1 (T-box 1), identified in an in vitro self-renewal RNA-interference (RNAi) screen of

transcription factors enriched in Bu-HFSCs relative to their progeny cells, is critical for Bu-HFSCs to maintain their numbers through multiple rounds of tissue regeneration (Chen et al., 2012). Additionally, NFIB (nuclear factor I B) mediates the crosstalk of HFSCs with melanocyte stem cells that also reside within the same niche to achieve behavioral synchrony between two distinct stem cell populations during tissue regeneration (Chang et al., 2013; Nishimura et al., 2002; Rabbani et al., 2011).

## **1.6 Stem cells and aging**

As an organism ages, the ability of its tissues to keep up with its demands wanes. Tissue self-renewal slows down. Adult stem cells residing within these tissues would have served their function of maintaining tissue turn-over for much of the lifetime of the organism, and potentially accumulated a substantial amount of oxidative stress, cellular and DNA damage, or become senescent. Aging also causes alterations to the cells that make up the stem cell niche, and changes the composite of systemically circulating factors. Overall, stem cell tissue-regenerative potential and self-renewal capacity become compromised with age (Chakkalakal et al., 2012; Flach et al., 2014; Keyes et al., 2013; Oh et al., 2014; Rossi et al., 2008; van Deursen, 2014). Therefore, much research is on-going to investigate stem cell aging mechanisms, find ways to rejuvenate aged stem cell function and improve the quality of life as we age.

Distinct adult stem cell populations have different levels of activity, depending on the needs and demands of their tissues. The intestinal crypt stem cells and skin epidermal stem cells self-renew more frequently as these epithelial tissues are constantly sloughed off and need to be replaced. On the other hand, hematopoietic stem cells divide infrequently as they leave the task of replacing blood cells to their transiently dividing multipotent progenitor cells which are more committed to differentiation. Skeletal muscles undergo limited self-renewal, thus their stem cells, termed satellite cells, also divide infrequently and play a more significant role during muscle injury (Busch et al., 2015; Collins et al., 2005; Fuchs, 2009; Sun et al., 2014).

Hair follicles undergo periodic regeneration bouts. Therefore, like hematopoietic stem cells and satellite cells, HFSCs stay in prolonged periods of quiescence, or inactivity, during telogen, with mechanisms in place to tightly regulate their activation. It has been demonstrated that as mice age, hair follicles stay in telogen for longer periods of time, and when they do enter anagen, the duration is shorter, resulting in a concomitant reduction in hair length. Indeed, when aged HFSCs (24-month old) were stimulated to proliferate and regenerate new hairs, they displayed a delayed response in proliferation when compared to young HFSCs (2-month old). This defect was recapitulated by the reduced in vitro colony forming efficiency of aged HFSCs compared to young HFSCs. Normally, HFSCs down-regulate the BMP signaling target gene *NFATc1* to exit quiescence and begin proliferating. However, in aged mice, BMP signals in the dermal environment are much higher, causing stimulated aged HFSCs to maintain high

levels of NFATc1, the inhibition of which can rescue their delayed response in proliferation. Importantly, repetitive stimulation of young HFSCs to undergo regeneration multiple times within a short duration caused them to acquire an aged HFSC phenotype, both in terms of their function, self-renewal capacity and gene expression (Keyes et al., 2013).

While quiescence is not a hallmark feature of stem cells, its establishment greatly restricts unnecessary stem cell proliferation, thereby protecting them against metabolic stress and preserving their genomic integrity. These ensure that stem cells can live long-term while retaining their stemness (Cheung and Rando, 2013; Stewart et al., 2008). Yet, inevitably, adult stem cell function still becomes compromised as the organism ages. For my thesis, I aim to explore the extent to which stem cells have an unlimited capacity for self-renewal and tissue regeneration, or whether there are intrinsic factors that restrict this capacity, using in vivo HFSCs as my paradigm. Are there novel ways by which HFSCs maintain quiescence? Are there autonomous mechanisms for stem cells to know when to proliferate and regenerate tissues, and when to remain quiescent? Is the quiescent state required to maintain the long-term self-renewal capacity and differentiation potential of HFSCs?

# CHAPTER 2: THE ROLE OF FOXC1 IN MAINTAINING HAIR FOLLICLE STEM CELL QUIESCENCE

## 2.1 Introduction

Similar to the quiescence factors LHX2 and NFATc1, the transcription factor Forkhead Box C1 (FOXC1) was first observed to be enriched in hair follicle progenitor cells (P-cadherin-positive) relative to inter-follicular basal epidermal cells (P-cadherin-negative) in the developing E17.5 embryo (Rhee et al., 2006). Expression of these transcription factors remain enriched in Bu-HFSCs relative to basal epidermal cells in the adult skin (Blanpain et al., 2004). Further, the regulatory regions of *Foxc1* and *Nfatc1* genes share similar epigenetic marks which suggest that both genes are strongly transcribed in the quiescent telogen Bu-HFSCs and down-regulated in anagen Bu-HFSCs (Lien et al., 2011).

FOXC1 belongs to the Forkhead Box transcription factor family whose members contain the conserved Forkhead (FH) DNA-binding domain. The FOXC1 FH domain is a variant of the helix-turn-helix motif, comprising 3  $\alpha$ -helices, 2  $\beta$ -sheets and 2 large loops that form “wing-like” structures that together contribute to the organization, nuclear localization, DNA-binding specificity and efficiency, and transactivation capability of FOXC1 (Saleem et al., 2004).

In humans, the most notable condition that features a mutation in FOXC1 is Axenfeld-Rieger syndrome, which is characterized by abnormalities in the anterior segment of the eye such as a thinner iris and an off-center pupil, and can lead to

glaucoma, vision loss or blindness often during late childhood or adolescence (<https://ghr.nlm.nih.gov/condition/axenfeld-rieger-syndrome>). In mice, pan-deletion of FOXC1 causes neonatal lethality with hydrocephalus (accumulation of cerebrospinal fluid in the brain), eye defects and skeletal abnormalities (Kume et al., 1998). In addition to brain, eye and bone, FOXC1 also plays important roles in embryonic development of somites, kidney, gonad, heart and vasculature (Kume et al., 2000; Kume et al., 2001; Mattiske et al., 2006a; Mattiske et al., 2006b; Seo et al., 2006; Seo and Kume, 2006; Zarbališ et al., 2007).

FOXC1 has been implicated in various signaling pathways. During vascular development, FOXC1 directly regulates the expression of two components of the Notch signaling pathway that specifies an arterial cell fate in endothelial cells: DLL4, the ligand for Notch signaling, and HEY2, the Notch signaling downstream target (Hayashi and Kume, 2008; Seo et al., 2006). During calvarial bone development, FOXC1 integrates FGF and BMP signaling to induce expression of *A/x4* and *Msx2* for the proliferation of bone osteoprogenitor cells and ensure proper bone patterning and growth (Rice et al., 2003; Rice et al., 2005). During eyelid development, binding of FGF10 to its receptor FGFR2 leads to expression of BMP4 and the downstream BMP signaling target gene FOXC1 that induces eyelid closure (Huang et al., 2009; Kidson et al., 1999; Kume et al., 2001; Smith et al., 2000). Last but not least, FOXC1 maintains corneal transparency by preventing vascular endothelial growth factor (VEGF) signaling and angiogenesis through the inhibition of metalloproteinases (MMPs), thereby restricting extra-cellular matrix (ECM) degradation and VEGF bioavailability, providing a pathological mechanism

for Axenfeld-Rieger syndrome (Seo et al., 2012). Many of these pathways have been implicated in HFSC maintenance (BMP), activation (FGF10) and differentiation (BMP, Notch) (Genander et al., 2014; Greco et al., 2009; Kobiela et al., 2007; Pan et al., 2004; Yamamoto et al., 2003).

Two recent studies have elucidated non-autonomous roles of FOXC1 on influencing stem and progenitor cell behavior via their niche. First, FOXC1 is necessary for specification and maintenance of the bone marrow mesenchymal progenitor CAR (CXCL12-abundant reticular) cells, and their expression of CXCL12 and SCF (stem cell factor), which in turn preserve hematopoietic stem/progenitor cell numbers (Omatsu et al., 2014). Second, FOXC1 expression in the head mesenchyme sustains radial glial cell proliferation in the cerebellar ventricular zone during embryonic development (Haldipur et al., 2014).

To investigate a potential role of FOXC1 in hair follicle stem cells, I engineered FOXC1 loss-of-function mouse models by crossing conditional *Foxc1<sup>fllox</sup>* mice to two different Cre-recombinase mouse lines. The entire coding region of the *Foxc1* gene is located in its single exon, hence loxP sequences were introduced into its 5' upstream region and 3' untranslated region such that its whole coding sequence will be deleted upon Cre recombination (Sasman et al., 2012). *K14-Cre* targeted the conditional knockout (cKO) of *Foxc1* in all epithelial cells, including hair follicles, from as early as E14.5, when K14 starts to be expressed in the embryo (hereby referred to as *Foxc1-K14Cre-cKO*) (Vasioukhin et al., 1999). *Sox9-CreER* targeted *Foxc1* ablation specifically in hair follicles (not epidermis) when mice were treated with tamoxifen to induce Cre nuclear localization at desired timepoints (hereby

referred to as *Foxc1-Sox9CreER-cKO*) (Soeda et al., 2010b). The *Sox9CreER* mouse line also had the *loxP-STOP-loxP-YFP* (yellow fluorescence protein) cassettes inserted into one of their *Rosa26* (*R26*) loci such that when Cre was active, it also acted on the loxP sites to remove the STOP codon and enable YFP expression, which thus acted as a faithful reporter for cells with Cre activity and all of their subsequent progeny. I did not introduce the *R26-YFP* allele into *Foxc1-K14Cre-cKO* mice when I first started the project so as to avoid introducing the *R26-YFP* mouse C57BL/6 background into their pure Black Swiss strain background and minimize hair cycle variations due to mouse strain differences (see details of mouse strains in Materials and Methods).

## **2.2 Results**

### **2.2.1 FOXC1 expression in adult mouse skin**

#### **2.2.1.1 Generating a FOXC1 antibody**

While a commercially available antibody efficiently detected FOXC1 in paraffin-embedded tissue sections, I also needed an antibody to co-stain FOXC1 with other proteins in frozen tissue sections. To that end, I generated a FOXC1 antibody. The coding region that encodes the last 200 amino acids of the FOXC1 protein, which is the least conserved among the FOX transcription factors and excludes the conserved Forkhead DNA binding domain, was cloned out and introduced into a pGEX vector for expression in BL21 *Escherichia coli* cells. The resultant GST-

tagged FOXC1 protein fragment was extracted, purified on a polyacrylamide gel and introduced into guinea pigs as an antigen to generate a polyclonal FOXC1 antibody (see Materials and Methods for details).

FOXC1 expression pattern in various stages of the hair cycle was observed in fresh-frozen and paraffin-embedded tissues obtained from *Foxc1-K14Cre-cKO* mice and their WT littermates at different stages of the hair cycle, namely 1<sup>st</sup> telogen, anagen and catagen. The newly generated FOXC1 antibody was validated by confirming its staining pattern in frozen tissue sections with that of the commercially available antibody in paraffin-embedded sections, and by verifying its absence of staining in *Foxc1-cKO* tissues.

#### **2.2.1.2 Expression of FOXC1 and other HFSC genes in telogen**

In 1<sup>st</sup> telogen, FOXC was detected in all compartments of the hair follicle, but was especially prominent in the infundibulum and isthmus, also known to contain stem cells that refuel these upper regions of the HF. In the bulge, FOXC1 could be found in both the Bu-HFSC layer and the inner K6+ bulge layer. It was also detected in a subset of HG-HFSCs that is closer to the bulge. While FOXC1 staining was also detected in the sebaceous gland appended to the hair follicle, it was absent in the inter-follicular epidermis. FOXC1 was not detected in *Foxc1-K14Cre-cKO* tissue sections, thereby validating the specificity of the antibodies and the efficiency of *Foxc1*-knockout by K14Cre (Figure 3A).

Expression of other key HFSC genes, including NFATC1, LHX2, SOX9 and TCF4, was also investigated in the *Foxc1*-cKO tissues, and was not found to be perturbed in the absence of FOXC1 (Figure 3B).

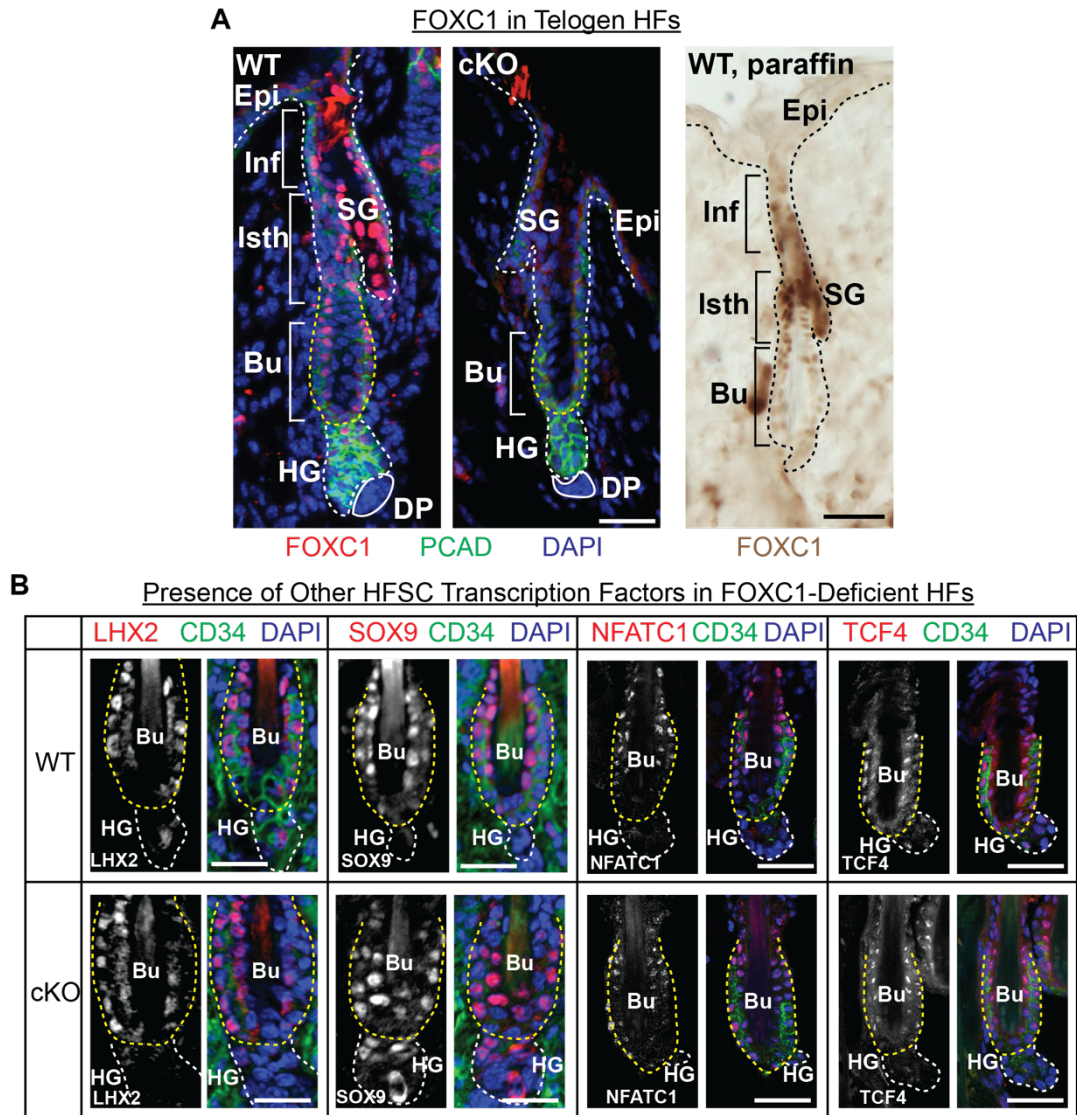


**Figure 3. Expression of FOXC1 and other key HFSC transcription factors in telogen.**

(A) FOXC1 expression pattern in telogen, and validation of *Foxc1*-cKO efficiency and FOXC1 antibody by immunofluorescence and paraffin immunohistochemistry. Antibodies (Abs) are color-coded according to the fluorescent secondary Abs used. Epi, epidermis; Inf, infundibulum; SG, sebaceous gland; Isth, isthmus; Bu, bulge; HG, hair germ; DP, dermal papilla.

(B) Expression of key HFSC transcription factors in WT vs. *Foxc1*-cKO. Note that CD34 expression in *Foxc1*-cKO bulge tends to be weaker than WT. Scale bars = 30  $\mu$ m.

### **2.2.1.3 *FOXC1* expression in anagen**

In anagen, *FOXC1* expression was maintained in all compartments of the hair follicle, as in telogen, be it when Bu-HFSCs were proliferating in earlier anagen (AnIII) or quiescent in later anagen (AnIV). *FOXC1* was also detected in some upper-most ORS cells just below the bulge, but absent in the mid- or lower-ORS. Within the newly emerging anagen hair bulb, *FOXC1* was expressed in the inner root sheath (IRS) as it co-localized with the IRS markers AE15 and GATA3. Therefore, in anagen, *FOXC1* was expressed in Bu-HFSCs, some Bu-HFSC progeny ORS cells, and in 3 of the 7 differentiated cell layers of the new hair follicle (Figures 4A and 4B). Loss of *FOXC1* did not seem to perturb the differentiation process as no differences were observed in the companion, IRS and hair shaft layers based on K6, AE13, AE15 and GATA3 expression (Figure 4B). However, *Foxc1-K14Cre*-cKO hair coat frequently appeared rough and dull, in contrast to WT hair coat which looked smooth and shiny. Surface electron microscopy (SEM) revealed that the ends of *Foxc1-K14Cre*-cKO hairs were kinked, which could account for the differences observed in hair coat appearance (Figure 4C, courtesy of Dr. Amalia Pasolli).

### **2.2.1.4 *FOXC1* expression in catagen**

As hair follicles degenerated, *FOXC1* was absent in the retracting epithelial strand, but was expressed in the bulging region above the epithelial strand. This bulging region would eventually enter the new bulge and constitute its inner K6+

layer. FOXC1 expression was also maintained in all other compartments of the hair follicle, including Bu-HFSCs, as in telogen and catagen (Figure 4D).

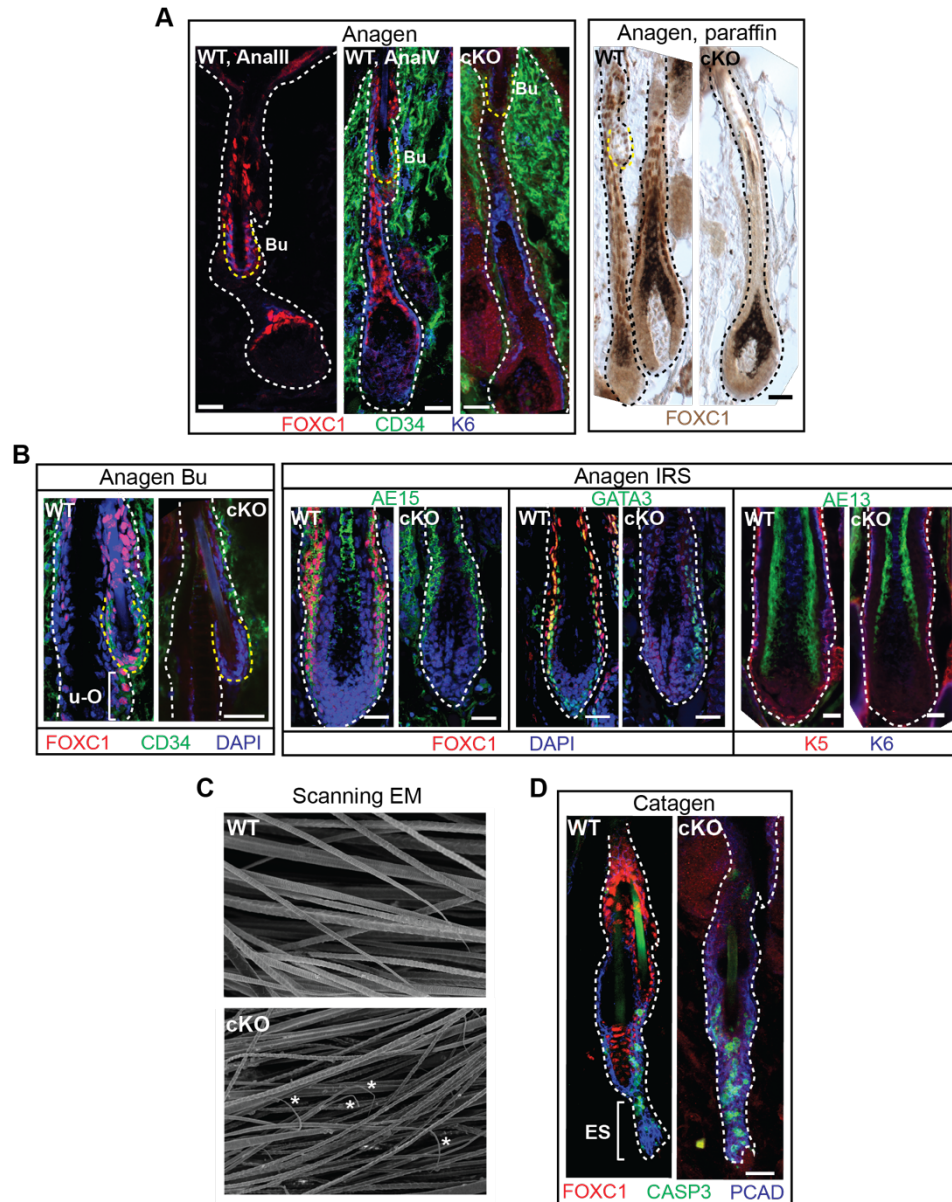


**Figure 4. Expression of FOXC1 in anagen and catagen.**

(A) FOXC1 expression in anagen.

(B) FOXC1 is expressed in anagen bulge, including HFSCs marked by CD34, and in the inner root sheath (IRS) layers marked by AE15 and GATA3.

(C) Scanning EM reveals kinked ends of *Foxc1*-cKO hairs, marked by asterisks (\*), courtesy of Dr. Amalia Pasolli.

(D) FOXC1 is expressed in the retracting portion of the catagen HF, above the caspase 3 (CASP3)-positive epithelial strand (ES).

Scale bars = 30  $\mu$ m.

### 2.2.2 Depletion of FOXC1 results in faster hair cycling and impacts long term hair coat maintenance

To observe hair cycle progression under native conditions, I shaved the dorsal back of *Foxc1-K14Cre-cKO* and WT mice after each round of hair cycling, starting from the first hair coat in 1<sup>st</sup> telogen at P19. Shaving clipped off hairs to reveal the skin surface without injuring the underlying hair follicular cells. This allowed for pinpointing of hair cycle stage according to the transition of skin color from pink (telogen) to grey and black (anagen), as melanocyte stem cells also proliferate together with HFSCs and differentiate to deposit black pigment onto the hair follicles, resulting in an increasing darkening of the skin (Muller-Rover et al., 2001; Plikus and Chuong, 2008). Generation of a second hair coat and entry into 2<sup>nd</sup> telogen occurred normally, suggesting that anagen and catagen were unperturbed by loss of FOXC1 (Figure 5A). However, *Foxc1-K14Cre-cKO* mice entered their next anagen and regenerated their third hair coat dramatically earlier than WT littermates (Figure 5B). Indeed, incorporation of the nucleotide analogue 5'-bromo-2'-deoxyuridine (BrdU) confirmed the precocious S-phase entry and proliferation of *Foxc1-cKO* HFSCs, indicating a shortening of the typically extended 2<sup>nd</sup> telogen (Figure 5C).

In subsequent hair cycles, *Foxc1-K14Cre-cKO* mice continued to display significantly shortened telogens relative to their WT counterparts. By 9 months of age, many *Foxc1-K14Cre-cKO* mice were in their 7<sup>th</sup> telogen, while WT mice were still in their 4<sup>th</sup> telogen as they had undergone significantly more hair cycles with shortened telogen durations during the same period of time (Figures 5D and 5E).

By these criteria, the major defect arising from loss of FOXC1 appeared to be a failure to maintain extended telogens, resulting in a dramatic increase in the frequency of hair cycling through most of the lifetime of the animal.

Despite the overall markedly abridged telogens, *Foxc1-K14Cre-cKO* HFs still experienced a modest age-related extension in telogen length, a feature that is more conspicuous in WT HFs and which has been attributed to a rise in macro-BMP levels in aging skin (Keyes et al., 2013). However, in contrast to their WT counterparts, even though young *Foxc1-K14Cre-cKO* mice generated grossly normal hair coats, their hair coats became strikingly sparser and frequently greyed as they aged (Figure 5F). This suggested that the bulge niche and its residents might be functionally impacted through excessive utilization during frequent hair cycling.

**Figure 5. Depletion of FOXC1 from HFs causes faster hair cycling, yielding a sparser hair coat with age.**

- (A) 1<sup>st</sup> hair coat of *Foxc1*-cKO and WT mice appeared at the same age. When shaved at P19 (1<sup>st</sup> Tel), skin of both *Foxc1*-cKO and WT were observed to darken from pink to grey and black in a similar way as they progressed through anagen (1<sup>st</sup> Ana). When the newly formed 2<sup>nd</sup> hair coat was shaved again at P35, skin of both *Foxc1*-cKO and WT were also observed to lose pigmentation in a similar way as they underwent catagen (Cat).
- (B) *Foxc1*-cKO mice regenerated their 3<sup>rd</sup> hair coat much earlier than WT mice.
- (C) Immunofluorescence of *Foxc1*-cKO HF sagittal section at P50, depicting precocious Bu-HFSC activation and earlier entry into anagen than WT.
- (D) Recovered hair coats of mice were shaved repeatedly to monitor hair cycles long-term.
- (E) *Foxc1*-cKO mice underwent more frequent hair cycling and exhibited markedly shorter intervals between hair cycles. Left, data are mean  $\pm$  SD. Right, “time between recovery” refers to the time at which > 80% of the hair coat had recovered after shaving; box-and-whisker plot: midline, median; box, 25<sup>th</sup> and 75<sup>th</sup> percentiles; whiskers, minimum and maximum. \*\* $p < 0.01$ ; \*\*\*\* $p < 0.0001$ .
- (F) Representative example of hair coat of WT and *Foxc1*-cKO mice at 1.5 to 2 years of age. Pink box indicates zoomed-in view of lateral side of hair coat. Note visibility of skin (with some pigmented spots) underneath a sparse hair coat in *Foxc1*-cKO. Scale bars = 30  $\mu$ m.



### **2.2.3 FOXC1 is necessary to establish a multiple-bulge hair follicle architecture, and maintain HFSC numbers and function with age**

To explore the consequences of FOXC1 loss further, I quantified Bu-HFSC numbers in young (P19, 1<sup>st</sup> telogen and P42, 2<sup>nd</sup> telogen) and aged ( $\geq 1.5$  years) mice. In 1<sup>st</sup> telogen, both WT and *Foxc1-K14Cre-cKO* HFs had one bulge with no significant differences in Bu-HFSC numbers. However, in 2<sup>nd</sup> telogen, while WT HFs had established a two-bulge architecture, *Foxc1-K14Cre-cKO* HFs still had only one bulge, and failed to expand their Bu-HFSC numbers like WT HFs did (Figures 6A-C). This one-bulge phenotype persisted in subsequent hair cycles: while WT hair follicles had up to three and four bulges in 3<sup>rd</sup> and 4<sup>th</sup> telogen respectively, *Foxc1-K14Cre-cKO* hair follicles continued to maintain only one (Figure 6D).

Once an old club hair is shed, the bulge structure disappears. Therefore, in aged mice, WT hair follicles continued to maintain a 2-4 bulge architecture, while *Foxc1-K14Cre-cKO* hair follicles still had only one bulge. Notably, their bulges were frequently smaller and contained dramatically fewer Bu-HFSCs when compared to both aged WT hair follicles and young *Foxc1-K14Cre-cKO* hair follicles (Figures 6C and 6E). By these criteria, starting from 2<sup>nd</sup> telogen, *Foxc1-K14Cre-cKO* Bu-HFSC numbers appeared to wane with subsequent hair cycles.

To test the ability of aged *Foxc1-K14Cre-cKO* HFSCs to regenerate hairs, I depilated the hair coat, which removed the club hair and its associated K6+ inner bulge layer, a potent source of HFSC-inhibitory factors BMP6 and FGF18, thereby stimulating HFSC proliferation and anagen entry (Hsu et al., 2011). Interestingly,

both young and aged *Foxc1-K14Cre*-cKO HFSCs proliferated one day earlier than their WT counterparts (Figures 6F and 6G). However, by 5 days post-depilation, young and aged WT hair follicles and young *Foxc1-K14Cre*-cKO hair follicles had progressed to mid-anagen, but some aged *Foxc1-K14Cre*-cKO hair follicles were still in early anagen, even though their HFSCs in the bulge and upper outer root sheath (ORS) showed signs of proliferation (Figure 6H). Consequently, despite an initial accelerated response, aged *Foxc1-K14Cre*-cKO HFSCs regenerated a hair coat more slowly than their aged WT and young mutant counterparts, suggesting a functional decline (Figure 6I).

**Figure 6. Without FOXC1, HF s fail to maintain multiple bulges and club hairs and display reduced HFSCs.**

- (A) Whole-mount immunofluorescence of WT and *Foxc1*-cKO 1<sup>st</sup> telogen (left panel) and 2<sup>nd</sup> telogen (right panel) HF s. CD34 (green) marks outer bulge layer (HFSCs); K6 (red) marks inner bulge layer; red autofluorescence marks club hair.
- (B) Quantification of 2<sup>nd</sup> telogen HF s with one bulge in dorsal skin (n ≥ 4 mice, ≥ 80 HF s from each mouse). Box-and-whisker plot: midline, median; box, 25<sup>th</sup> and 75<sup>th</sup> percentiles; whiskers, minimum and maximum. \*\*\*\*p < 0.0001.
- (C) Quantification of total number of CD34+ HFSCs (both basal-Bu and suprabasal-Bu) per whole-mount HF (n ≥ 2 mice, ≥ 10 HF s per mouse). \*\*\*\*p < 0.0001; ns, non-significant.
- (D) Whole-mount immunofluorescence of WT and *Foxc1*-cKO HF s in 3<sup>rd</sup> and 4<sup>th</sup> telogen. Note the increase in bulge numbers in WT but persistent one-bulge phenotype in *Foxc1*-cKO. CD34 expression is frequently weaker in *Foxc1*-cKO.
- (E) Whole-mount immunofluorescence of HF s in aged (≥ 1.5 years) WT and *Foxc1*-cKO animals. Bu, bulge; HG, hair germ; SG, sebaceous gland.
- (F) Sagittal section immunofluorescence of HF s which were depilated and then pulsed with BrdU for 24 hr. Skin biopsies were retrieved at t = 24 and 48 hr post-depilation (pd). PCAD (P-cadherin) stains HG and outlines Bu. Note that both aged and young *Foxc1*-cKO HF s responded faster than WT.
- (G) Quantification of BrdU+ cells in Bu and HG 24 hr post-depilation (n = 2 mice, ≥ 10 HF s per mouse). \*\*, p < 0.01; \*\*\*\* p < 0.0001.
- (H) Sagittal sections from Day 5 post-depilated mice indicated that aged *Foxc1*-cKO HF s progressed to regenerate new hairs more slowly than WT.
- (I) Tracking of hair coat recovery post-depilation. Note that despite the faster response to depilation, hair coat recovery was delayed in aged *Foxc1*-cKO mice. Scale bars = 30 μm unless indicated otherwise.



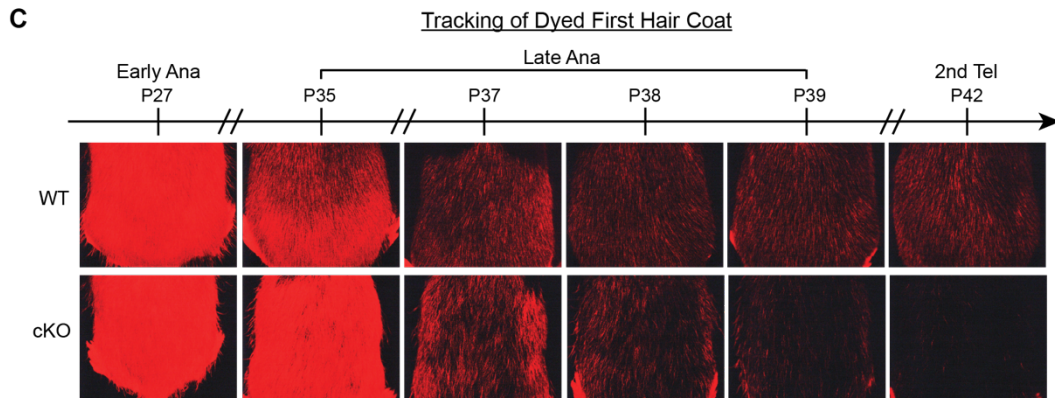
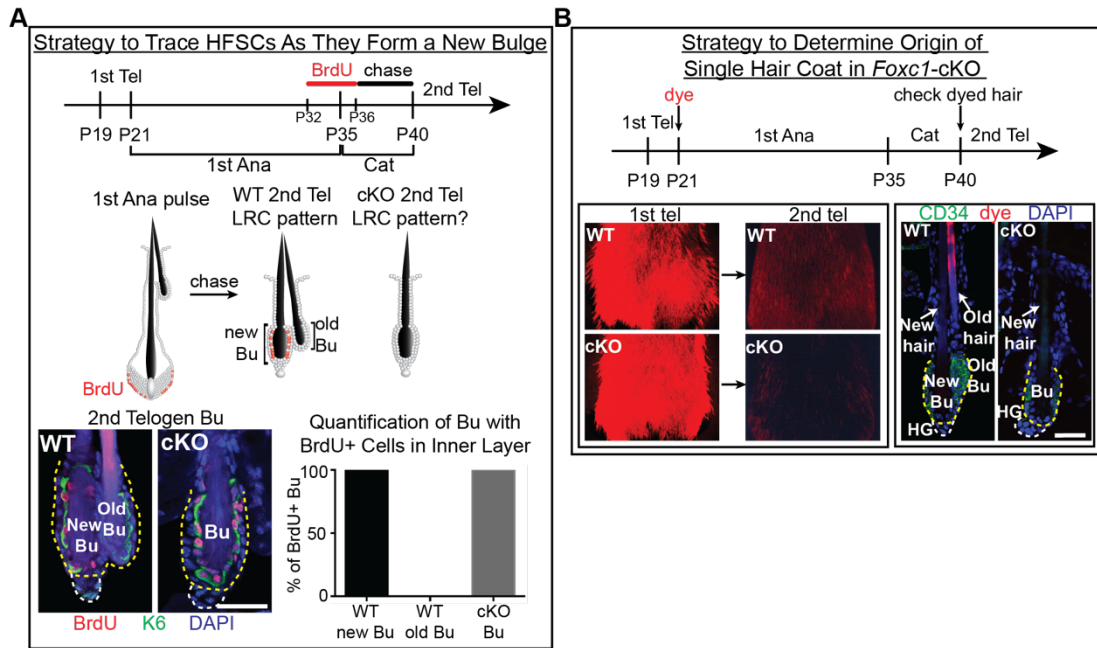
#### **2.2.4 FOXC1-deficient hair follicles can make a new bulge but fail to maintain the older one**

Intrigued by the one-bulge phenotype, I wanted to know how it arises, and if it results in more than just thinning of the hair coat. I first determined whether FOXC1-deficient HFs failed to establish their new bulge or precociously lost their old one. To test the former, I employed a nucleotide analogue pulse-chase strategy. In late anagen (anagen VI), while Bu-HFSCs and cells in the upper and middle ORS had ceased proliferation, lower ORS cells were still proliferating. When these lower ORS cells were pulsed with BrdU and chased, some of these BrdU-labeled ORS cells in WT HFs survived the ensuing catagen and made the K6<sup>+</sup> inner layer of the telogen new bulge, while the old bulge remained unlabeled (Hsu et al., 2011). In *Foxc1-K14Cre*-cKO HFs, the single bulge displayed BrdU-retaining K6<sup>+</sup> cells, indicating that it was newly formed, just like the WT new bulge (Figure 7A).

To confirm that the old bulge was lost, I traced the old (first) hair coat by dyeing it in 1<sup>st</sup> telogen and tracking it through 1<sup>st</sup> anagen (Figure 7B). In WT late anagen hair follicles, the dyed hairs persisted, but most of the dyed hairs in *Foxc1-K14Cre*-cKO hair follicles were gradually lost during late anagen (Figure 7C). Immunofluorescence confirmed that WT hair follicles consisted of an old bulge which anchored a dyed hair and a new bulge which anchored a non-dyed hair; by contrast, *Foxc1-K14Cre*-cKO hair follicles consisted of a single new bulge anchoring a non-dyed hair (Figure 7B). These data indicated that with every hair cycle, *Foxc1-K14Cre*-cKO hair follicles were able to generate a new bulge and new club hair, but failed to maintain the old ones.

**Figure 7. FOXC1-deficient HFs can make a new bulge but fail to maintain the old one.**

- (A) Strategy to pulse proliferating lower ORS cells with BrdU during 1<sup>st</sup> anagen and analyze the pattern of label-retaining cells (LRCs) in 2<sup>nd</sup> telogen. Note that the *Foxc1*-cKO single bulges displayed the LRC pattern expected of a newly formed and not old bulge. Quantification shown is respective percentages of WT new bulge, WT old bulge and *Foxc1*-cKO bulge that had retained BrdU label in their inner layer (n = 2 mice, 30 HFs per mouse).
- (B) Dyeing of 1<sup>st</sup> telogen hair coat and tracing it through 1<sup>st</sup> adult hair cycle to 2<sup>nd</sup> telogen. Note the retention of dyed hairs in WT 2<sup>nd</sup> telogen, but the near absence of dyed hairs in *Foxc1*-cKO 2<sup>nd</sup> telogen. Immunofluorescence of 2<sup>nd</sup> telogen HFs depicts WT old bulge anchoring old (dyed) hair, WT new bulge anchoring new (non-dyed) hair, and *Foxc1*-cKO single bulge also anchoring a new (non-dyed) hair. Scale bars = 30  $\mu$ m.
- (C) Dyed mice were tracked closely in late anagen to monitor fate of dyed hairs. Note that mice illustrated here entered 1<sup>st</sup> anagen ~2 days later than described in Figure 1.



### 2.2.5 Preservation of the old bulge contributes to HFSC quiescence

To investigate whether the old bulge plays a functional role in regulating hair cycling, I forced WT hair follicles to lose their old bulge precociously, thereby phenocopying *Foxc1-K14Cre-cKO* HF. To do so, I depilated them in 1<sup>st</sup> telogen (P19) to remove the club hair and inner K6+ bulge layer, and then allowed them to generate a new bulge and club hair. I also shaved the un-depilated posterior region to monitor natural hair cycle progression (Figures 8A and 8B). Both depilated and un-depilated halves generated new hairs and entered 2<sup>nd</sup> telogen by ~P40 (Figure 8B). However, while the posterior hair follicles now had two bulges and two club hairs, the anterior hair follicles had only one (Figure 8C).

I then shaved the new hairs to continue monitoring the hair cycle. While the posterior two-bulge hair follicles stayed in 2<sup>nd</sup> telogen for ~6.5 weeks, the anterior one-bulge HF remained in 2<sup>nd</sup> telogen for only ~2.5 weeks before regenerating a full hair coat precociously (Figures 8B and 8H, WT 2-Bu vs. WT 1-Bu). The anterior-posterior boundary was maintained throughout both hair cycles, indicating that precocious anagen occurred specifically in one-bulge hair follicles only. The converse experiment was repeated (posterior half, depilated; anterior half, shaved) with analogous results (Figure 8E). Under the conditions used, hair follicles were age-, sex- and strain-matched, thereby providing compelling evidence that the presence of the old bulge contributed to HFSC quiescence. Based upon the existing literature, I attribute this to the contribution of inhibitory signals, particularly FGF18 and BMP6, emanating from 1) the suprabasal Bu-HFSCs, which arise from

the interface between two adjacent bulges and which are no longer present in one-bulge hair follicles (Blanpain et al., 2004), and 2) the K6+ inner layer of the old bulge (Hsu et al., 2011).

Consistent with this notion and with a prior report that *Foxc1* is a downstream target of BMP signaling in proliferative hair progenitors (Genander et al., 2014), I did not see significant changes in *Fgf18* and *Bmp6* transcripts on a per K6+ inner bulge cell basis in *Foxc1-K14Cre-cKO* one-bulge hair follicles, but we confirmed a reduction of inner bulge cell numbers, in addition to the complete absence of suprabasal Bu-HFSCs (Figure 8D). In this regard, the microenvironment of the *Foxc1-K14Cre-cKO* bulge was likely to be reduced over WT for these inhibitory factors, a feature that would allow stimulatory signals to overcome the threshold for HFSC activation more easily.

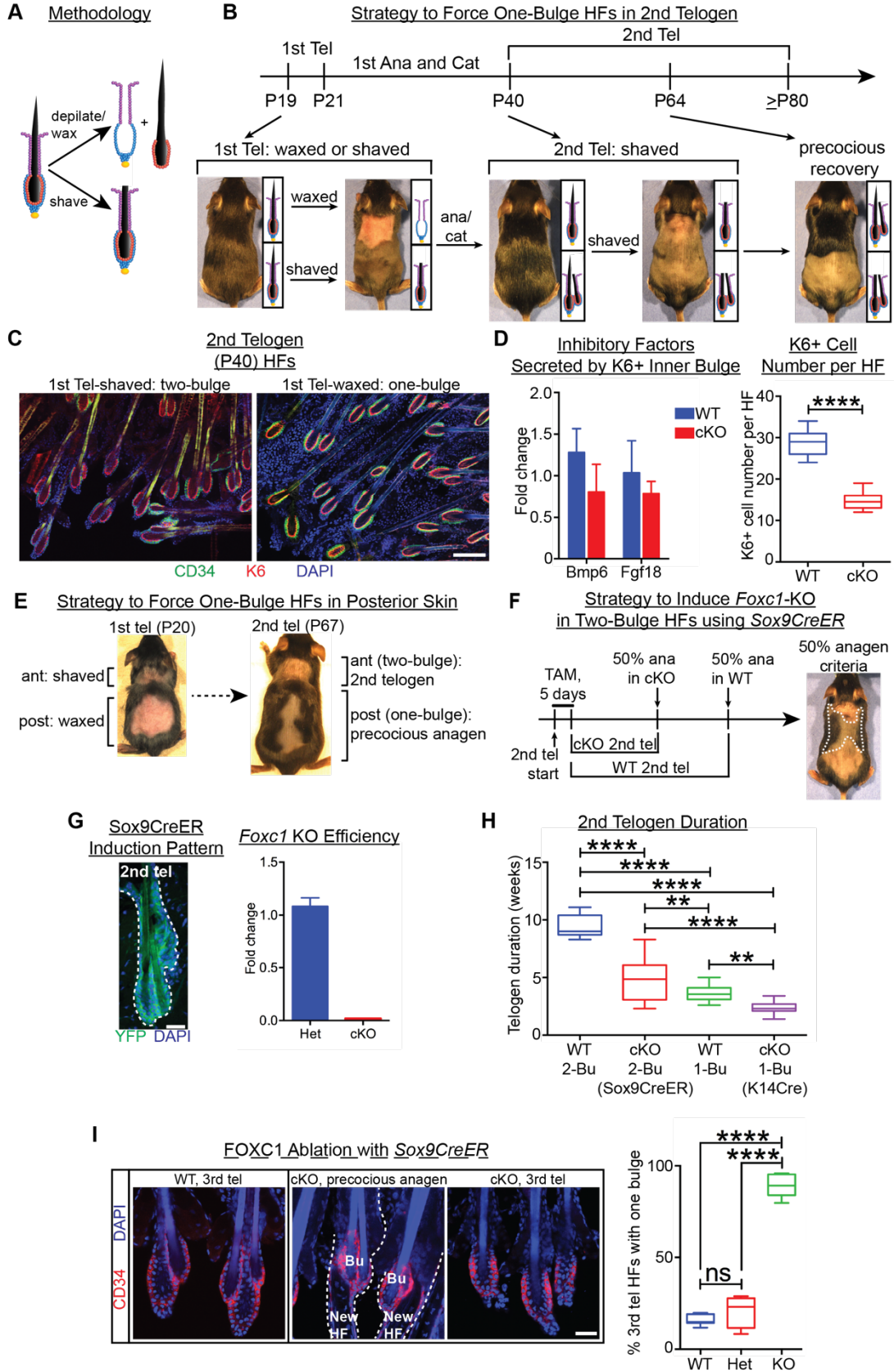
### **2.2.6 Loss of FOXC1 in the presence of the old bulge also shortens telogen**

Despite the impact of the old bulge, its loss was not sufficient to fully account for the acutely constrained telogen observed in *Foxc1-K14Cre-cKO* hair follicles (Figure 8H, WT 1-Bu vs. cKO 1-Bu). Therefore, it was important to determine whether FOXC1 loss alone was sufficient to elicit telogen shortening under conditions where two bulges existed. To accomplish this, I used *Sox9CreER* to induce *Foxc1* ablation in two-bulge hair follicles during 2<sup>nd</sup> telogen (at ~P50), shaved hair coats to observe hair cycle progression, and quantified telogen duration as time taken for at least 50% of the shaved skin to enter anagen (Figures

8F and 8G). I found that loss of FOXC1 alone shortened the 2<sup>nd</sup> telogen of these two-bulge hair follicles, but to a lesser extent than when coupled with loss of the bulge (Figure 8H). It was important to note that these hair follicles maintained their old bulges when they precociously entered anagen, but would lose them later and display a one-bulge phenotype in their next telogen (Figure 8I). This lends further support to my hair dye experiment results (Figure 7C) which suggested that the process of bulge loss occurred during late anagen. Taken together, these data demonstrated that loss of FOXC1 influenced HFSC activity in at least two different ways.

**Figure 8. The old bulge contributes to HFSC quiescence.**

- (A) Methodology of hair-shaving and hair-depilation/waxing. Note that depilation of HFs removes the club hair and associated K6+ inner layer from the bulge, while shaving only clips away hairs at the skin surface.
- (B) Strategy to force WT 2<sup>nd</sup> telogen HFs to have only one bulge. HF schematics next to mouse photos depict HF state after waxing/shaving and completion of anagen/catagen. 1<sup>st</sup> telogen (P19) HFs were depilated by waxing, and entered 1<sup>st</sup> anagen at the same time as their shaved counterparts. By 2<sup>nd</sup> telogen (P40), shaved-HFs had two bulges/club hairs, while waxed-HFs had only one bulge/club hair. All HFs were then shaved to observe entry into 2<sup>nd</sup> anagen. Tel, telogen; Ana, anagen; Cat, catagen.
- (C) Whole-mount-immunofluorescence to validate strategy. Most 1<sup>st</sup> telogen-shaved-HFs had two bulges/club hairs, whereas 1<sup>st</sup> telogen-waxed-HFs largely had one bulge/club hair only. Scale bar = 100  $\mu$ m.
- (D) Left, qRT-PCR of SC-inhibitory factors from FACS-purified K6+ inner bulge cells. Data are mean  $\pm$  SEM. Right, quantification of K6+ cell number per HF. Box-and-whisker plot: midline, median; box, 25<sup>th</sup> and 75<sup>th</sup> percentiles; whiskers, minimum and maximum ( $n \geq 2$  mice,  $\geq 10$  HFs per mouse). Note that although *Bmp6* and *Fgf18* were only slightly reduced on a per cell level, there were fewer K6+ inner bulge cells in *FOXC1*-deficient HFs, resulting in an overall reduced density of cells expressing these inhibitory factors.
- (E) When HFs in the posterior (post) dorsal skin were forced to have one bulge, they recapitulated the precocious anagen phenotype of the anterior (ant) one-bulge HFs in (B), as evidenced by greying and darkening of posterior skin while anterior skin remained pink.
- (F) Strategy to induce *Foxc1*-KO in 2<sup>nd</sup> telogen two-bulge HFs using *Sox9CreER*. Mice were treated with tamoxifen for 5 days and observed for progression into anagen. Inset of mouse image depicts criteria to determine telogen duration, which was time taken for at least 50% of dorsal skin to enter anagen (as judged by greying, blackening or appearance of hair).
- (G) Left, *Sox9CreER* induces *R26-YFP* expression efficiently and specifically in HFs. Right, qRT-PCR shows the efficient deletion of *Foxc1* in FACS-purified Bu-HFSCs. Data are mean  $\pm$  SEM ( $n = 3$  mice). Scale bar = 30  $\mu$ m.
- (H) 2<sup>nd</sup> telogen duration determined by criteria described in (F). WT two-bulge HFs, WT one-bulge HFs (post-depilation-recovery), *Foxc1-Sox9CreER*-cKO two-bulge HFs and *Foxc1-K14Cre*-cKO one-bulge HFs were compared. Box-and-whisker plot: midline, median; box, 25<sup>th</sup> and 75<sup>th</sup> percentiles; whiskers, minimum and maximum ( $n \geq 10$  mice). \*\* $p < 0.01$ ; \*\*\*\* $p < 0.0001$ .
- (I) Left, after tamoxifen treatment in 2<sup>nd</sup> telogen and allowing HFs to progress through anagen  $\rightarrow$  3<sup>rd</sup> telogen, *Foxc1-Sox9CreER*-WT HFs had 2 or 3 bulges, while cKO HFs maintained their old bulges when they entered anagen precociously, but lost them by 3<sup>rd</sup> telogen. Right, quantification of number of bulges per 3<sup>rd</sup> telogen HF ( $n \geq 4$  mice, 70  $\geq$  HFs from each mouse). ns, non-significant; \*\*\*\* $p < 0.0001$ . Scale bar = 30  $\mu$ m.



### 2.2.7 FOXC1 re-establishes and maintains quiescence of HFSCs after their activation

To explore Bu-HFSC-intrinsic effects resulting from the loss of FOXC1, I performed RNA sequencing (RNA-seq) on late anagen and 2<sup>nd</sup> telogen Bu-HFSC populations purified by fluorescence activated cell sorting (FACS). Late anagen Bu-HFSCs were obtained from *Foxc1-Sox9CreER-cKO* mice in which *Foxc1* deletion was induced in the prior 1<sup>st</sup> telogen, while 2<sup>nd</sup> telogen Bu-HFSCs were purified from both *Foxc1-K14Cre-cKO* (one-bulge) and *Foxc1-Sox9CreER-cKO* (two-bulge) hair follicles. In addition to YFP (for *Foxc1-Sox9CreER*), antibodies against CD34 (Bu-HFSC marker),  $\alpha 6$  (marker of basal epithelial cells, including Bu-HFSCs) and SCA1 (marker of epidermis, for exclusion) were used for FACS purification (Figure 9A). I first investigated transcripts (with FPKM > 1) that were significantly up-regulated (p-value < 0.05, false-discovery rate (q-value) < 0.05) upon FOXC1 loss and found that these were enriched for genes encoding cell cycle-associated proteins, be it anagen or 2<sup>nd</sup> telogen hair follicles with one bulge or two bulges (Figures 9B-F and 10A; see Materials and Methods for RNA-seq data analysis details).

Since up-regulation of cell cycle genes upon FOXC1 loss was persistent across all stages of the hair cycle, I asked if these *Foxc1-cKO* Bu-HFSCs could even exist in a quiescent state. Cell cycle profiling was performed on FACS-purified Bu-HFSCs using a DNA dye to quantify DNA content, and Ki67 to distinguish G0 (quiescent) cells from cells in G1, S, G2 or M phases of the cell cycle. Analysis in late anagen confirmed that while WT Bu-HFSCs had largely returned to

quiescence (G0, as judged by DNA content and absence of Ki67) following their proliferative activity in early anagen, an appreciable fraction of *Foxc1*-cKO Bu-HFSCs remained in the cell cycle (non-G0), although most cells had also returned back to quiescence (Figure 10B). A similar trend was observed in 2<sup>nd</sup> telogen, at a time when almost all WT Bu-HFSCs were in quiescence (Figure 10C).

Further evidence to support the increased proliferative capacity of *Foxc1*-cKO Bu-HFSCs came from in vitro studies in which FACS-purified Bu-HFSCs were co-cultured with feeder fibroblasts for 2 weeks and allowed to make colonies. Indeed, *Foxc1*-cKO Bu-HFSCs exhibited greater colony formation efficiency, analogous to that displayed by cultured HG-HFSCs that were also more primed to proliferate in vivo (Greco et al., 2009) (Figure 10D).

Taken together, loss of FOXC1 delayed the return of anagen Bu-HFSCs from an activated state to a quiescent state, and also primed telogen Bu-HFSCs to proliferate precociously, suggesting that FOXC1 acts to re-establish Bu-HFSC quiescence during anagen and maintain it during telogen.

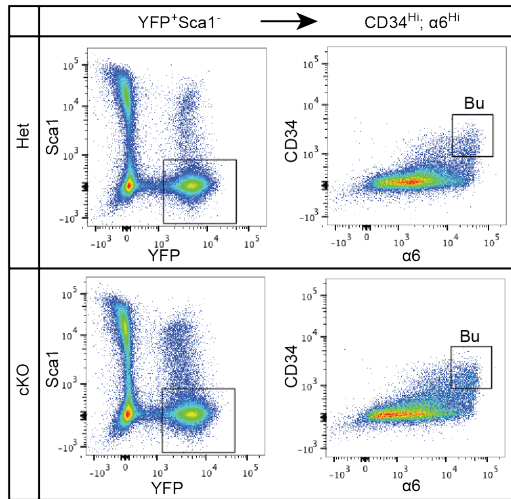
Previously, it was shown that absence of the quiescence-associated NFATc1 causes de-repression of the cell cycle gene *Cdk4*, precocious HFSC activation and premature hair cycling (Horsley et al., 2008). Interestingly, when I conditionally ablated *Nfatc1* in hair follicles, I discovered that in addition to their precocious hair cycle entry, hair follicles also displayed a one-bulge phenotype (Figure 10E). These data led me to hypothesize that upon loss of either FOXC1 or NFATc1, the HFSC-intrinsic proliferative activity itself may contribute to both faster hair cycling and loss of the bulge; the bulge loss in turn couples with this HFSC-intrinsic

proliferative nature to further accelerate future hair cycles. I will re-address this hypothesis in a later section.

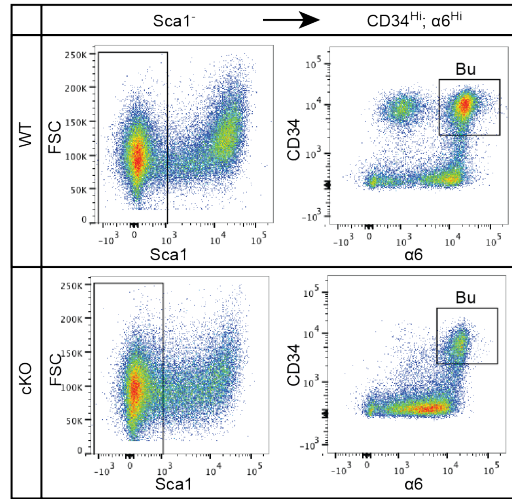
**Figure 9. RNA-seq summary of up-regulated genes in *Foxc1*-cKO Bu-HFSCs.**

- (A) FACS strategies to purify Bu-HFSCs from late anagen and 2<sup>nd</sup> telogen.
- (B) Summary of transcriptional profiling of *Foxc1*-cKO vs. WT Bu-HFSCs in late anagen by RNA-seq. Shown here are significantly up-regulated genes (FPKM > 1,  $p < 0.05$ ,  $q < 0.05$ ).
- (C) Gene ontology (GO)-biological process (BP) term analysis of significantly up-regulated genes in late anagen.
- (D) Summary of transcriptional profiling of *Foxc1*-cKO vs. WT Bu-HFSCs in 2<sup>nd</sup> telogen by RNA-seq. Shown here are significantly up-regulated genes (FPKM > 1,  $p < 0.05$ ,  $q < 0.05$ ).
- (E) GO-BP term analysis of significantly up-regulated genes in 2<sup>nd</sup> telogen.
- (F) Genes in the GO-cell cycle term, commonly up-regulated in both late anagen and 2<sup>nd</sup> telogen, are shown.

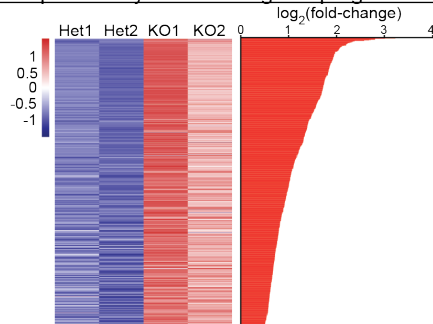
**A FACS Strategy to Purify Late Anagen Bu-HFSCs**



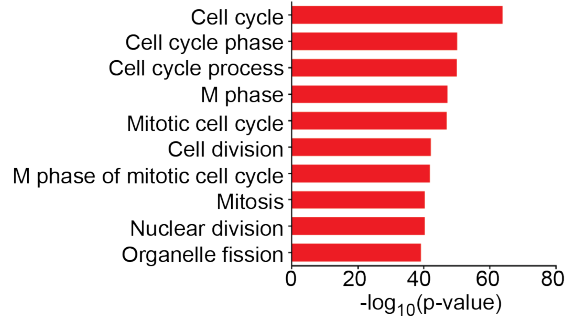
**FACS Strategy to Purify 2nd Telogen Bu-HFSCs**



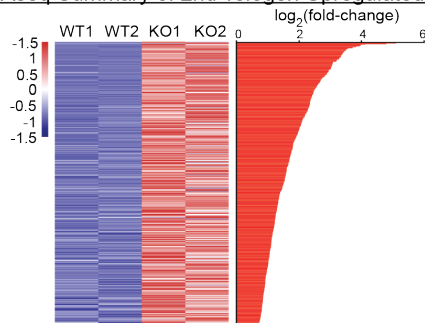
**B RNAseq Summary of Late Anagen Upregulated Genes**



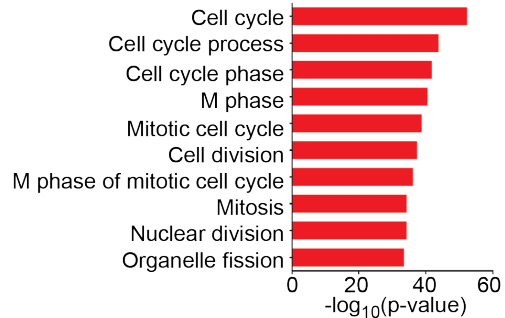
**C GO Analysis of Late Anagen Upregulated Genes**



**D RNAseq Summary of 2nd Telogen Upregulated Genes**



**E GO Analysis of 2nd Telogen Upregulated Genes**



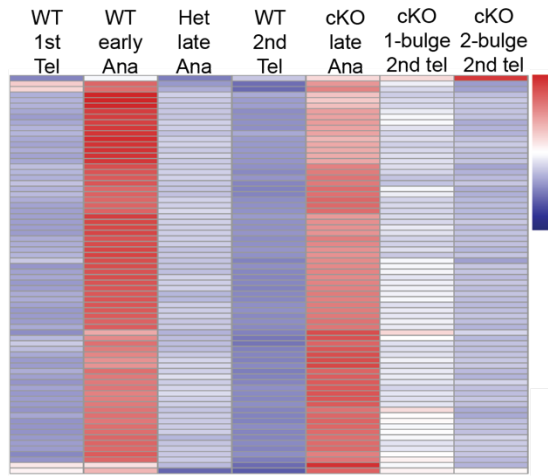
**F**

Cell cycle	<i>Cks2, Mcm6, Ube2c, Ccna2, Ccnb1, Birc5, Cdca3, Prc1, Uhrf1, Mki67, Mcm3, Anln, Cdk1, Ccnb2, Mad2l1, Ckap2, Cdca8, Racgap1, Nusap1, Tpx2, Tacc3, Smc2, Bub1b, Hells, Kif11, Rad51, Ncaph, Plk1, Nuf2, Dbf4, Cdc45, Cep55, Aurkb, Aurka, Cdkn3, Cenph, Esco2, Zwilch, Dlgap5, Spag5, Ndc80, Cdca5, Nek2, Cdc25c, Bub1, Timeless, Trip13, Kif20b, Cenpf, Chek1, Cenpe, Sgol1, Kifc1, Kntc1, Aspm, Dscc1, Sgol2, Nsl1, Cdca2, Clspn, Brca1, Ercc6l, Ska1, Cdc6, Gas2l3, Exo1</i>
------------	---

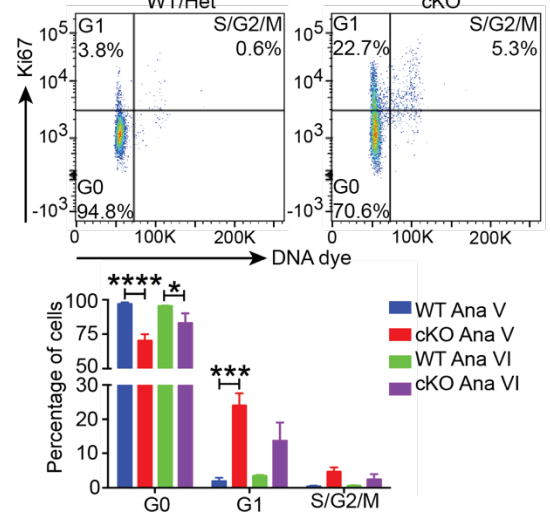
**Figure 10. Governance of HFSC quiescence is necessary to maintain the old bulge.**

- (A) Heat map to illustrate changes in expression of cell cycle genes (listed in Figure 9F) through the 1<sup>st</sup> hair cycle. Tel, telogen; Ana, anagen.
- (B) Cell cycle analysis of late anagen (substages Ana V and Ana VI) Bu-HFSCs by flow cytometry and quantification of percentages of cells in various phases of the cell cycle. Ki67 marks cycling cells; DNA content distinguishes cells in S/G2/M from G1/G0). Data are mean  $\pm$  SEM (n  $\geq$  3 mice). \*p < 0.05; \*\*\*p < 0.001; p\*\*\*\* < 0.0001.
- (C) Cell cycle analysis of 2<sup>nd</sup> telogen Bu-HFSCs by flow cytometry and quantification of percentages of cells in various phases of the cell cycle. “Mid” and “sides” refer to midline and lateral regions of dorsal skin from which cells were analyzed. Data are mean  $\pm$  SEM (n  $\geq$  3 mice). \*\*\*p < 0.001; \*\*\*\*p < 0.0001.
- (D) Colony formation efficiency of *Foxc1*-cKO compared to *Foxc1*<sup>+/-</sup> Het Bu-HFSCs. Left, 2<sup>nd</sup> telogen FACS-purified Bu-HFSCs were cultured *in vitro* for two weeks and allowed to form colonies, which were then fixed and stained with Rhodamine B. Middle, number of colonies formed per 33,000 cells plated. Right, area of each colony. Data are mean  $\pm$  SEM (n  $\geq$  3 mice, triplicates per mouse). \*\*p < 0.01; \*\*\*\*p < 0.0001.
- (E) Whole-mount immunofluorescence of *Nfatc1*-cKO HFAs, showing a one-bulge phenotype. Since NFATC1 loss enhances Bu-HFSC proliferative activity, the one-bulge phenotype suggests that deregulation of quiescence may contribute to premature loss of the old bulge. Scale bar = 100  $\mu$ m.

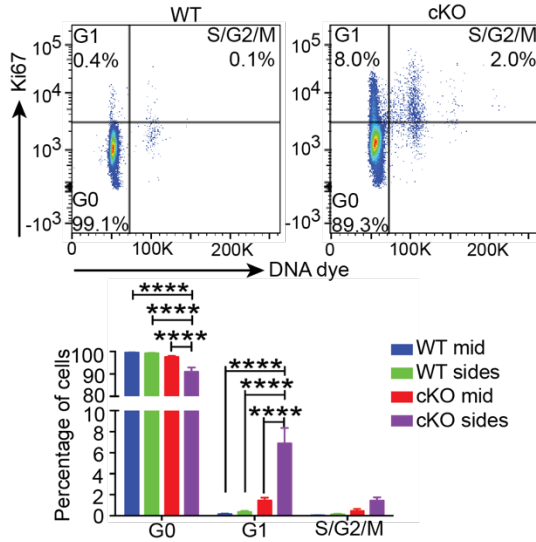
**A** Cell Cycle Gene Expression During Hair Cycle



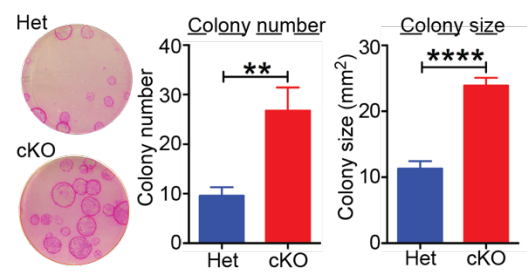
**B** Cell Cycle Profile of Ana Bu-HFSCs



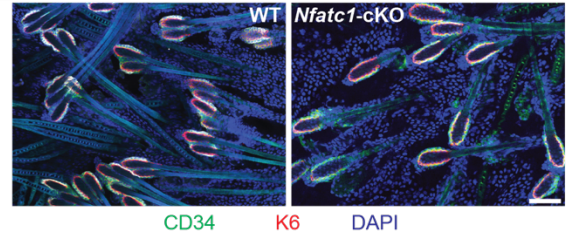
**C** Cell Cycle Profile of 2nd Tel Bu-HFSCs



**D** Colony Formation Efficiency



**E** NFATc1-Deficient HFSCs



### 2.2.8 FOXC1 ensures anchorage of old bulge to prevent its loss during anagen

Before exploring the possible relation between stem cell quiescence and bulge maintenance, I sought to understand how FOXC1 acts to preserve the old bulge. Since the old hairs were lost in anagen (Figures 7C and 8I), I examined the genes that were significantly down-regulated in *Foxc1*-cKO anagen Bu-HFSCs prior to their loss, and found an enrichment of cell-cell and cell-extracellular matrix (ECM) adhesion transcripts, along with those encoding various intermediate filament components (Figure 11).

Hypothesizing adhesion to be the underlying defect causing the bulge loss, I tracked the fate of the old bulge and club hair using keratin 24 (K24). In 1<sup>st</sup> telogen, K24 was expressed specifically by Bu-HFSCs (Figure 12A). In anagen, besides labeling the old Bu-HFSCs, K24 also labeled a region of the newly growing HF that was adjacent to the old bulge, hence marking the site of the future new bulge. Throughout WT anagen, the old bulge resided next to this new bulge site and below the adipophilin-expressing sebaceous gland (Figures 12B and 12D, top panel).

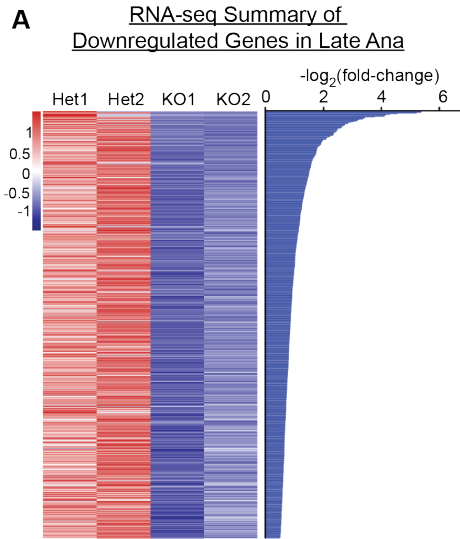
In striking contrast, the *Foxc1*-cKO old bulge became separated from the new bulge site as the emerging new hair moved past it. As anagen progressed, the old bulge was seen above the sebaceous gland and sometimes even near the skin surface, being completely excluded from the new bulge region (Figures 12B and 12D, bottom panel). This process eventually resulted in the one-bulge hair follicle observed in 2<sup>nd</sup> telogen (Figure 12C).

I further observed that this process sometimes left a trail of K24+ cells behind the old bulge, suggesting that HFSCs were being lost along with it (Figure 12D, bottom panel). Indeed, by flow cytometry, *Foxc1*-cKO HFs displayed few if any suprabasal Bu-HFSCs (CD34<sup>Hi</sup>α6<sup>Lo</sup>), and a reduction in the proportion of basal Bu-HFSCs (CD34<sup>Hi</sup>α6<sup>Hi</sup>) (Figure 12E). Additionally, as quantified earlier, *Foxc1*-cKO Bu-HFSC numbers were lower than WT beginning in their 2<sup>nd</sup> telogen (Figure 6C).

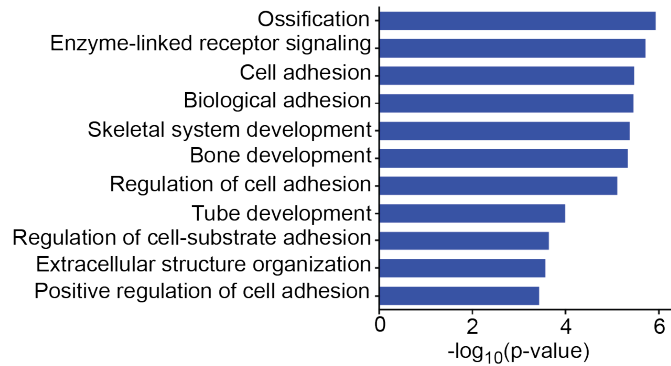
Finally, I performed a “hair-pull test” by applying an adhesive surgical tape and then peeling it off from the hair coat. Indeed, many more hairs came out from *Foxc1*-cKO than WT skin, indicating that *Foxc1*-cKO hairs were plucked out more easily than WT hairs (Figure 12F). Together, these data suggest that FOXC1 functions in part to ensure adequate adhesion of the old bulge to prevent its loss during anagen.

**Figure 11. RNA-seq summary of down-regulated genes in *Foxc1*-cKO Bu-HFSCs.**

- (A) Summary of transcriptional profiling of *Foxc1*-cKO vs. WT Bu-HFSCs in late anagen by RNA-seq. Shown here are significantly down-regulated genes (FPKM > 1,  $p < 0.05$ ,  $q < 0.05$ ).
- (B) Gene ontology (GO)-biological process (BP) term analysis of significantly down-regulated genes in late anagen.
- (C) GO-cellular component (CC) term analysis of significantly down-regulated genes in late anagen.



**B** GO-Biological Process Term Analysis



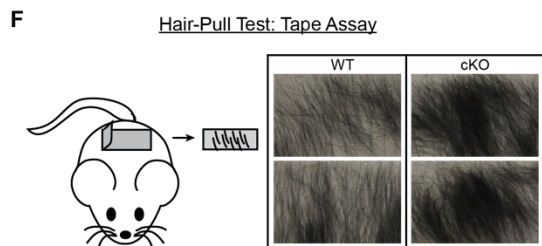
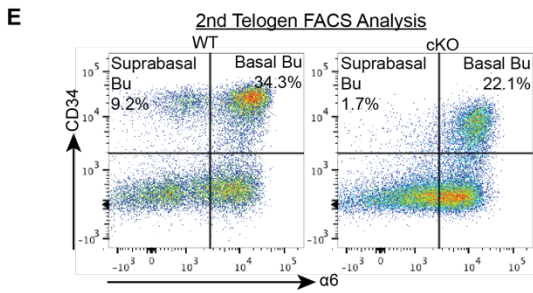
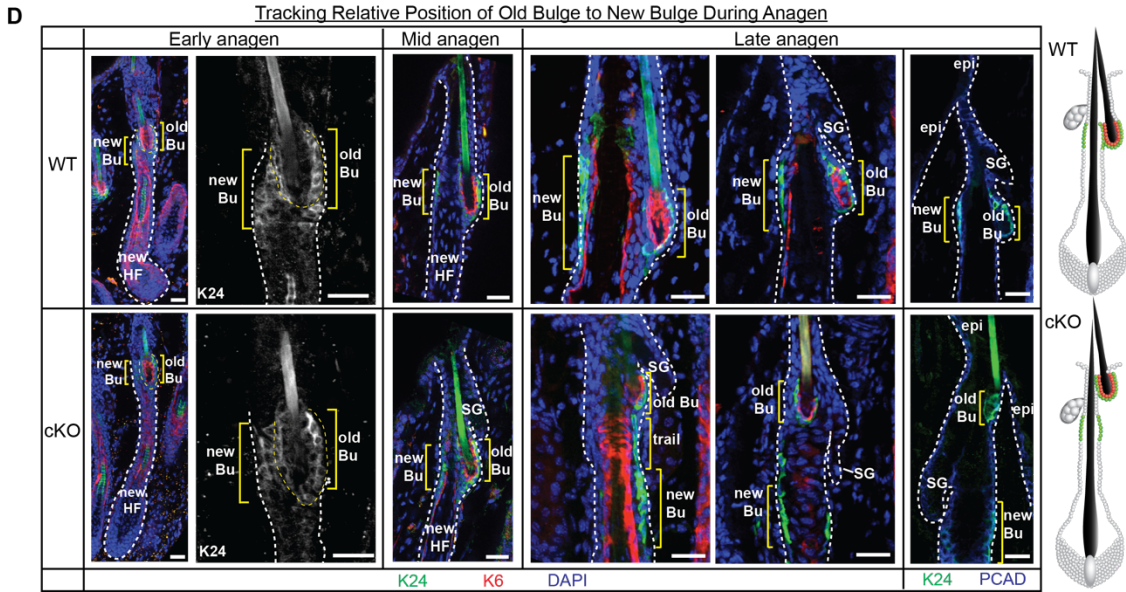
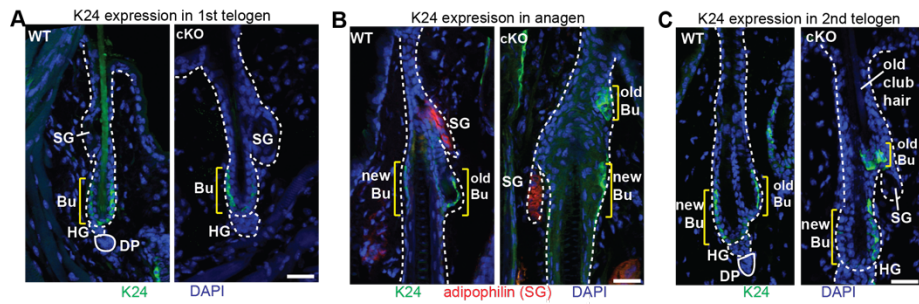
Cell adhesion	<i>Cd34, Npnt, Cd24a, Col6a1, Ctgf, Rhob, Spon2, Cadm1, Col7a1, Thra, Col8a2, Col6a2, Cdon, Egfl6, Antxr1, Fat2, Celsr2, Bcar1, Wnt7b, Pcdh1, Eda, L1cam, Gpmb, Podxl2, Igfals, Frem2, Thbs3, Cadm3, Itga5, Sdk2, Bcl2l11, Tek, Aplp1, Ror2, Nrcam, Sned1, Col20a1, Cadm4, Thbs4, Nell1</i>
---------------	---

**C** GO-Cellular Component Term Analysis

GO-term	P-value	Genes
Extra-cellular matrix	5.51E-14	<i>Ltbp1, Npnt, Adamtsl4, Col3a1, Adamtsl5, Eln, Gpld1, Spock1, Vit, Wnt4, Gpc2, Hmcn1, Col7a1, Ctgf, Smoc1, Gpc6, Col6a3, Tgm2, Col6a2, Col6a1, Spon2, Prss36, Col8a2, Col4a4, Egfl6, Olfml2b, Cilp, Ccdc80, Papln, Mmp15, Mmp14, Ntn1, Mmp11, Prelp, Wnt7b, Clec3b, Frem2, Col1a2, Mfap2, Col1a1, Adam15</i>
Intermediate filament	2.99E-9	<i>Krtap8-1, Krtap7-1, Krtap15, Krt31, Krt35, Krt33a, Krt33b, Krtap13-1, Krt24, Krt73, Krt81, Gm10229, Kt28, Krt36, Krt80, Krtap3-3, Krtap14, Krtap17-1, Krtap1-5, Krt86, Krt83</i>

**Figure 12. FOXC1 functions to anchor the old bulge during hair growth.**

- (A) K24 expression in 1<sup>st</sup> telogen HFs. Note its restriction to the outer layer of bulge, i.e. Bu-HFSCs.
- (B) Position of old bulge relative to new bulge (marked by K24) and sebaceous gland (marked by adipophilin) in anagen HFs.
- (C) K24 expression in 2<sup>nd</sup> telogen HFs. Note the persistence of the old bulge/club hair but its complete exclusion from the new bulge in *Foxc1*-cKO HF.
- (D) Immunofluorescence of sagittal sections of anagen HFs. K24 marks the old-Bu-HFSCs and the new bulge region in newly growing HFs. K6 marks the inner layer of the old bulge and the companion layer of the new HF. PCAD (P-cadherin) marks the relatively undifferentiated progenitors of the HF, including those of the bulge and sebaceous gland (SG). Scale bars = 30  $\mu$ m
- (E) Flow cytometry analysis of dorsal skin epithelial cells in 2<sup>nd</sup> telogen. Depicted are singly dissociated HF cells that were negative for SCA1 (marker of basal epidermis) and positive for CD34 (surface marker of Bu-HFSCs) and  $\alpha$ 6 integrin (surface marker of all basal epithelial cells). Note that *Foxc1*-cKO HFs have only CD34<sup>Hi</sup> basal Bu-HFSCs, but lack the suprabasal-Bu-HFSC population characteristic of the interface between two bulges.
- (F) Tape assay. A surgical tape was affixed to the hair coat, then peeled off to assess amount of hairs that come off with the tape (n = 3 mice).



### 2.2.9 Proliferative Bu-HFSCs display reduced E-cadherin

Since loss of FOXC1 perturbed the transcription of genes encoding cell-ECM adhesion molecules, I FACS-purified Bu-HFSCs and tested their ability to adhere to different ECM components in vitro. Although cell-ECM adhesion defects could still be rooted in matrix production and organization, I did not observe significant differences in the ability of *Foxc1*-cKO and WT Bu-HFSCs to adhere to these various substrata (Figure 13A).

On the other hand, my data presented in Chapter 2.2.7 raised the intriguing possibility of a link between stem cell-intrinsic proliferative behavior and a reduction in intercellular adhesion. These two cellular events often occur concomitantly in different biological contexts, prompting me to address whether the propensity of *Foxc1*-cKO Bu-HFSCs to proliferate might impact their intercellular adhesion.

I first noticed a possible compromise in adhesion between *Foxc1*-cKO Bu-HFSCs in vitro, when I performed immunofluorescence for E-cadherin (ECAD), the central core of adherens junctions, to distinguish between epithelial cells (ECAD-positive) and co-cultured fibroblast feeder cells (ECAD-negative). I frequently observed reduction in ECAD intensity in cultured *Foxc1*-cKO Bu-HFSCs when compared to WT Bu-HFSCs (Figure 13B). When RNA-seq indeed revealed reduced expression of cell adhesion transcripts in the absence of FOXC1 loss (Figure 11), I focused on analyzing ECAD expression as a read-out of cell adhesion in vivo. In WT telogen HFs (Figure 13D, left panel), both basal (inset a)

and suprabasal (inset b) CD34<sup>+</sup> Bu-HFSCs showed intense junctional ECAD immunolabeling, irrespective of whether they were in contact with themselves or with the inner K6<sup>+</sup> layer. However, in *Foxc1*-cKO HFs, junctional ECAD immunolabeling was reduced, especially at sites where Bu-HFSCs contacted each other (Figure 13D, right panel). This was intriguing given that ECAD's gene, *Cdh1*, was not affected transcriptionally by loss of FOXC1 (Figure 13C). Additionally, in contrast to the well-organized bi-layer of compacted cells in WT bulge, *Foxc1*-cKO bulge often consisted of three layers of disorganized and elongated cells (Figure 13D).

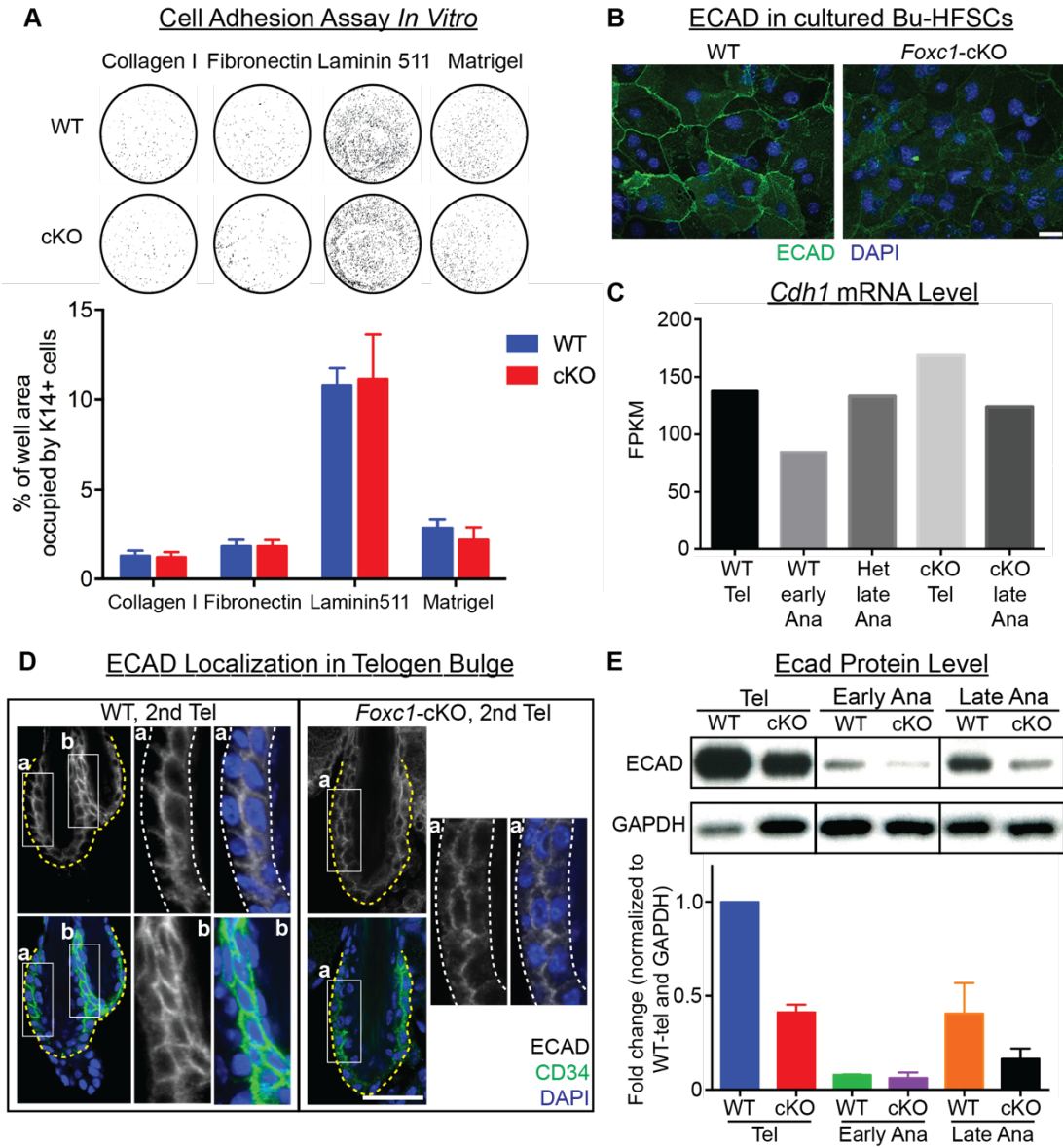
I pursued these tantalizing hints at a relation between cell proliferation and intercellular adhesion by monitoring ECAD protein levels in WT Bu-HFSCs as they underwent the hair cycle (Figure 13E). Interestingly, Bu-HFSCs displayed their highest levels of ECAD when they were quiescent during telogen. Strikingly, they down-regulated ECAD protein levels dramatically as they became proliferative during early anagen. ECAD levels were up-regulated again as Bu-HFSCs returned back to quiescence in late anagen (Figure 13E). In this way, ECAD protein (but not mRNA, Figure 13C) expression inversely correlated with cell cycle gene expression, which was high in early anagen, down-regulated in late anagen, and further reduced in telogen (Figure 10A).

Although *Foxc1*-cKO Bu-HFSCs exhibited similar ECAD expression dynamics, they exhibited lower levels than WT Bu-HFSCs at each stage throughout the hair cycle. This was especially evident in late anagen and telogen (Figure 13E), a feature which corresponded to their atypical persistence in the cell cycle as

revealed by RNA-seq and cell cycle profiling (Figure 10). Taken together, the failure of *Foxc1*-cKO Bu-HFSCs to return to quiescence and up-regulate ECAD promptly in late anagen could generate a mechanically weakened cell-cell adhesion state, which could account for the loss of the old bulge as the newly growing hair pushed pass it.

**Figure 13. Exploring cell-ECM and cell-cell adhesion properties of *Foxc1*-cKO Bu-HFSCs.**

- (A) *In vitro* cell adhesion assay. Top, FACS-purified WT and *Foxc1*-cKO Bu-HFSCs were plated on collagen I, fibronectin, laminin-511 or matrigel-coated polyethylene-glycol 24-well culture plates in equal numbers in triplicates (n=2 mice). After 1 hr, non-adherent cells were washed away and adherent cells were fixed, permeabilized and stained for keratin-14 (K14). Odyssey infrared scanner was used to visualize K14+ cells, which are depicted here as individual greyscale dots within each well (see Materials and Methods). Bottom, total area of individual adherent cells covering each well was calculated using Image J and presented as percentage of total well area.
- (B) Immunofluorescence of cultured Bu-HFSCs *in vitro*. Note the localization of ECAD at WT cell-cell junctions but reduced ECAD intensity at *Foxc1*-cKO cell borders. Scale bar = 30  $\mu$ m.
- (C) *Cdh1* transcript level from RNA-seq. FPKM, fragments per kilobase of transcript per million mapped reads.
- (D) Immunofluorescence of 2<sup>nd</sup> telogen HFs to analyze ECAD localization. Inset (a) zooms in on basal-Bu-HFSC layer in both WT and *Foxc1*-cKO; note that the compacted, organized bilayer of cells, characteristic of the WT bulge, is disorganized and displays extraneous cells in the *Foxc1*-cKO bulge. Inset (b) zooms in on suprabasal-Bu-HFSC layer in WT. Scale bar = 30  $\mu$ m.
- (E)
- (F) Immunoblotting of FACS-purified Bu-HFSCs illustrates dynamic changes in ECAD levels during the hair cycle. Quantifications are mean  $\pm$  SEM of  $\geq$  3 independent replicates normalized to WT using GAPDH as loading control. Note that FOXC1 loss reduces overall ECAD levels but does not alter their dynamics during the hair cycle.



### 2.2.10 Direct perturbation to cell-cell adhesion is sufficient for bulge loss

Finally, to functionally test if reduction in ECAD was sufficient to cause the bulge loss in *Foxc1*-cKO hair follicles, I conditionally ablated *Cdh1*. Since *Cdh1<sup>fl/fl</sup>* x *K14Cre* mice exhibit early aberrations in hair follicles (Tinkle et al., 2004), I used *Sox9CreER* to efficiently induce *Cdh1* ablation in 2<sup>nd</sup> telogen hair follicles (Figure 14A). At this time, some hair follicles had begun to display a disorganized bulge with three cell layers (Figure 14A), similar to that frequently observed in *Foxc1*-cKO hair follicles (Figure 13D). I then allowed hair follicles to progress from 2<sup>nd</sup> telogen → 2<sup>nd</sup> anagen → 3<sup>rd</sup> telogen.

I checked for timing of 2<sup>nd</sup> anagen entry. Unlike FOXC1 loss mediated by the same *Sox9CreER* (Figure 8H), ECAD loss did not result in precocious anagen, suggesting its putative role downstream of Bu-HFSC proliferation. However, like *Foxc1*-cKO HFs (Figure 12D), as *Cdh1*-cKO HFs were undergoing their 2<sup>nd</sup> anagen, their bulge was mis-localized relative to the newly specified bulge region (Figure 14B). Moreover, as the old bulge moved upward, some K24+ cells moved with it and were excluded from the new bulge region, while others were left behind ectopically (Figure 14B, arrow).

Subsequently by 3<sup>rd</sup> telogen, like *Foxc1*-cKO hair follicles (Figures 6A, 6B and 8I), most *Cdh1*-cKO hair follicles displayed single bulges (Figure 14C). Overall, with the exception of the precocious entry into the hair cycle, the bulge loss phenotype seen with depletion of ECAD bore resemblance to that of *Foxc1*-cKO hair follicles.

Consistent with the fact that *Foxc1*-cKO Bu-HFSCs displayed only reduced and not silenced ECAD, the full *Cdh1* ablation in hair follicles resulted in a more severe phenotype, evident in their single bulge displaying a highly aberrant structure (Figure 14C). Based upon these collective data, I conclude that the loss of the old bulge in *Foxc1*-cKO hair follicles was predicated upon enhanced proliferative activity of Bu-HFSCs, coupled with reduced ECAD.

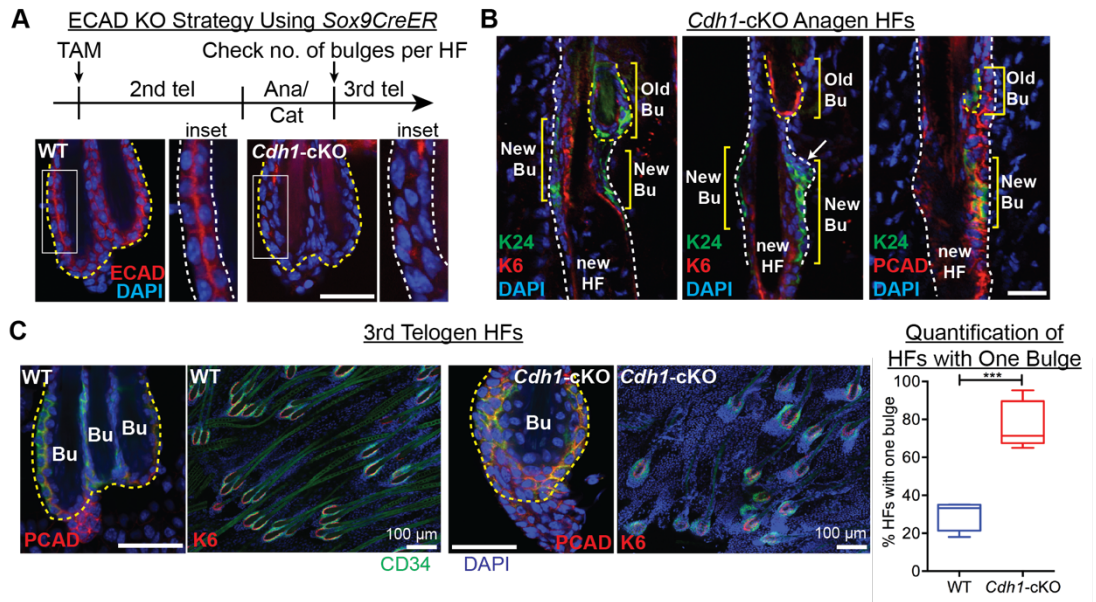


**Figure 14. Reducing intercellular junctions between HFSCs contributes to the loss of the old bulge during new hair growth.**

- (A) Strategy to ablate *Cdh1* gene expression in skin HFSCs by using *Sox9-CreER* mice. Immunofluorescence images depict loss of ECAD after tamoxifen treatment and appearance of disorganized cells within the bulge, compared with WT.
- (B) Immunofluorescence of sagittal sections of *Cdh1*-cKO anagen HFSCs depicting the position of the old bulge relative to the newly specified bulge. Arrow points to a trail of K24+ cells, left behind as the old bulge moved upwards.
- (C) Immunofluorescence of WT and *Cdh1*-cKO 3<sup>rd</sup> telogen HFSCs. Quantifications show that most *Cdh1*-cKO HFSCs had only one bulge by their 3<sup>rd</sup> telogen. Box-and-whisker plot: midline, median; box, 25<sup>th</sup> and 75<sup>th</sup> percentiles; whiskers, minimum and maximum ( $n \geq 4$  mice,  $\geq 80$  HFSCs per mouse). \*\*\* $p < 0.001$ . Scale bars = 30  $\mu$ m unless indicated otherwise.

## **2.3 Discussion**

### **2.3.1 Summary of results**

The ability to make tissue(s) is a necessary feature of all stem cells, regardless of differences in the dynamics of tissue regeneration. In vitro, many tissue stem cells, including epidermal and HFSCs, can be passaged long-term without loss of their tissue regenerating capability (Green, 1991; Huch et al., 2013; Jones et al., 1995; Sato and Clevers, 2015; Sato et al., 2009). In vivo, stem cell markers can lineage-trace progeny that survive in tissues long-term (Barker et al., 2007; Samokhvalov et al., 2007), although a recent detailed study of hematopoietic stem cells (HSCs) self-renewal suggests that adult homeostasis may be sustained by multiple short-term stem cells that receive rare input from polyclonal long-term HSCs (Busch et al., 2015; Sun et al., 2014). In all of these cases, the outcome is long-term ability to regenerate the tissue.

Less is clear about the multiple facets which are required to balance stem cell usage within the native tissue. Mice lacking FOXC1 in their hair coat allowed me to explore this captivating issue. In dissecting their complex phenotype that arises by the loss of a single transcription factor, I unearthed a variety of ways in which HFSCs interact with their environment to govern their proliferation and conserve their tissue regenerating potential. Specifically, I found that FOXC1 loss in hair follicles causes the following: 1) Bu-HFSCs become primed to proliferate, as evidenced by their cell cycle status, earlier response to an activating stimulus in

vivo, and increased colony forming efficiency in vitro; 2) Bu-HFSCs express lower ECAD levels in part due to their proliferative nature; 3) hair follicles lose their old bulge as a result of the compromised cell-cell adhesion, and fail to expand their stem cell numbers and thicken the animal's hair coat; 4) hair follicles consequently accelerate their hair cycling; 5) when aged, hair follicles fail to maintain Bu-HFSC numbers and regenerate new hairs promptly, leading to a markedly sparse hair coat.

### **2.3.2 Two is better than one: the role of the older bulge**

My work has established an importance for the unique property of mouse pelage hair follicles to preserve their older bulge(s). Following embryonic and early postnatal morphogenesis, both WT and *Foxc1*-cKO adult P19 hair follicles exist in 1<sup>st</sup> telogen as a single bulge anchoring a single club hair. 1<sup>st</sup> telogen typically lasts only 2 to 3 days, because shortly after, HFSCs proliferate in anagen to make a new hair and new bulge. However, unlike WT hair follicles which will retain the older bulge(s) as they undergo more rounds of regeneration, *Foxc1*-cKO hair follicles always lose their prior bulge whenever they make a new one, and thus never advance past their initial starting point of having only one bulge. A critical repercussion is the loss of local inhibitory factors emanating from both K6+ inner bulge (Hsu et al., 2011) and suprabasal Bu-HFSCs that normally form the interface between two bulges (Blanpain et al., 2004). This becomes manifest in the failure of either FOXC1-deficient Bu-HFSCs, or WT Bu-HFSCs in a one-bulge

environment, to stay in prolonged quiescence. Moreover, although ablation of *Foxc1* in a two-bulge hair follicle did shorten the stem cell quiescence period, indicative of an intrinsic defect, the presence of the second bulge nevertheless delayed the precocious anagen entry of the active bulge as compared to that seen in *Foxc1*-cKO one-bulge hair follicles.

These findings are relevant in light of other hair follicles such as rodent whiskers, which do not accumulate multiple bulges and, like *Foxc1*-cKO pelage hair follicles, also exhibit shorter telogen durations, as evident in the appearance of a new whisker shortly after (~1 week) the old whisker has stopped growing in length. Similar to the old club hair and bulge loss observed in *Foxc1*-cKO anagen hair follicles, the old whisker also falls off when the new whisker is still growing. Intriguingly, the whisker could undergo 7 growth cycles within the first 8 months, resembling *Foxc1*-cKO hair follicles that could undergo up to 6 hair cycles within the first 9 months of age (Figure 4E) (Ibrahim and Wright, 1975).

Overall, my results provide compelling evidence that prior bulges participate in regulating HFSC quiescence and hair cycling. Indeed, excessive tissue regeneration and stem cell expenditure have no favorable outcome in FOXC1-deficient mice, as their hair coat remains thin. My findings suggest that furry mammals have acquired a means to generate new bulges and preserve the older ones in order to maintain tissue regenerative potential for the lifetime of the animal.

It has been demonstrated that HFSCs that have undergone fewer divisions are set aside in the old bulge to participate in wound healing, while those with more divisions are recycled into the new bulge and tasked with homeostatic hair

regeneration (Hsu et al., 2011). A WT hair follicle almost never accommodates more than four bulges. What happens to the older bulges is still unknown. An intriguing idea is that once a bulge sheds its old hair, its HFSCs with their low division history fold into the newer bulge(s) and “rejuvenate” the HFSC pool to improve its efficiency in hair cycling and wound repair.

### **2.3.3 A distinct hair loss mechanism**

Intercellular adhesion defects are also at the root of another mouse mutant that fails to maintain its hair coat, namely mice lacking the desmosomal glycoprotein, desmoglein 3 (DSG3) (Koch et al., 1998). That said, the mechanism of bulge and club hair loss by *Foxc1*-cKO hair follicles seems to be distinct from *Dsg3*-KO mice, which lose their entire hair coat during telogen, and hence undergo cyclical balding. By contrast, *Foxc1*-cKO mice lose only their old club hairs (and not the newly generated hair) during anagen, and thus continuously display a new hair coat layer. Moreover, the adhesive defect in *Dsg3*-KO hair follicles was attributed to reduced adhesion between the two bulge layers, while that in *Foxc1*-cKO hair follicles appears to involve inter-HFSC adhesion, resulting in a failure to retain the old bulge HFSCs.

The hair loss process that is thought to occur naturally is termed exogen, in which the club hair is shed from the hair follicle. Because it happens infrequently in WT pelage hair follicles, multiple bulges accumulate. When it does happen, it largely coincides with anagen (Higgins et al., 2009; Milner et al., 2002).

Interestingly, *Foxc1*-cKO hair follicles also lose their club hairs in late anagen. However, while exogen is thought to involve the proteolytic shedding of the club hair from the bulge *in situ* without loss of Bu-HFSCs, due to the balance between proteases and protease inhibitors tipping in favor of the former (Higgins et al., 2009), *Foxc1*-cKO hair follicles appear to lose their old bulge (K24<sup>+</sup> HFSCs, K6<sup>+</sup> inner cells, and club hair) in its entirety. Expression of the transcripts encoding these proteases and protease inhibitors that influence exogen was also not changed in *Foxc1*-cKO Bu-HFSCs. Additionally, *Foxc1*-cKO bulge loss appears to take place only when subjected to a stimulus, which in the hair cycle is the mechanical force imposed by the newly growing hair during anagen. By contrast, during telogen, the single bulge remains in position. As more is learned about the normal process of exogen, the extent to which *Foxc1*-cKO mice might serve as a model of premature exogen should become more apparent.

#### **2.3.4 An aged phenotype not normally observed in WT**

Mouse pelage hair follicles employ multiple strategies to keep their stem cells quiescent and restrict the number of hair cycles to only what is necessary to maintain a full hair coat. As such, the hair coats of aged and young mice are usually quite similar in appearance. However, when mice are forced by repeated depilation to undergo excessive hair cycling, their hair coat greys, suggesting a deleterious impact on melanocyte stem cells which are activated along with Bu-HFSCs during regeneration (Endou et al., 2014). In this regard, it is interesting that the *Foxc1*-

cKO hair coat also greyed as mice aged. Since *Foxc1* ablation was restricted to the epithelium, its effects on melanocytes appeared to be a secondary consequence. While future studies will be needed to dissect the precise mechanisms, the hair greying could reflect over-usage of melanocyte stem cells during the more frequent hair cycling, a failure of a smaller bulge to accommodate sufficient melanocyte stem cells, or defective crosstalk between FOXC1-deficient HFSCs and WT melanocyte stem cells.

In the context of hematopoietic SCs (HSCs), their “exhaustion” is typically determined by their decline in ability to reconstitute the entire hematopoietic system when subjected to serial transplantation. It has been suggested that the less proliferative HSCs from aged mice of longer-lived strains reconstitute the blood more efficiently than the more proliferative HSCs from aged mice of shorter-lived strains, suggesting a more rapid functional exhaustion in the latter (Orford and Scadden, 2008). Here, I propose a highly analogous case of HFSC exhaustion, in which FOXC1-deficient Bu-HFSCs are able to cope with tissue maintenance in young mice but, having undergone more rounds of cell division and tissue regeneration than WT, find themselves impaired in their ability to maintain their numbers and make new hairs promptly in aged mice. This is especially intriguing given that hair follicles naturally set aside stem cells that have divided more frequently for new rounds of hair production (Hsu et al., 2011), and FOXC1 loss further expends their activity.

### 2.3.5 Intercellular adhesion, E-cadherin and stem cell biology

ECAD serves important functions in the *Drosophila* germline stem cells (GSCs). In the testis, ECAD orientates the centrosome and spindle of GSCs in mediating their adhesion to their niche hub cells (Inaba et al., 2010). In the ovary, GSCs adhere to their niche cap cells via ECAD, whose loss results in their departure from their niche (Song et al., 2002). As such, ECAD mediates the competition of female GSCs for niche occupancy, whereby only WT GSCs with higher ECAD expression stay adhered to the cap cells. This potentially acts as a quality control mechanism to keep only the functional and less differentiated GSCs within their niche (Jin et al., 2008).

In the hair follicle bulge, HFSCs also adhere to their niche K6+ cells via ECAD, as evidenced by high ECAD expression between these two cell layers. Additionally, the adherence of Bu-HFSCs to one another is also mediated at least in part by ECAD (Figure 12B). My results indicated that when ECAD-mediated cell adhesion was perturbed, either by reducing ECAD protein levels (as in *Foxc1*-cKO hair follicles) or by completely ablating ECAD expression (as in *Cdh1*-cKO hair follicles), bulge integrity became perturbed 1) within the bulge, in which the usually well-compacted bilayer of bulge cells became disorganized, sometimes having extraneous cells present in between the two cell layers; and 2) between two bulges, in which the adhesion of the older bulge to the newly forming bulge became compromised, consequently resulting in its complete loss in every hair cycle.

The timing of bulge loss in anagen suggests that the reduction of ECAD leads to a weakening of intercellular connections within the bulge that are necessary to withstand the mechanical pressures of hair protrusion. In this regard, it is notable that adherens junctions are needed to organize actin-myosin based filament networks across skin epithelial cells and are also important in sensing and activating tension-based signaling (Schlegelmilch et al., 2011; Silvis et al., 2011; Vasioukhin et al., 2000). Although the precise mechanisms involved in bulge retention remain to be elucidated and could involve more than ECAD, these relations provide a plausible working model for how loss of FOXC1 might be linked functionally to the reduced threshold in withstanding the mechanical tension necessary to anchor the reserve SC pool throughout subsequent hair cycles.

My studies suggest that the proliferative nature of *Foxc1*-cKO Bu-HFSCs can partly account for their reduced ECAD protein levels. Thus, as evidenced in WT Bu-HFSCs, ECAD levels inversely correlated with cell cycle status throughout the periodic bouts of tissue regeneration. FOXC1 plays a critical role to re-establish Bu-HFSC quiescence and restore levels of adhesion proteins, including ECAD. In its absence, cells remain proliferative while cell adhesion gene expression and ECAD levels remain low, ultimately causing the loss of the bulge and its associated consequences.

As for *Cdh1*-cKO bulge, while ECAD expression was completely abolished, there was detectable up-regulation of P-cadherin (PCAD) expression, consistent with previous reports (Figure 13C; Tinkle et al., 2007). PCAD could be partially compensating for ECAD loss by maintaining adhesion of Bu-HFSCs to their K6+

niche cells, but it could not rescue the loss of the old bulge. Notably, its organizational defects became more apparent after completing one round of hair cycle, whereby multiple Bu-HFSC layers were more obviously detected. This could be due to retention of cells left behind by the old bulge that got lost in the prior hair cycle, or due to defects in making the new bulge. It would be interesting to address these issues and improve our understanding of how adhesion molecules function to enable SCs to take up residence in and organize themselves within their niche.

## 2.4 Materials and Methods

### ***Mice and procedures***

*Foxc1<sup>flox</sup>* mice were obtained from Dr. Tsutomu Kume (Sasman et al., 2012). *K14-Cre*, *Sox9-CreER*, *Nfatc1<sup>flox</sup>*, *Cdh1<sup>flox</sup>* and *Rosa26<sup>Flox-Stop-Flox-YFP</sup>* were described previously (Aliprantis et al., 2008; Boussadia et al., 2002; Mao et al., 1999; Soeda et al., 2010a; Vasioukhin et al., 1999). *Sox9-CreER* was activated by intraperitoneal (i.p.) injection of tamoxifen (75 µg/g body weight, in corn oil) once a day for 2-3 days. 5-bromo-2'-deoxyuridine (BrdU, Sigma, 25 µg/g body weight) or 5-ethynyl-2'-deoxyuridine (EdU, Thermo Fisher Scientific, 25 µg/g body weight) was injected intra-peritoneal (i.p.) into mice twice a day before putting mice under anesthesia to obtain a skin biopsy or before lethal administration of CO<sub>2</sub>. For depilation experiments, molten wax was applied onto the hair coats of anesthetized mice and peeled off after hardening. For the tape assay to analyze hair adhesion, a narrow strip of cloth surgical tape of fixed length was attached onto hairs of anesthetized mice and peeled off. For hair dye experiment, hairs of anesthetized mice were dyed using a glow-in-the-dark red hair color cream for 30-40 min before rinsing dye off under warm water. Dyed hair coats were visualized by fluorescence under Leica dissection scope. All animals were maintained in an animal facility approved by The Association for Assessment and Accreditation of Laboratory Animal Care (AAALAC), and procedures were performed with protocols approved by Rockefeller University's institutional animal care and use committee (IACUC) members and staff.

### ***Hair Cycle Analysis***

HFs were staged based on Muller-Rover et al. (Muller-Rover et al., 2001). To track hair cycles, full-length telogen hairs were trimmed with electric clippers to reveal back skin. HF entry into anagen was determined by darkening of skin and reappearance of hair. Completion of anagen and catagen and re-entry into telogen were determined by appearance of full-length hairs and loss of pigmentation in skin. Hairs were trimmed again to observe entry into next anagen. Mice were checked in this way twice a week for long-term monitoring of hair cycle status. Progression of first and second hair cycles in Black Swiss and C57BL/6J strains were verified to be largely similar. *Foxc1<sup>flox</sup>* (Black Swiss) X *K14-Cre* (CD1) mice were back-crossed for  $\geq 4$  generations to pure Black Swiss mice to achieve a background strain of  $> 90\%$  Black Swiss. *Foxc1<sup>flox</sup>* (Black Swiss) X *Sox9CreER* ; *R26-YFP* (C57BL/6J) mice were of mixed background. *Cdh1<sup>flox</sup>* (C57BL/6J) X *Sox9CreER* ; *R26-YFP* mice were of C57BL/6J strain. Hair cycle phenotypes were consistently observed in both genders of mice.

### ***Antibodies***

The following antibodies and dilutions were used: FOXC1 (guinea pig, 1:1000, Fuchs Lab), P-cadherin (goat, 1:200, R&D), CD34 (rat, 1:100, eBioscience), LHX2 (rabbit, 1:2000, Fuchs Lab), SOX9 (rabbit, 1:1000, Fuchs Lab), NFATc1 (mouse, 1:100, Santa Cruz), TCF4 (rabbit, 1:250, Cell Signaling), BrdU (rat, 1:100, Abcam), K6 (guinea pig, 1:2000, Fuchs Lab), K24 (rabbit, 1:5000, Fuchs Lab), K14 (rabbit,

1:500, Fuchs Lab), E-cadherin (rabbit, 1:5000, Cell Signaling), glyceraldehyde phosphate dehydrogenase (GAPDH, mouse, 1:2500, Abcam). Nuclei were stained with 4'6'-diamidino-2-phenylindole (DAPI). EdU click-iT reaction was performed according to manufacturer's directions (Thermo Fisher).

### ***FOXC1 antibody construction***

The coding region that encodes the last 200 amino acids of FOXC1 was cloned into pGEX-4T1 vector (GE Healthcare). BL21 *Escherichia coli* cells were transformed with the construct and induced to express the GST-tagged FOXC1 protein fragment by isopropyl  $\beta$ -D-1-thiogalactopyranoside (IPTG). Bacterial cultures were lysed with bacterial protein extraction reagent (B-PER, Pierce) then sonicated and centrifuged. Agarose-glutathione beads were added to the supernatant to allow binding of GST-tagged protein overnight. Beads were washed on cellulose acetate filter spin cups (Pierce). Glutathione solution was used to elute the GST-tagged protein. The eluted protein was purified on a 4-12% Bis-Tris polyacrylamide gel and excised. The purified protein was introduced as an antigen into guinea pigs to generate FOXC1 polyclonal antibody (Covance). Bleeds from guinea pigs were obtained every 3 weeks and tested, with the 8<sup>th</sup> bleed starting to reveal strong and specific FOXC1 signal.

### ***Histology and Immunofluorescence***

To prepare sagittal skin sections for immunofluorescence microscopy, backskins were embedded in OCT, frozen and cryosectioned (20  $\mu$ m). Sections were fixed

for 10 min in 4% paraformaldehyde (hereby termed PFA) in phosphate-buffered saline (hereby termed PBS) at room temperature (hereby termed RT) and permeabilized for 20 min in PBS + 0.3% Triton (hereby termed PBST). To prepare whole-mounts for immunofluorescence microscopy, adipose tissue was scraped from backskins, which were then incubated (dermis side down) on 2.5 U/ml dispase + 20 mM EDTA for 2 hr at 37°C. Epidermis and hair follicles were separated from dermis, fixed in 4% PFA for 30 min at RT and permeabilized for 30 min in 0.5% PBST. Sections and whole-mounts were blocked for 1-2 hr at RT in 2% fish gelatin, 5% normal donkey serum, 1% BSA, 0.2% - 0.3% Triton in PBS. Primary antibodies (Abs) were incubated overnight at 4°C and secondary Abs conjugated to Alexa 488, 546 or 647 were incubated for 1-2 hr at RT. Mouse antibodies were incubated with M.O.M. block (Vector Laboratories) according to manufacturer's directions. Images were acquired with Zeiss Axio Observer Z1 equipped with ApoTome.2 through a 20x air objective or Zeiss LSM780 laser-scanning confocal microscope through a 40x water objective.

### ***Immunohistochemistry***

Backskins were fixed in 4% PFA at 4°C overnight, washed twice with PBS at RT, dehydrated through an ethanol series (50%, 70%, 80%, 95%, 100%) and citrus clearing solvent, and incubated in molten paraffin at 37°C overnight. Backskins were then embedded in paraffin and 8 µm sections were cut using a microtome. De-paraffinization and rehydration of sections was performed through a series of citrus clearing solvent and ethanol (100%, 95%, 70%, 50%). Sections were then

washed in PBS before undergoing antigen retrieval, which was performed in 0.01 M sodium citrate, pH 6.0, in a pressure cooker. Endogenous peroxidase activity was quenched with 0.3% hydrogen peroxide in PBS for 30 minutes at RT. Blocking and incubation of primary and secondary antibodies were done as per immunofluorescence procedure (see above). Primary antibody used was FOXC1 (goat, 1:500, Abcam). ImmPRESS horseradish peroxidase (HRP) anti-goat IgG polymer (Vector Laboratories) and 3,3-diaminobenzidine (DAB) peroxidase substrate kit (Vector Laboratories) were used to detect FOXC1. Sections were mounted with cyto seal (Richard-Allan Scientific) and imaged on Zeiss Axioskop 2 through a 20x objective lens.

### ***Fluorescence-activated cell sorting (FACS)***

To prepare single cell suspensions from telogen backskin, subcutaneous fat was scraped off with a scalpel and backskin was placed (dermis side down) on 0.25% trypsin-EDTA (Gibco) at 37°C for 35-45 min. To prepare single cell suspensions from anagen backskin, backskin was placed (dermis side down) on 2.5 mg/ml collagenase (Sigma) in Hank's balanced salt solution (HBSS, Gibco) at 37°C for 45 min, dermal side was scraped off with a scalpel, and remaining epidermal side was transferred to trypsin at 37°C for 20 min. To obtain single epithelial cell suspensions, hair follicles and epidermal cells were scraped off gently from all trypsinized backskins with a scalpel and filtered with strainers (70 µm, followed by 40 µm). Dissociated cells were re-suspended in 4% chelated fetal bovine serum (FBS) in PBS (vol/vol) and incubated with the appropriate antibodies for 20 min at

4°C. For cell cycle profiling, dissociated cells were fixed with 4% PFA for 30 min at RT and permeabilized with 0.1% PBST for 20-25 min at RT prior to antibody incubation for 20 min at RT. The following antibodies were used: CD34-eFluor660 (1:100, eBioscience), α6-PE (1:100, BD Biosciences), Sca1-Percp-Cy5.5 (1:1000, eBioscience), Ki67-Pe-Cy7 (1:400, eBioscience). DAPI was used to exclude dead cells. FxCycle violet stain (Invitrogen) was used to analyze DNA content. Cell purification was performed on FACS Aria sorters equipped with Diva software (BD Biosciences). FACS analyses were performed using LSRII FACS Analyzers and then analyzed using FlowJo program.

### ***Cell Culture***

FACS-purified HFSCs were plated in equal numbers, in triplicates, onto mitomycin C-treated 3T3-J2 dermal fibroblasts in E-media supplemented with 15% (vol/vol) serum and 0.3 mM calcium. For colony forming efficiency assay, cells were cultured for 14 days, then fixed and stained with 1% (wt/vol) Rhodamine B (Sigma). Colony diameter and colony number were quantified using scanned images of culture plates in Image J. For cell adhesion assay, FACS-purified HFSCs were plated in equal numbers, in triplicates, onto polyethylene-glycol 24-well culture plates coated with matrigel (BD Biosciences), collagen I (BD Biosciences), fibronectin (Millipore) or laminin 511 (BioLamina). After 1 hr, non-adherent cells were washed off and adherent cells were fixed with 4% PFA for 10 min at RT and permeabilized with 0.3% PBST. Cells were incubated with antibody against keratin 14 (K14) overnight at 4°C and with Odyssey secondary antibody for 1 hr at RT.

Imaging was performed on an Odyssey infrared scanner (LI-COR). Quantification of well area occupied by K14+ adherent cells was performed using Image J.

### ***RNA purification, RNA-Seq and qRT-PCR***

Total RNA was purified from FACS-purified cells by directly sorting cells in Trizol LS (Sigma), followed by extraction using Direct-Zol RNA mini-prep kit (Zymo Research). RNA quality was determined using an Agilent 2100 Bioanalyzer and all samples sequenced had RNA integrity numbers >8. mRNA library preparation using Illumina TrueSeq mRNA sample preparation kit and single-end sequencing on Illumina HiSeq 2000 were performed at Weill Cornell Medical College Genomic Core Facility (New York). Alignment of reads was done using Tophat with the mm9 build of the mouse genome. Transcript assembly and differential expression were performed using Cufflinks with Refseq mRNAs to guide assembly (Trapnell et al., 2012). Differentially expressed genes were used in GO term analysis to find enriched functional annotations using DAVID (Huang da et al., 2009a, b). All RNA-seq datasets have been deposited in the Gene Expression Omnibus (GEO) database, with accession no. GSE77256. For real-time qRT-PCR, equivalent amounts of RNA were reverse-transcribed using Superscript III (Thermo Fisher). cDNAs were normalized to equal amounts using primers against *Ppib2*. qRT-PCR was performed with SYBR green PCR Master Mix (Sigma) on an Applied Biosystems 7900HT Fast Real-Time PCR system.

### ***Immunoblotting***

FACS-purified Bu-HFSC protein lysates were prepared using RIPA buffer. Gel electrophoresis was performed using 4% - 12% NuPAGE Bis-Tris gradient gels (Thermo Fisher) and transferred to nitrocellulose membranes (Amersham). Membranes were blocked in 5% milk in PBS containing 0.1% Tween 20 (PBSTw) for 1 hr at RT, incubated with primary antibodies overnight at 4°C and with secondary antibodies conjugated with HRP for 1 hr at RT. HRP was detected using ECL (Amersham).

### ***Scanning electron microscopy***

Samples were fixed in 2% glutaraldehyde, 4% PFA and 2 mM CaCl<sub>2</sub> in 0.05 M sodium cacodylate buffer, pH 7.2, at RT for > 1 hr, dehydrated, critical-point dried, mounted, and sputter coated with gold palladium. Scanning electron microscopy images were obtained using a field emission scanning electron microscope (model 1550; LEO Electron Microscopy, Inc.).

### ***Statistical Analysis***

Data were analyzed and statistics were performed using unpaired two-tailed Student's t test and ANOVA (Prism5 GraphPad). Significant differences between two groups were noted by asterisks (\*:p<0.05; \*\*:p<0.01; \*\*\*:p<0.001; \*\*\*\*:p<0.0001).

## CHAPTER 3: STEM CELL ADHESION AND ACTIVITY

### 3.1 Introduction

#### 3.1.1 Comparing *Foxc1*-cKO and *Cdh1*-cKO hair follicles

The proliferative propensity of *Foxc1*-cKO Bu-HFSCs and the associated reduction in adhesion protein levels led me to uncover the dynamic changes in E-cadherin (ECAD) expression that normally occur in Bu-HFSCs as they switch between quiescence and activation during the hair cycle. Re-establishment of the quiescent state and a concomitant increase in ECAD are critical to preventing the loss of older bulges and hairs as new ones are being made.

Although both *Foxc1*-cKO and *Cdh1*-cKO hair follicles displayed perturbations in their bulge architecture and failed to maintain the old bulge during anagen, they also exhibited differences in their phenotypes. First, the bulge structure was more perturbed in *Cdh1*-cKO wherein ECAD was completely ablated, as opposed to the subtler changes observed in *Foxc1*-cKO in which ECAD was still present at reduced levels. Second, while *Foxc1*-cKO hair follicles entered anagen precociously, *Cdh1*-cKO hair follicles were not observed to have such a hair cycle entry phenotype.

Since compromised cell adhesion seems to occur downstream of the inability of *Foxc1*-cKO Bu-HFSCs to maintain an extended quiescence, and it can indirectly accelerate *Foxc1*-cKO Bu-HFSC re-entry into a proliferative state via causing

bulge loss, I next asked if perturbing cell adhesion is sufficient to directly cause Bu-HFSCs to exit quiescence prematurely. Given my initial findings in *Cdh1*-cKO hair follicles, I wondered how ECAD loss causes such dramatic changes in the stem cell niche architecture. If loss of cell-cell adhesion does influence cell proliferation, why do ECAD-deficient hair follicles not cycle prematurely like FOXC1-deficient hair follicles do? If it does not influence cell proliferation, does the perturbation of the stem cell niche influence the timing of hair regeneration?

### **3.1.2 Cell-ECM and cell-cell adhesion**

Cellular adhesion is paramount to maintaining tissue integrity. Both cell-ECM and cell-cell interactions enable cells to form contiguous physical and communication networks with their surroundings, and integrate signaling pathways to influence their shape, motility, polarity, proliferation and differentiation, both during homeostasis and in response to changes in their environment. In the skin, basal cells express adhesion receptors known as integrins, which are  $\alpha\beta$  heterodimers that bind various ECM proteins including collagen, laminin and fibronectin. Integrins connect skin epithelial cells to their ECM via two molecular complexes: a) hemidesmosomes, which link the keratin intermediate filaments to the ECM, and b) focal adhesions, which connect their actin cytoskeleton to the ECM (Barczyk et al., 2010; Winograd-Katz et al., 2014).

On the other hand, cells adhere to each other via four major junctions. Gap junctions facilitate the exchange of small molecules and electrolytes between cells,

while tight junctions, adherens junctions and desmosomes, arranged in this order from apical side to basal side of cells, form the junctional complex. Tight junctions seal neighboring cells and allow paracellular diffusion of ions and solutes between cells, while adherens junctions and desmosomes link up the actin and intermediate filament components of the cytoskeleton of connected cells respectively (Nekrasova and Green, 2013; Zihni et al., 2016).

### **3.1.3 Adherens junctions and loss-of-function studies**

The adherens junction is a calcium-dependent adhesion complex that consists of three distinct components: transmembrane cadherins, armadillo family members and cytoskeletal adapter proteins. In the skin, the main cadherins expressed are the classical cadherins E-cadherin (ECAD) and P-cadherin (PCAD). The extracellular portion of ECAD and PCAD is composed of five repetitive extracellular cadherin (EC) domains that physically bind cadherin-expressing neighboring cells, while the intracellular portion is composed of a juxtamembrane domain and a catenin-binding domain. The juxtamembrane portion is bound by the armadillo family member, p120, which serves to stabilize the adherens junction complex, and the catenin-binding domain is bound by the cytoskeletal adapter protein  $\beta$ -catenin.  $\beta$ -catenin in turn binds to  $\alpha$ -catenin which ultimately serves as the physical link between the adherens junction complex and the actin cytoskeleton of the cell (Gumbiner, 2005; Takeichi, 2014).

In the skin, the functions of the adherens junction and its various components have been explored in detail. In the embryonic epithelium, ECAD needs to be repressed by the WNT signaling transcription factor LEF1 to enable placode downgrowth during HF morphogenesis, which is inhibited when ECAD is overexpressed (Jamora et al., 2003). When the developing epidermis lacks ECAD, the basal layer remains largely intact due to an upregulation of PCAD, but the terminally differentiated layers, which do not upregulate PCAD, become perturbed (Tinkle et al., 2004). A combined loss of ECAD and PCAD in turn causes more severe cell junction perturbations and a defective skin barrier (Tinkle and Fuchs, 2008). p120 and  $\alpha$ -catenin have been found to play roles beyond their cell adhesion function. While p120-cKO epidermis does not display a barrier defect, it becomes hyperplastic due to an upregulation of NF $\kappa$ B signaling and expression of inflammatory cytokines, which is rescued by immune cell suppression with dexamethasone (Perez-Moreno et al., 2006).  $\alpha$ -catenin-cKO epidermis also exhibits hyperproliferation due to sustained RAS-MAP-kinase signaling and increased Yap signaling following its nuclear translocation, independent of cell adhesion defects (Schlegelmilch et al., 2011; Vasioukhin et al., 2001; Vasioukhin et al., 2000).

While most studies have focused on the roles of various adherens junction components in the epidermis, less emphasis has been placed on HFs. HFs that lack ECAD are short, brittle and mis-angled as intercellular gaps appear in the differentiated layers that form during anagen (Tinkle et al., 2004). While dissecting the function of WNT signaling in HFSCs, one study demonstrated that HFs that

have  $\beta$ -catenin ablated only in Bu-HFSCs remain in telogen for prolonged periods without entering anagen, but when stimulated to regenerate, these  $\beta$ -catenin-cKO Bu-HFSCs adopt a sebaceous gland fate instead (Lien et al., 2014; Merrill et al., 2001).

Since I had found that reduction of ECAD expression in Bu-HFSCs occurs downstream of increased proliferation, I wanted to investigate if direct perturbation of cell adhesion would have a downstream effect on proliferative activity of adult stem cells. Much of the work on how ECAD influences cell proliferation have been performed in vitro (Benham-Pyle et al., 2015; Kim et al., 2011; McClatchey and Yap, 2012; Perrais et al., 2007). The mouse hair follicle presents an ideal model system to elucidate the functions of ECAD in vivo, specifically in adult stem cells, for the following reasons: a) HFSCs reside in an architecturally defined niche, the bulge, which anchors and maintains the hair coat; b) HFSCs adhere to each other at least via ECAD-based adherens junctions (Figure 12D); c) HFSCs also adhere to their inner bulge K6<sup>+</sup> niche cells at least via ECAD (Figure 12D); and d) the periodic nature of HF regeneration provides a tractable model to investigate how cell-cell adhesion can influence stem cell activity and therefore tissue production.

## 3.2 Results

### 3.2.1 ECAD-cKO HFs exhibit an aberrant stem cell niche architecture

As described in Chapter 2.2.10, I engineered ECAD-cKO mice by introducing *Sox9CreER* ; *R26-LSL-YFP* to *Cdh1<sup>fl/fl</sup>* background, in which flox sites were inserted to flank exons 6 to 11 of *Cdh1* (Boussadia et al., 2002). Using an inducible CreER that was specific to hair follicles allowed me to control the timing of knocking-out ECAD only in the hair follicles and avoid defects in the epidermis (hereby termed ECAD-cKO). When 2<sup>nd</sup> telogen mice were treated with tamoxifen, ECAD was efficiently depleted by one month post-tamoxifen. At this time, the bulge structure began to show abnormalities. Instead of an organized bi-layer of cells, in which the outer Bu-HFSCs were uniformly arranged next to the inner bulge cells, many ECAD-cKO bulges displayed more than two cell layers. Careful analysis revealed that these extra cell layers were CD34+ and expressed one of the stem cell markers, TCF4, suggesting that they were likely Bu-HFSCs and not extra K6+ inner bulge cells, of which there was still only one layer (Figure 15A). Quantification of multiple hair follicles in backskin samples revealed that most ECAD-cKO hair follicles had perturbations in their bulges, be it in the new bulge or old bulge (Figure 15B).

Immunofluorescence of various adhesion proteins further demonstrated the disorganization of the HFSC niche upon ECAD loss. F-actin, the cytoskeletal component to which the adherens junction complex binds, revealed the highly

disorganized cells within the bulge, and  $\beta$ 4-integrin staining showed some discontinuities in the basement membrane. PCAD antibody signal is usually stronger in the hair germ than in the bulge of WT HF $s$ , but when ECAD was ablated, the bulge expressed PCAD as highly as the hair germ, consistent with previous reports that PCAD was upregulated in the absence of ECAD (Tinkle and Fuchs, 2008; Tinkle et al., 2004). Despite the disorganization, Bu-HFSCs appeared to maintain junctions with each other, as further demonstrated by antibody staining against the adherens junction proteins p120,  $\alpha$ -catenin and  $\beta$ -catenin, and desmosomal components including desmoglein 3, plakoglobin and desmoplakin (Figures 15C and 15D).

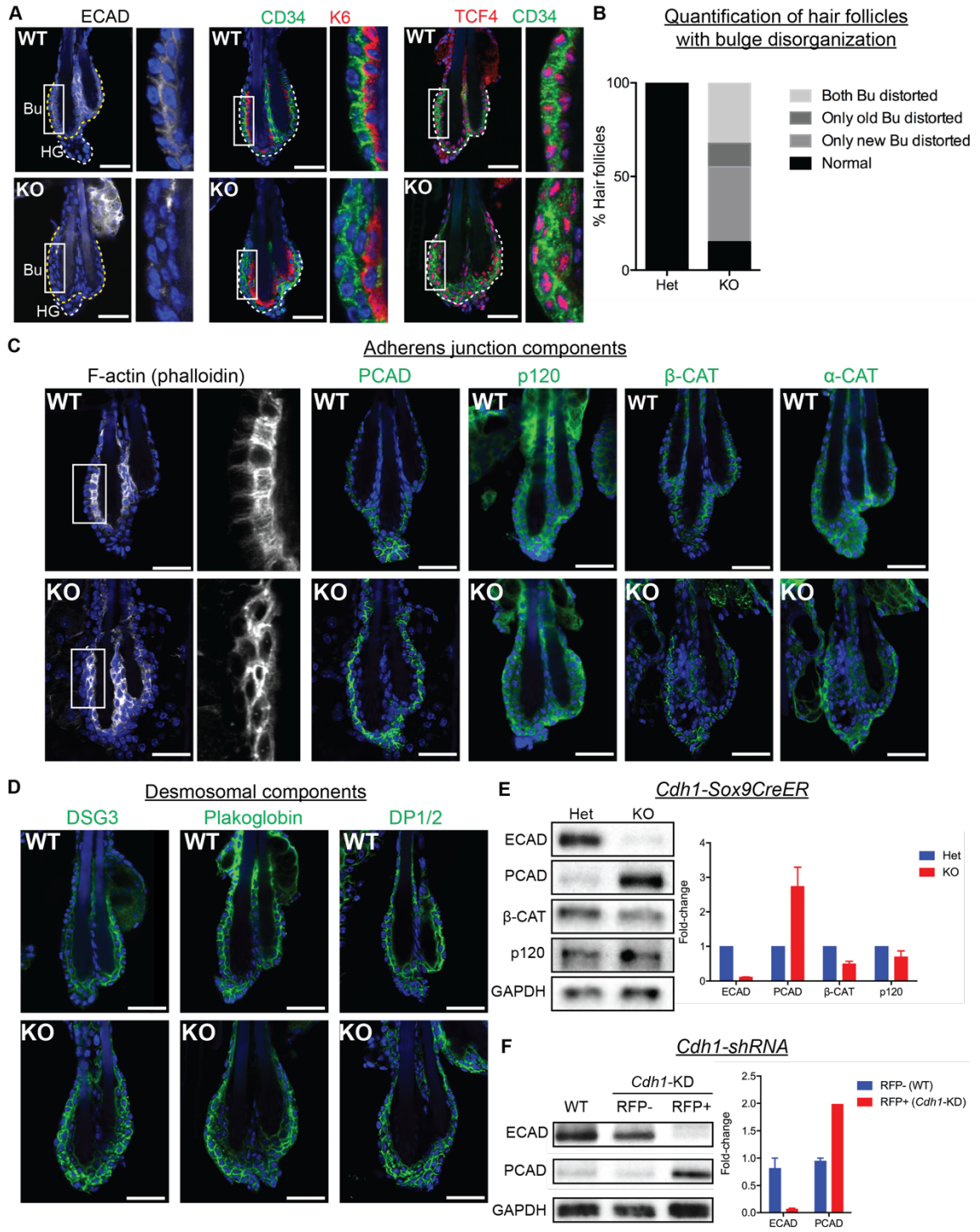
Western blotting of FACS-purified Bu-HFSC protein lysates confirmed the efficient deletion of ECAD and the striking up-regulation of PCAD in ECAD-cKO HF $s$  (Figure 15E). Since the genes encoding ECAD (*Cdh1*) and PCAD (*Cdh3*) are located in tandem on the same chromosome, the increase in PCAD could be due to the disruption in the genome following the removal of six exons upon *Sox9CreER* induction. To test this, I generated lentiviruses harboring a H2B-RFP reporter and a short hairpin RNA (shRNA) that efficiently knocked down *Cdh1* transcripts without perturbing the genome, injected these lentiviruses into E9.5 WT embryos in utero, and allowed these *Cdh1*-KD mice to grow to the age of 2<sup>nd</sup> telogen (~P50). While the bulge architecture of these *Cdh1*-KD HF $s$  was not perturbed due to the mosaicism of the knockdown, western blotting of FACS-purified *Cdh1*-KD RFP(+) Bu-HFSCs and WT uninfected RFP(-) Bu-HFSCs from the same mice revealed the efficient knockdown of ECAD and the upregulation of

PCAD, suggesting that the robust PCAD increase in the absence of ECAD did not occur at the genomic level, but rather as a functional compensation (Figure 15F).

**Figure 15. Analyzing bulge architecture and expression of junctional complex proteins upon ECAD loss.**

- (A) Left, ECAD is more highly expressed in bulge (Bu) than hair germ (HG) of WT HF, and is efficiently deleted in KO. Insets show magnified view of organized bilayer in WT bulge and disorganized KO bulge with extraneous cells. Middle, WT bulge exhibits one layer of K6+ inner bulge cells and one layer of CD34+ Bu-HFSCs, while KO bulge exhibits one layer of K6+ cells and two layers of CD34+ Bu-HFSCs. Insets show magnified view. Right, extra KO Bu-HFSCs maintain expression of a HFSC transcription factor TCF4. Insets show magnified view.
- (B) Hair follicles are scored based on whether they have distortions (extra cell layers) in new bulge only, old bulge only, or both bulges (n = 2 mice, N = 40 HFs).
- (C) Expression of F-actin and various adherens junction proteins.  $\alpha$ -CAT,  $\alpha$ -catenin;  $\beta$ -CAT,  $\beta$ -catenin.
- (D) Expression of various desmosomal proteins. DSG3, desmoglein 3; DP1/2, desmoplakin 1/2.
- (E) Western blotting of various adherens junction proteins in FACS-purified Bu-HFSCs from *Cdh1-Sox9CreER* mice.
- (F) Western blotting of ECAD and PCAD in FACS-purified Bu-HFSCs from *Cdh1-KD* mice.

Scale bars = 30  $\mu$ m.



### **3.2.2 Bu-HFSCs proliferate precociously without contributing to new HF regeneration in the absence of ECAD**

To test if the extraneous cell layers in the ECAD-cKO bulge was due to proliferation of Bu-HFSCs, I pulsed mice with EdU for 24 hr before harvesting skin samples. Indeed, ECAD-cKO bulges displayed varying degrees of proliferation, as revealed by quantification of EdU+ Bu-HFSCs within each bulge of individual HFs (Figure 16A). This precocious proliferative activity in the ECAD-cKO bulge preceded any hair germ proliferation, going against the well-established 2-step sequential activation of HG-HFSC → Bu-HFSC at anagen initiation during WT HF regeneration. Strikingly, the old bulge, which is highly quiescent and proliferates only in response to wounding (Hsu et al., 2011), became proliferative in the absence of ECAD (Figure 16A). These data strongly suggest that the aberration of the telogen HF bulge upon ECAD loss was due to the premature proliferation of the otherwise quiescent Bu-HFSCs.

One would expect that the increased proliferative capacity of the ECAD-cKO Bu-HFSCs would result in precocious hair cycling, similar to that observed in *Foxc1*-cKO HFs. However, the opposite result was observed: ECAD-cKO HFs stayed in telogen for longer durations than Het or WT HFs before eventually entering anagen to generate a new hair coat (Figure 16B). Interestingly, when challenged by depilation, both HG-HFSCs and Bu-HFSCs of ECAD-cKO HFs responded, initiated anagen and regenerated new hairs at around the same time as those of WT or Het HFs (Figure 16C).

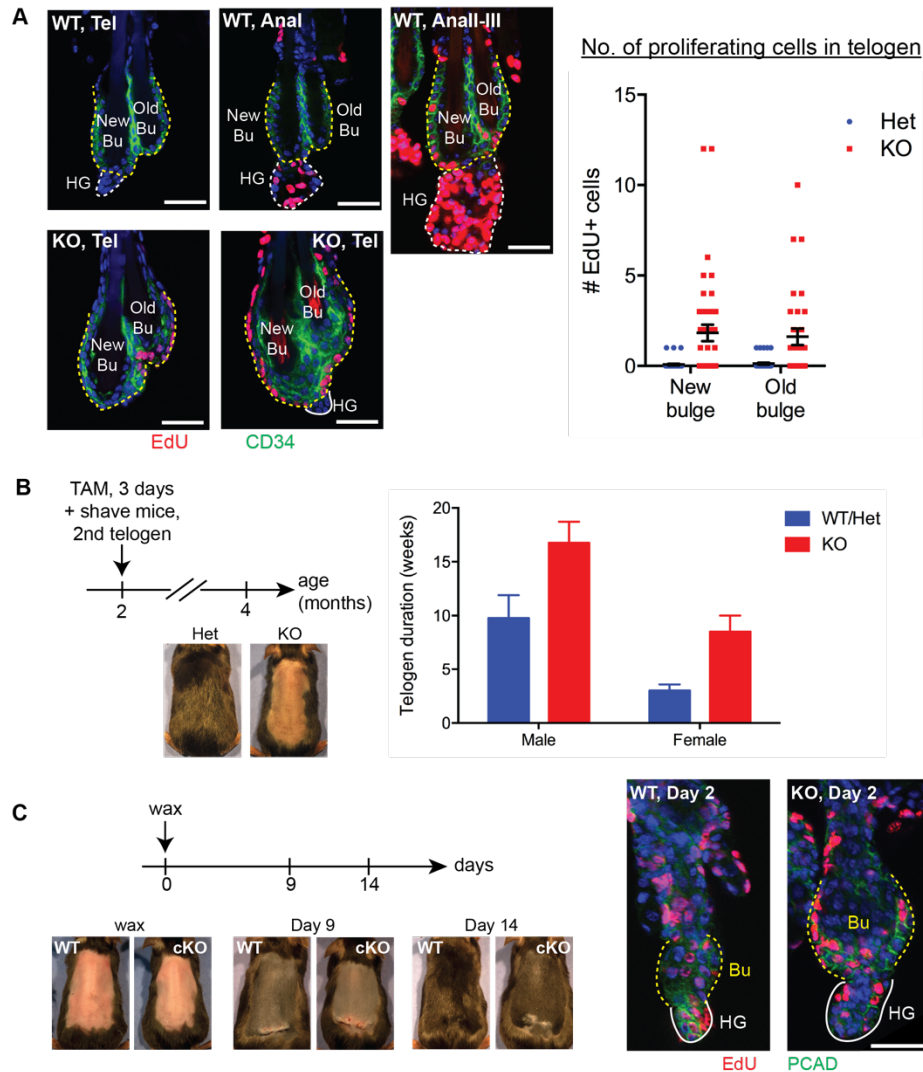


**Figure 16. ECAD-cKO Bu-HFSCs proliferate precociously without regenerating new hairs.**

(A) Left, WT telogen (Tel) Bu-HFSCs are largely quiescent (as judged by absence of EdU), and begin to proliferate only after HG-HFSCs are activated (EdU+) in anagen I (Anal); in contrast, KO telogen Bu-HFSCs are proliferative even in the absence of HG-HFSC proliferation. Right, Quantification of number of EdU+ cells in old bulge and new bulge, with black bars denoting mean $\pm$ SEM (n = 2 mice, N = 40 HF per mouse).

(B) Telogen duration of ECAD-cKO HF is longer than sex-matched WT or Het counterparts. By 4 months of age, WT or Het mice have generated a new hair coat and entered 3<sup>rd</sup> telogen, but KO mice are still in 2<sup>nd</sup> telogen (n  $\geq$  3 mice per genotype).

(C) ECAD-cKO HG-HFSCs and Bu-HFSCs respond upon depilation (waxing), as shown by incorporation of EdU at Day 2 post-wax, and regenerate a new hair coat at the same time as WT. Scale bars = 30  $\mu$ m.

### **3.2.3 RNA-seq revealed enrichment of genes associated with inflammatory response following ECAD loss**

Various signaling pathways have been found to be inhibited by ECAD-based adherens junctions to result in the inhibition of cell growth and proliferation in vitro, including epidermal growth factor receptor (EGFR) and Hippo-YAP signaling (Kim et al., 2011; Perrais et al., 2007). Indeed, cultured FACS-purified ECAD-cKO Bu-HFSCs grew as clusters of cells that did not form junctions with one another (Figure 17A), despite expressing PCAD (Figure 17B), and remained proliferative even upon reaching confluency (Figure 17C), as opposed to WT Bu-HFSCs that formed cell-cell junctions within well-defined colonies (Figures 17A and 17B) and exhibited contact inhibition (Figure 17C). ECAD-cKO Bu-HFSCs also exhibited a more elongated cell shape that resembled that of mesenchymal cells, but were still epithelial in nature as evidenced by K14 staining and absence of the mesenchymal marker vimentin (Figure 17D).

To identify novel signaling pathways that could act downstream of ECAD and confer a quiescence property to Bu-HFSCs, I performed RNA-seq on Bu-HFSCs FACS-purified from ECAD-cKO and Het mice. Alignment of reads to the mm10 build of the mouse genome was performed using Sliced Transcripts Alignment to a Reference (STAR) software (Dobin et al., 2013), and read counts were analyzed for differentially expressed genes using DESeq2 (Love et al., 2014). 1987 genes were statistically significantly changed ( $p < 0.05$ ), of which 793 were down-regulated (fold change  $\leq -1.5$ ) and 1194 were up-regulated (fold change  $\geq 1.5$ ) in the absence of ECAD.

I performed KEGG (Kyoto Encyclopedia of Genes and Genome) pathway analysis to identify signaling pathways and networks that were altered downstream of ECAD loss. Among the down-regulated genes, signaling pathways that were significantly changed include TGF $\beta$ , Ras, Rap1, Wnt and Mapk (Table 1). On the other hand, the most significantly changed pathway among the up-regulated genes was cell cycle, which was expected given the proliferation phenotype of the ECAD-cKO Bu-HFSCs. Surprisingly, a huge number of pathways that were significantly changed below that were related to immune responses. These included tumor necrosis factor (TNF) signaling, herpes simplex infection, antigen processing and presentation, cytokine-cytokine receptor interaction, human T-cell lymphotropic virus type 1 (HTLV-1) infection, Hepatitis B, Influenza A, Jak-STAT signaling and NF $\kappa$ B signaling amongst others. Indeed, the two most highly up-regulated genes, with a 32-fold increase, were chemokine ligands 2 and 1 (*Ccl2*, *Ccl1*), both of which function to recruit immune cells such as dendritic cells and monocytes to sites of inflammation. “DNA replication” was also ranked highly as expected, and further below the list were apoptosis, p53 signaling pathway, Fanconi anemia pathway, base excision repair and homologous recombination, all of which pointed towards an up-regulation of DNA repair mechanisms or components of the apoptotic pathway, likely following damage incurred during cell division and DNA replication (Table 2).

To validate the RNA-seq data, especially with respect to the up-regulated genes, I investigated the skin immune cell milieu after loss of ECAD by performing immunofluorescence for CD45, a general immune cell marker. Notably, immune

cells did not reside near the bulge of the WT HF, where the HFSCs reside. However, in the absence of ECAD, an increased number of CD45+ immune cells accumulated around the bulge, which had already developed defects in its organization and cell layers (Figure 18). This specificity of immune cell localization to the bulge, and not to the epidermis, which still expressed ECAD and did not exhibit a hyperproliferative phenotype, ruled out a general skin inflammatory response. This supports the notion that an up-regulation of cytokine expression and immune responses specifically within the ECAD-cKO Bu-HFSCs, as revealed by RNA-seq, recruited immune cells to their vicinity. Whether this is a cause or consequence of the Bu-HFSC proliferation and disorganization phenotypes remains to be determined.

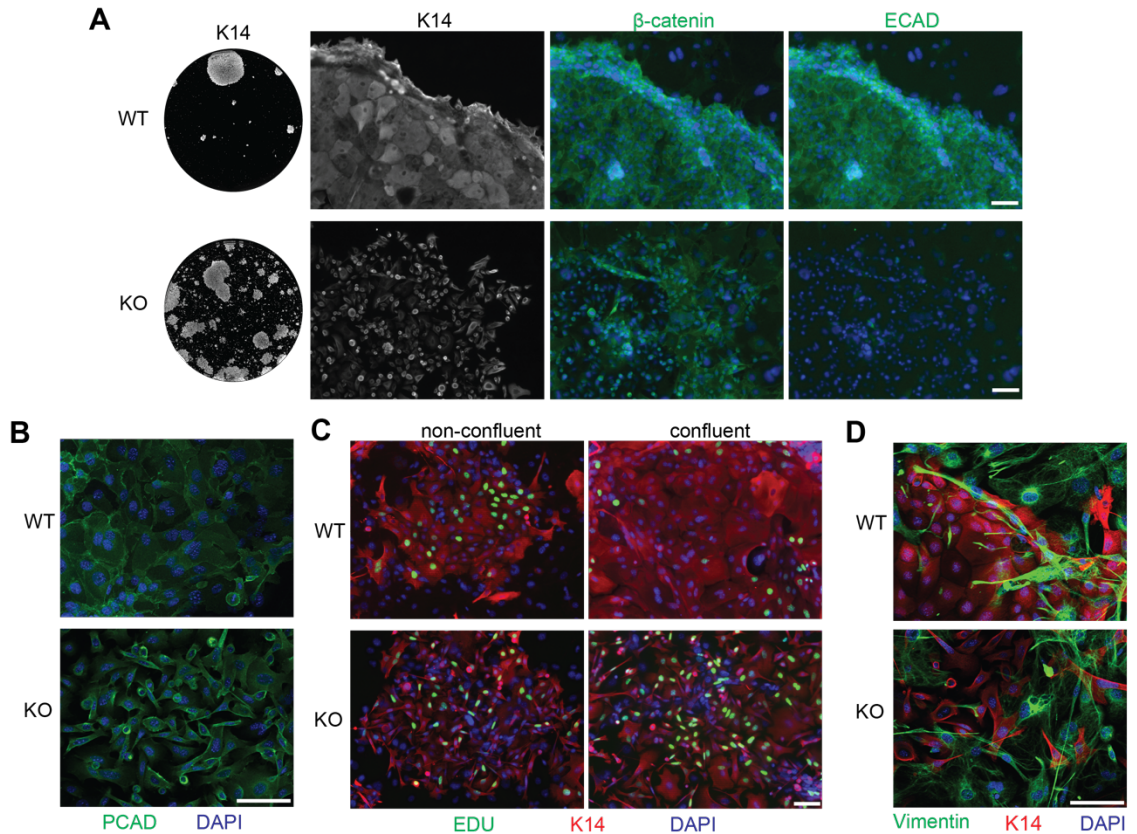


**Figure 17. ECAD-cKO Bu-HFSCs differ from WT in cell and colony morphology in vitro.**

(A) WT and KO Bu-HFSCs were FACS-purified and co-cultured with feeder fibroblast cells in vitro for 2 weeks. While WT cells form junctions with each other in a colony with well-defined edges, KO cells do not form junctions and merely exist as clusters. K14 was used to distinguish Bu-HFSCs from feeder cells.

(B) Cultured KO Bu-HFSCs express PCAD but still fail to form cell-cell junctions.

(C) WT Bu-HFSCs exhibit contact inhibition when confluent, but KO Bu-HFSCs continue to proliferate despite reaching confluency.

(D) KO Bu-HFSCs maintain their epithelial nature (K14+) and do not express vimentin, which are expressed by the surrounding feeder cells.

Scale bars = 30  $\mu$ m

**Table 1. KEGG pathway analysis of genes down-regulated in ECAD-cKO Bu-HFSCs vs. Het**

<b>KEGG term</b>	<b>P-value</b>
Neuroactive ligand-receptor interaction	0.004391511
Metabolism of xenobiotics by cytochrome P450	0.004709852
TGF-beta signaling pathway	0.004791515
Glutamatergic synapse	0.007290345
Ras signaling pathway	0.010791497
Vascular smooth muscle contraction	0.012891568
Drug metabolism - cytochrome P450	0.022813837
Rap1 signaling pathway	0.038260611
Glutathione metabolism	0.045820465
Glycosphingolipid biosynthesis - ganglio series	0.051275016
Wnt signaling pathway	0.058900993
Metabolic pathways	0.059078362
Ether lipid metabolism	0.093338613
MAPK signaling pathway	0.094182488
Melanogenesis	0.096680445

**Table 2. KEGG pathway analysis of genes up-regulated in ECAD-cKO Bu-HFSCs vs. Het**

<b>KEGG term</b>	<b>P-value</b>
Cell cycle	4.78E-14
TNF signaling pathway	3.56E-10
Herpes simplex infection	6.00E-10
Antigen processing and presentation	2.67E-08
DNA replication	3.09E-07
Cytokine-cytokine receptor interaction	5.42E-07
HTLV-I infection	5.48E-07
Apoptosis	5.91E-06
Osteoclast differentiation	9.92E-06
Hepatitis B	9.93E-06
Influenza A	1.57E-05
p53 signaling pathway	2.29E-05
Viral myocarditis	3.90E-05
Jak-STAT signaling pathway	8.63E-05
Measles	1.02E-04
Inflammatory bowel disease (IBD)	1.16E-04
NF-kappa B signaling pathway	1.28E-04
Graft-versus-host disease	1.54E-04
Viral carcinogenesis	1.56E-04
Toxoplasmosis	2.53E-04
Epstein-Barr virus infection	2.77E-04
Small cell lung cancer	3.00E-04
Allograft rejection	3.07E-04
Amoebiasis	3.86E-04
Tuberculosis	5.11E-04
Type I diabetes mellitus	7.65E-04
Cell adhesion molecules (CAMs)	0.001062282
RIG-I-like receptor signaling pathway	0.001684951
Hepatitis C	0.00215579
Fanconi anemia pathway	0.00236418
Phagosome	0.002539278

MicroRNAs in cancer	0.005114966
Rheumatoid arthritis	0.007426065
Autoimmune thyroid disease	0.007463676
Adipocytokine signaling pathway	0.008232676
Leishmaniasis	0.011006194
Progesterone-mediated oocyte maturation	0.011464807
Primary immunodeficiency	0.012402721
ECM-receptor interaction	0.012442698
Toll-like receptor signaling pathway	0.013616957
Base excision repair	0.01425673
African trypanosomiasis	0.01425673
Homologous recombination	0.020880764
Pathways in cancer	0.022390129
Hematopoietic cell lineage	0.022922273
Oocyte meiosis	0.025205421
Pertussis	0.026605432
Natural killer cell mediated cytotoxicity	0.040441231
NOD-like receptor signaling pathway	0.041940809
Legionellosis	0.045531159
Focal adhesion	0.05526631
MAPK signaling pathway	0.060914272
Staphylococcus aureus infection	0.06776068
Amyotrophic lateral sclerosis (ALS)	0.073227421
Chagas disease (American trypanosomiasis)	0.074860544
Pyrimidine metabolism	0.074860544
Pancreatic cancer	0.08127409
FoxO signaling pathway	0.088221055
Intestinal immune network for IgA production	0.093966324
One carbon pool by folate	0.094306301

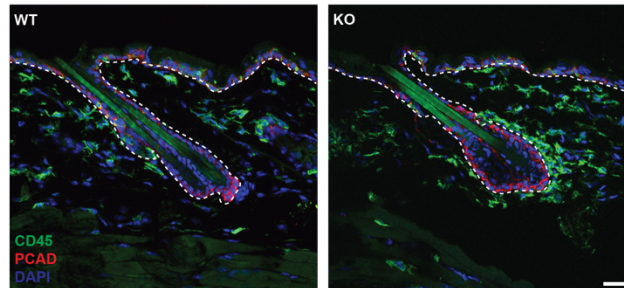


**Figure 18. Skin sagittal sections reveal recruitment of CD45+ immune cells around ECAD-cKO bulge.**

Scale bar = 30  $\mu$ m.

### **3.3 Discussion and future directions**

#### **3.3.1 ECAD loss causes downstream ectopic proliferation of Bu-HFSCs, resulting in stem cell niche architectural disruption**

Following embryonic hair follicle morphogenesis that forms the first hair coat, and a round of early adult hair cycling thereafter to form the second hair coat, hair follicles enter an extended telogen phase, during which HFSCs remain quiescent. It was during this time when I induced knock-out of *Cdh1*, the gene encoding the adherens junction component ECAD, in hair follicles.

During a normal telogen  $\rightarrow$  anagen transition, quiescent Bu-HFSCs respond to activating cues and become proliferative, during which ECAD becomes down-regulated (Figure 13D), perhaps to allow Bu-HFSCs and their progeny to divide and move out of their bulge niche. Interestingly, these Bu-HFSC progeny do not

divide perpendicularly to their basement membrane and cause an expansion of the bulge. Rather, they divide along their basement membrane and move downwards to form an ORS that encases the newly growing anagen hair follicle in an orchestrated manner (Hsu et al., 2011; Niessen et al., 2013).

When ECAD was ablated from quiescent Bu-HFSCs, they exited quiescence and proliferated despite the absence of activating cues that drive anagen entry. In the absence of a down-growing hair follicle, Bu-HFSCs and their progeny remained within the bulge. The disruption to adherens junctions within and between the two bulge layers, together with this consequent proliferation of the outer Bu-HFSC layer, resulted in a “remodeling” of the bulge to accommodate the extra cells. In spite of this, these bulge cells could still form cell-cell junctions, since components of desmosomes appeared to be unaffected, at least based on immunofluorescence and RNA-seq data. PCAD staining at the cell junctions also intensified, suggesting that PCAD could be compensating partially for ECAD loss. However, it has been reported that ECAD is required for proper localization of key proteins that form tight junctions in the developing embryonic skin (Tunggal et al., 2005). It would be necessary to dissect if inducing loss of ECAD in the adult HF will affect tight junctions that have already been established. Further validation of the expression of these various junctional proteins by western blotting, and ultrastructural analysis by electron microscopy (EM), are required.

However, the precocious proliferation of ECAD-cKO Bu-HFSCs did not set off anagen entry. This was due to the absence of HG-HFSC proliferation, since the hair germ did not express junctional ECAD as highly as the bulge and could be

spared of phenotypes directly associated with ECAD loss (Figure 14A). However, it was surprising that these hair follicles remained in telogen longer than their Het or WT counterparts, for which there could be several reasons. First, the hair germs of ECAD-cKO HF s were frequently smaller or indistinguishable from the bulge (Figures 15 and 16 immunofluorescence panels); careful quantification of whole-mount hair follicles and skin sagittal sections is required. Second, ECAD-cKO Bu-HFSCs could be secreting factors that non-autonomously inhibit HG-HFSC activity; more thorough analysis of the RNA-seq data and validation by qPCR will provide more insights. Third, immune cells recruited to the bulge could exert a non-autonomous inhibition on HG-HFSC proliferation, or influence the surrounding dermal cells by delaying the reduction in global BMP signals that is necessary to initiate anagen entry.

If formation, maintenance and turn-over of tight junctions are indeed affected by ECAD loss, a consequent defect in the skin barrier could elicit the observed gene expression changes associated with immune responses and the recruitment of immune cells. While the inter-follicular epidermis remains intact, external agents could still enter the skin through the hair follicle orifice along the club hair, and come into contact with the suprabasal layers of the hair follicle, including the K6+ inner bulge layer that is also ECAD-deficient. Ultrastructural analysis by EM, and devising an adult barrier assay to check for penetration of colored dyes through the hair follicle, are critical to determine the presence of a hair follicle barrier defect.

### 3.3.2 An immune response was mounted in the absence of ECAD

The recruitment of immune cells to the ECAD-cKO bulge was striking and surprising. Are the immune cells a cause or consequence of the ectopic Bu-HFSC proliferation and bulge niche disruption? To distinguish between the two possibilities, the timing of events by sampling hair follicles at regular timepoints following induction of *Cdh1*-cKO has to be elucidated. This would answer the following questions: a) when ECAD is efficiently depleted; b) when the precocious proliferation of Bu-HFSCs begins; c) whether the recruitment of immune cells to the bulge occurs before or after Bu-HFSC proliferation and bulge disorganization; and d) how long the immune cells persist around the bulge, and how they behave as HFs eventually overcome the delay and enter anagen.

Next, it is important to investigate the types of immune cells that are recruited to the bulge by both immunofluorescence of sagittal skin sections and flow cytometry analysis of dissociated skin samples using a panel of antibodies against various immune cell type-specific surface markers, including CD3 (T-cells), CD64 (macrophages), MHC Class II (dendritic cells, macrophages) and CD11c (dendritic cells, monocytes) amongst others. Finally, it would be critical to suppress the immune response at an appropriate timepoint before immune cell recruitment, either by dexamethasone, a general immune suppressant, or by immune cell type-specific antibody depletion. If the bulge phenotype is rescued, the immune cells are likely a cause; if the phenotype persists or worsens, they are probably a consequence.

Up-regulation of genes associated with DNA damage repair and apoptosis could suggest that Bu-HFSCs are accumulating damage from their precocious proliferative activity, and those that die by apoptosis need to be cleared out. Consequently, this could account for the up-regulation of genes associated with immune cell recruitment and response. Immunofluorescence can be performed on whole-mount and sagittal sections of HFs for phosphorylated H2AX check for DNA double-stranded breaks, and caspase 3 and terminal deoxynucleotidyl transferase dUTP nick end labeling (TUNEL) to detect apoptosis and DNA fragmentation. If more cell death is occurring, differences in caspase 3 staining between basal and suprabasal Bu-HFSCs can be quantified, given that basal epidermal cells without the adherens junction component  $\alpha$ -catenin are much less susceptible to apoptosis than their suprabasal counterparts (Livshits et al., 2012).

### **3.3.3 Investigating the direct cause of Bu-HFSC proliferation upon ECAD loss**

Mice with an epithelial-specific knockout of another adherens junction component, p120, display a hyper-proliferative skin epidermis. The mechanism is cell adhesion-independent, because even in the presence of an intact skin barrier, p120-cKO epidermal keratinocytes up-regulate NF $\kappa$ B signaling, which induces pro-inflammatory responses. In this case, the hyper-proliferation was rescued when immune cells were suppressed with dexamethasone (Perez-Moreno et al., 2006).

Here, I present a similar proliferative phenotype but in the context of the hair follicles and in particular their stem cells, a less explored area compared to the interfollicular epidermis in terms of hyper-proliferative phenotypes caused by perturbation to cell junctions. If the immune cells are not causing the phenotype, investigating the mechanism immediately downstream of ECAD loss will be critical to understanding how these Bu-HFSCs proliferate and result in a profound recruitment of immune cells. This signaling pathway might, or might not, be occurring in proliferating WT Bu-HFSCs during a physiological telogen → anagen entry. To this end, gene expression profiling of WT anagen II proliferating Bu-HFSCs vs. telogen quiescent Bu-HFSCs can be performed to uncover the changes that normally occur during Bu-HFSC proliferation, then compared to those observed with ECAD-cKO Bu-HFSC proliferation, along with the differences that occurred upon FOXC1 loss that also influences Bu-HFSC quiescence. Some of the possible signaling pathways as suggested from the ECAD-cKO RNA-seq data include TNF and NFκB signaling (Table 2). It has been demonstrated that drug inhibition of Jak-Stat signaling is sufficient to induce anagen entry (Harel et al., 2015), and intriguingly, the up-regulation of Jak-Stat signaling in ECAD-cKO Bu-HFSCs (Table 2) could account for the delayed entry of these hair follicles into anagen. Immunohistochemistry, immunofluorescence and western blotting for transcriptional effectors of these various signaling pathways, including p65, phosphorylated-Stat1 and phosphorylated-Stat3 must be performed to analyze changes in their expression and localization patterns upon ECAD loss.

### 3.3.4 Implications for EMT and cancer biology

The transcriptional repression of ECAD expression occurs during epithelial-to-mesenchymal transition (EMT), which is believed to be a critical driver of cancer progression. Cells in the invasive front of an epithelial tumor tend to exhibit characteristics of EMT, including expression of the EMT-initiating transcription factors Snail, Twist and Zeb, elongated cell shape, reduced ECAD levels and overall weakened intercellular adhesion, all of which are believed to enable tumor progression as these leading edge cells gain motility, remodel and invade through the basement membrane (Nieto et al., 2016). Moreover, increasing evidence have also pointed to functional roles of increased PCAD levels in tumor progression, such as promoting dissemination and migration of ovarian epithelial cancer cells, and potentiating insulin-like growth factor 1 receptor signaling and increasing Snail expression in oral squamous cell carcinoma (Ko and Naora, 2014; Paredes et al., 2012).

Here, I present an in vivo stem cell model, in which Bu-HFSCs that are genetically knocked out for ECAD gain higher PCAD levels, become more proliferative and are able to remodel their surrounding basement membrane and ECM such that the bulge can now expand and accommodate extraneous Bu-HFSCs, recapitulating at least in part cells in the invasive front of a malignant tumor. However, expression of the EMT-initiating transcription factors was not changed upon loss of ECAD, consistent with a previous study reporting that ECAD loss does not induce EMT in non-malignant breast cancer cells (Chen et al., 2014). While

this fits with the notion that ECAD repression occurs as a consequence of the EMT process, delineating the direct downstream consequences of ECAD loss will help dissect how EMT can contribute to malignant tumor progression through ECAD repression. Over-expression of PCAD in WT HF<sub>s</sub> will delineate whether the phenotypes in ECAD-cKO HF<sub>s</sub> are caused by a loss of ECAD, over-expression of PCAD or a combination of both.

### **3.4 Materials and Methods**

#### ***Antibodies and immunofluorescence***

The following antibodies were used for immunofluorescence:  $\beta$ 4 (1:200, BD Biosciences),  $\alpha$ -catenin (1:1000, Sigma),  $\beta$ -catenin (1:1000, BD Biosciences), desmoglein 3 (1:500, MBL), plakoglobin (1:500, BD Biosciences), desmoplakin 1&2 (1:500, Millipore), keratin 14 (1:500, Biolegend), vimentin (1:500, Cell Signaling) and CD45 (1:100, Biolegend). Phalloidin (1:100, Fisher) was used to detect F-actin. The following antibodies were used for immunoblotting: p120 (1:500, Zymed), PCAD (1:1000, R&D) and  $\beta$ -catenin (1:1000, BD Biosciences).

## CHAPTER 4: CONCLUSION

My findings best fit a model as follows. During early anagen, WT Bu-HFSCs proliferate and down-regulate ECAD expression so as to move out of their niche and fuel hair regeneration. As anagen progresses, WT Bu-HFSCs cease proliferation, re-establish quiescence and restore ECAD levels. As such, they are able to anchor the old bulge in place as the new hair follicle emerges and grows alongside it. When hair follicles return to telogen, they retain the old bulge alongside the newly made bulge. The presence of the old bulge helps to keep HFSCs in quiescence, by virtue of inhibitory factors emanating from its inner bulge layer and the suprabasal cells existing between the two bulges. In this way, telogen becomes longer, and hair cycling is restricted. When WT mice age, their HFSC numbers are maintained, and hair coats remain thick and replete with pigmentation (Figure 19, top panel).

Loss of FOXC1 leads to elevated cell cycle transcripts and enhanced HFSC activity, resulting in premature entry of HFSCs into anagen. Proliferating *Foxc1*-cKO Bu-HFSCs also down-regulate ECAD expression during early anagen. However, as anagen progresses, they fail to re-establish quiescence and up-regulate ECAD promptly. This heightens the sensitivity of the old bulge to mechanical stress induced by new hair growth. Eventually, the old bulge becomes extruded and lost as *Foxc1*-cKO Bu-HFSCs are unable to anchor it in place. Hair follicles re-enter telogen with only the newly made bulge. The absence of the old bulge, together with the intrinsic inability of *Foxc1*-cKO HFSCs to remain quiescent

for prolonged periods, further accelerates *Foxc1*-cKO HFSC activity and usage by lowering the threshold for their activation. This results in *Foxc1*-cKO hair follicles undergoing many more rounds of regeneration than WT hair follicles do over time. As *Foxc1*-cKO mice age, their Bu-HFSC numbers and function decline, resulting in a sparser hair coat that is often depigmented (Figure 19, bottom panel).

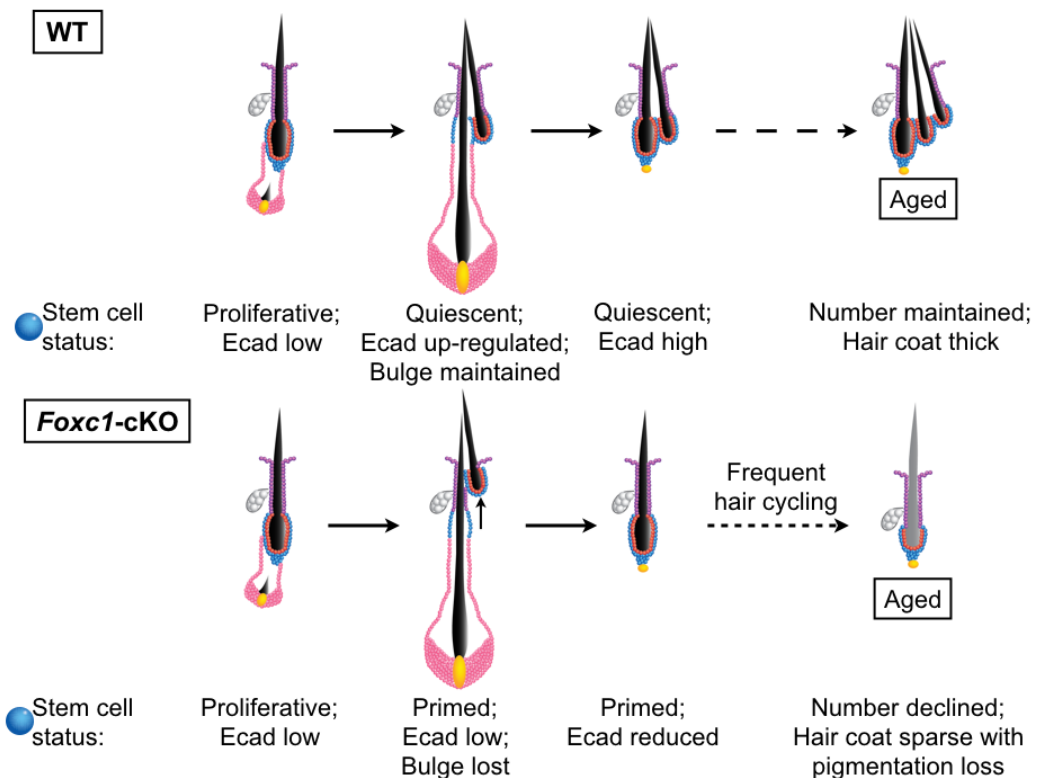


**Figure 19. Proposed model for the role of FOXC1 and adhesion in HFSCs.**

While stem cell activity results in dynamic downstream changes in ECAD during progression of the hair cycle, direct perturbation to ECAD in turn is sufficient to affect stem cell quiescence downstream. In the near complete absence of ECAD, Bu-HFSCs become proliferative. An up-regulation of PCAD does not seem to

compensate, since an otherwise organized bulge structure now becomes perturbed as extra Bu-HFSCs persist. However, the precocious Bu-HFSC proliferation did not result in earlier entry into anagen. Rather, hair follicles remain in telogen for an even longer time as HG-HFSCs remain quiescent. Intriguingly, ECAD-cKO Bu-HFSCs up-regulate genes involved in immune responses, and immune cells become recruited specifically to the bulge and not to other regions of the skin. It is noteworthy that *Foxc1*-cKO Bu-HFSCs do not exhibit such increases in expression of immune response-associated genes. Ongoing work will elucidate the sequence of Bu-HFSC proliferative and immune cell recruitment events, and whether the immune cells are a cause or consequence of the phenotypes associated with ECAD loss.

In conclusion, distinct tissues of the adult body have different turnover rates during homeostasis, necessitating various stem cell activity and usage. When not utilized for self-renewal or differentiation, many adult stem cells adopt, or are maintained, in a reversible state of inactivity known as quiescence. It is believed that the quiescence state can protect stem cells from metabolic stresses and preserve their genomic integrity, so that they can last through the lifetime of the organism. For my thesis, I asked if quiescence is essential to preserve this life-long tissue-regenerating ability of adult stem cells. Indeed, at least for the pelage hair follicle in the context of its native environment, prudence in conserving its stem cell activity, through the role of FOXC1 in establishment and coupling of stem cell quiescence to adhesion, is essential to maintain its stem cell numbers and preserve its tissue-regenerating potential throughout the lifetime of the animal.

## BIBLIOGRAPHY

Aliprantis, A.O., Ueki, Y., Sulyanto, R., Park, A., Sigrist, K.S., Sharma, S.M., Ostrowski, M.C., Olsen, B.R., and Glimcher, L.H. (2008). NFATc1 in mice represses osteoprotegerin during osteoclastogenesis and dissociates systemic osteopenia from inflammation in cherubism. *The Journal of Clinical Investigation* 118, 3775-3789.

Barczyk, M., Carracedo, S., and Gullberg, D. (2010). Integrins. *Cell Tissue Res* 339, 269-280.

Barker, N., van Es, J.H., Kuipers, J., Kujala, P., van den Born, M., Cozijnsen, M., Haegebarth, A., Korving, J., Begthel, H., Peters, P.J., *et al.* (2007). Identification of stem cells in small intestine and colon by marker gene Lgr5. *Nature* 449, 1003-1007.

Benham-Pyle, B.W., Pruitt, B.L., and Nelson, W.J. (2015). Cell adhesion. Mechanical strain induces E-cadherin-dependent Yap1 and beta-catenin activation to drive cell cycle entry. *Science* 348, 1024-1027.

Blanpain, C., Lowry, W.E., Geoghegan, A., Polak, L., and Fuchs, E. (2004). Self-renewal, multipotency, and the existence of two cell populations within an epithelial stem cell niche. *Cell* 118, 635-648.

Botchkarev, V.A., Botchkareva, N.V., Nakamura, M., Huber, O., Funa, K., Lauster, R., Paus, R., and Gilchrist, B.A. (2001). Noggin is required for induction of the hair follicle growth phase in postnatal skin. *Faseb J* 15, 2205-2214.

Boussadia, O., Kutsch, S., Hierholzer, A., Delmas, V., and Kemler, R. (2002). E-cadherin is a survival factor for the lactating mouse mammary gland. *Mech Dev* 115, 53-62.

Busch, K., Klapproth, K., Barile, M., Flossdorf, M., Holland-Letz, T., Schlenner, S.M., Reth, M., Hofer, T., and Rodewald, H.R. (2015). Fundamental properties of unperturbed haematopoiesis from stem cells in vivo. *Nature* 518, 542-546.

Chakkalakal, J.V., Jones, K.M., Basson, M.A., and Brack, A.S. (2012). The aged niche disrupts muscle stem cell quiescence. *Nature* 490, 355-360.

Chang, C.Y., Pasolli, H.A., Giannopoulou, E.G., Guasch, G., Gronostajski, R.M., Elemento, O., and Fuchs, E. (2013). NFIB is a governor of epithelial-melanocyte stem cell behaviour in a shared niche. *Nature* 495, 98-102.

Chen, A., Beetham, H., Black, M.A., Priya, R., Telford, B.J., Guest, J., Wiggins, G.A., Godwin, T.D., Yap, A.S., and Guilford, P.J. (2014). E-cadherin loss alters cytoskeletal organization and adhesion in non-malignant breast cells but is insufficient to induce an epithelial-mesenchymal transition. *BMC Cancer* 14, 552.

Chen, T., Heller, E., Beronja, S., Oshimori, N., Stokes, N., and Fuchs, E. (2012). An RNA interference screen uncovers a new molecule in stem cell self-renewal and long-term regeneration. *Nature* 485, 104-108.

Cheung, T.H., and Rando, T.A. (2013). Molecular regulation of stem cell quiescence. *Nat Rev Mol Cell Biol* 14, 329-340.

Collins, C.A., Olsen, I., Zammit, P.S., Heslop, L., Petrie, A., Partridge, T.A., and Morgan, J.E. (2005). Stem cell function, self-renewal, and behavioral heterogeneity of cells from the adult muscle satellite cell niche. *Cell* 122, 289-301.

Cotsarelis, G., Sun, T.T., and Lavker, R.M. (1990). Label-retaining cells reside in the bulge area of pilosebaceous unit: implications for follicular stem cells, hair cycle, and skin carcinogenesis. *Cell* 61, 1329-1337.

Dobin, A., Davis, C.A., Schlesinger, F., Drenkow, J., Zaleski, C., Jha, S., Batut, P., Chaisson, M., and Gingeras, T.R. (2013). STAR: ultrafast universal RNA-seq aligner. *Bioinformatics* 29, 15-21.

Endou, M., Aoki, H., Kobayashi, T., and Kunisada, T. (2014). Prevention of hair graying by factors that promote the growth and differentiation of melanocytes. *J Dermatol* 41, 716-723.

Festa, E., Fretz, J., Berry, R., Schmidt, B., Rodeheffer, M., Horowitz, M., and Horsley, V. (2011). Adipocyte lineage cells contribute to the skin stem cell niche to drive hair cycling. *Cell* 146, 761-771.

Flach, J., Bakker, S.T., Mohrin, M., Conroy, P.C., Pietras, E.M., Reynaud, D., Alvarez, S., Diolaiti, M.E., Ugarte, F., Forsberg, E.C., *et al.* (2014). Replication stress is a potent driver of functional decline in ageing haematopoietic stem cells. *Nature* 512, 198-202.

Folgueras, A.R., Guo, X., Pasolli, H.A., Stokes, N., Polak, L., Zheng, D., and Fuchs, E. (2013). Architectural Niche Organization by LHX2 Is Linked to Hair Follicle Stem Cell Function. *Cell Stem Cell* 13, 314-327.

Fuchs, E. (2009). The tortoise and the hair: slow-cycling cells in the stem cell race. *Cell* 137, 811-819.

Genander, M., Cook, P.J., Ramskold, D., Keyes, B.E., Mertz, A.F., Sandberg, R., and Fuchs, E. (2014). BMP signaling and its pSMAD1/5 target genes differentially regulate hair follicle stem cell lineages. *Cell Stem Cell* 15, 619-633.

Greco, V., Chen, T., Rendl, M., Schober, M., Pasolli, H.A., Stokes, N., Dela Cruz-Racelis, J., and Fuchs, E. (2009). A two-step mechanism for stem cell activation during hair regeneration. *Cell Stem Cell* 4, 155-169.

Green, H. (1991). Cultured cells for the treatment of disease. *Sci Am* 265, 96-102.

Gumbiner, B.M. (2005). Regulation of cadherin-mediated adhesion in morphogenesis. *Nat Rev Mol Cell Biol* 6, 622-634.

Haldipur, P., Gillies, G.S., Janson, O.K., Chizhikov, V.V., Mithal, D.S., Miller, R.J., and Millen, K.J. (2014). Foxc1 dependent mesenchymal signalling drives embryonic cerebellar growth. *eLife* 3.

Harel, S., Higgins, C.A., Cerise, J.E., Dai, Z., Chen, J.C., Clynes, R., and Christiano, A.M. (2015). Pharmacologic inhibition of JAK-STAT signaling promotes hair growth. *Sci Adv* 1, e1500973.

Hayashi, H., and Kume, T. (2008). Foxc transcription factors directly regulate Dll4 and Hey2 expression by interacting with the VEGF-Notch signaling pathways in endothelial cells. *PLoS One* 3, e2401.

Higgins, C.A., Westgate, G.E., and Jahoda, C.A. (2009). From telogen to exogen: mechanisms underlying formation and subsequent loss of the hair club fiber. *J Invest Dermatol* 129, 2100-2108.

Horsley, V., Aliprantis, A.O., Polak, L., Glimcher, L.H., and Fuchs, E. (2008). NFATc1 balances quiescence and proliferation of skin stem cells. *Cell* 132, 299-310.

Hsu, Y.C., Li, L., and Fuchs, E. (2014). Transit-amplifying cells orchestrate stem cell activity and tissue regeneration. *Cell* 157, 935-949.

Hsu, Y.C., Pasolli, H.A., and Fuchs, E. (2011). Dynamics between stem cells, niche, and progeny in the hair follicle. *Cell* 144, 92-105.

Huang da, W., Sherman, B.T., and Lempicki, R.A. (2009a). Bioinformatics enrichment tools: paths toward the comprehensive functional analysis of large gene lists. *Nucleic Acids Res* 37, 1-13.

Huang da, W., Sherman, B.T., and Lempicki, R.A. (2009b). Systematic and integrative analysis of large gene lists using DAVID bioinformatics resources. *Nat Protoc* 4, 44-57.

Huang, J., Dattilo, L.K., Rajagopal, R., Liu, Y., Kaartinen, V., Mishina, Y., Deng, C.X., Umans, L., Zwijsen, A., Roberts, A.B., *et al.* (2009). FGF-regulated BMP signaling is required for eyelid closure and to specify conjunctival epithelial cell fate. *Development* 136, 1741-1750.

Huch, M., Dorrell, C., Boj, S.F., van Es, J.H., Li, V.S., van de Wetering, M., Sato, T., Hamer, K., Sasaki, N., Finegold, M.J., *et al.* (2013). In vitro expansion of single Lgr5+ liver stem cells induced by Wnt-driven regeneration. *Nature* 494, 247-250.

Ibrahim, L., and Wright, E.A. (1975). The growth of rats and mice vibrissae under normal and some abnormal conditions. *J Embryol Exp Morphol* 33, 831-844.

Inaba, M., Yuan, H., Salzmann, V., Fuller, M.T., and Yamashita, Y.M. (2010). E-Cadherin Is Required for Centrosome and Spindle Orientation in *Drosophila* Male Germline Stem Cells. *PLoS ONE* 5, e12473.

Jamora, C., DasGupta, R., Kocieniewski, P., and Fuchs, E. (2003). Links between signal transduction, transcription and adhesion in epithelial bud development. *Nature* 422, 317-322.

Jin, Z., Kirilly, D., Weng, C., Kawase, E., Song, X., Smith, S., Schwartz, J., and Xie, T. (2008). Differentiation-defective stem cells outcompete normal stem cells for niche occupancy in the *Drosophila* ovary. *Cell Stem Cell* 2, 39-49.

Jones, P.H., Harper, S., and Watt, F.M. (1995). Stem cell patterning and fate in human epidermis. *Cell* 80, 83-93.

Kadaja, M., Keyes, B., Lin, M., Pasolli, H., Genander, M., Polak, L., Stokes, N., Zheng, D., and Fuchs, E. (2014). SOX9: a stem cell transcriptional regulator of secreted niche signaling factors. *Genes Dev* 28, 328-341.

Keyes, B.E., Segal, J.P., Heller, E., Lien, W.H., Chang, C.Y., Guo, X., Oristian, D.S., Zheng, D., and Fuchs, E. (2013). Nfatc1 orchestrates aging in hair follicle stem cells. *Proc Natl Acad Sci U S A*.

Kidson, S.H., Kume, T., Deng, K., Winfrey, V., and Hogan, B.L. (1999). The forkhead/winged-helix gene, Mf1, is necessary for the normal development of the cornea and formation of the anterior chamber in the mouse eye. *Dev Biol* 211, 306-322.

Kim, N.G., Koh, E., Chen, X., and Gumbiner, B.M. (2011). E-cadherin mediates contact inhibition of proliferation through Hippo signaling-pathway components. *Proc Natl Acad Sci U S A* 108, 11930-11935.

Ko, S.Y., and Naora, H. (2014). HOXA9 promotes homotypic and heterotypic cell interactions that facilitate ovarian cancer dissemination via its induction of P-cadherin. *Mol Cancer* 13, 170.

Kobielak, K., Pasolli, H.A., Alonso, L., Polak, L., and Fuchs, E. (2003). Defining BMP functions in the hair follicle by conditional ablation of BMP receptor IA. *J Cell Biol* 163, 609-623.

Kobielak, K., Stokes, N., de la Cruz, J., Polak, L., and Fuchs, E. (2007). Loss of a quiescent niche but not follicle stem cells in the absence of BMP signaling. *PNAS* *104*, 10063-10068.

Koch, P.J., Mahoney, M.G., Cotsarelis, G., Rothenberger, K., Lavker, R.M., and Stanley, J.R. (1998). Desmoglein 3 anchors telogen hair in the follicle. *J Cell Sci* *111 ( Pt 17)*, 2529-2537.

Kume, T., Deng, K., and Hogan, B.L. (2000). Murine forkhead/winged helix genes *Foxc1* (*Mf1*) and *Foxc2* (*Mfh1*) are required for the early organogenesis of the kidney and urinary tract. *Development* *127*, 1387-1395.

Kume, T., Deng, K.Y., Winfrey, V., Gould, D.B., Walter, M.A., and Hogan, B.L. (1998). The forkhead/winged helix gene *Mf1* is disrupted in the pleiotropic mouse mutation congenital hydrocephalus. *Cell* *93*, 985-996.

Kume, T., Jiang, H., Topczewska, J.M., and Hogan, B.L. (2001). The murine winged helix transcription factors, *Foxc1* and *Foxc2*, are both required for cardiovascular development and somitogenesis. *Genes Dev* *15*, 2470-2482.

Lien, W.-H., Polak, L., Lin, M., Lay, K., Zheng, D., and Fuchs, E. (2014). In vivo transcriptional governance of hair follicle stem cells by canonical Wnt regulations. *Nature Cell Biology* *16*, 179-190.

Lien, W.H., Guo, X., Polak, L., Lawton, L.N., Young, R.A., Zheng, D., and Fuchs, E. (2011). Genome-wide maps of histone modifications unwind In vivo chromatin states of the hair follicle lineage. *Cell Stem Cell* *9*, 219-232.

Livshits, G., Kobiela, A., and Fuchs, E. (2012). Governing epidermal homeostasis by coupling cell-cell adhesion to integrin and growth factor signaling, proliferation, and apoptosis. *Proc Natl Acad Sci U S A* *109*, 4886-4891.

Lo Celso, C., Prowse, D.M., and Watt, F.M. (2004). Transient activation of beta-catenin signalling in adult mouse epidermis is sufficient to induce new hair follicles but continuous activation is required to maintain hair follicle tumours. *Development* *131*, 1787-1799.

Love, M.I., Huber, W., and Anders, S. (2014). Moderated estimation of fold change and dispersion for RNA-seq data with DESeq2. *Genome Biol* *15*, 550.

Lowry, W.E., Blanpain, C., Nowak, J.A., Guasch, G., Lewis, L., and Fuchs, E. (2005). Defining the impact of beta-catenin/Tcf transactivation on epithelial stem cells. *Genes Dev* *19*, 1596-1611.

Mao, X., Fujiwara, Y., and Orkin, S.H. (1999). Improved reporter strain for monitoring Cre recombinase-mediated DNA excisions in mice. *Proc Natl Acad Sci U S A* *96*, 5037-5042.

Mattiske, D., Kume, T., and Hogan, B.L. (2006a). The mouse forkhead gene *Foxc1* is required for primordial germ cell migration and antral follicle development. *Dev Biol* *290*, 447-458.

Mattiske, D., Sommer, P., Kidson, S.H., and Hogan, B.L. (2006b). The role of the forkhead transcription factor, *Foxc1*, in the development of the mouse lacrimal gland. *Dev Dyn* *235*, 1074-1080.

McClatchey, A.I., and Yap, A.S. (2012). Contact inhibition (of proliferation) redux. *Curr Opin Cell Biol* 24, 685-694.

Merrill, B.J., Gat, U., DasGupta, R., and Fuchs, E. (2001). Tcf3 and Lef1 regulate lineage differentiation of multipotent stem cells in skin. *Genes Dev* 15, 1688-1705.

Milner, Y., Sudnik, J., Filippi, M., Kizoulis, M., Kashgarian, M., and Stenn, K. (2002). Exogen, Shedding Phase of the Hair Growth Cycle: Characterization of a Mouse Model. *119*, 639-644.

Morris, R.J., Liu, Y., Marles, L., Yang, Z., Trempus, C., Li, S., Lin, J.S., Sawicki, J.A., and Cotsarelis, G. (2004). Capturing and profiling adult hair follicle stem cells. *Nat Biotechnol* 22, 411-417.

Morrison, S.J., and Spradling, A.C. (2008). Stem cells and niches: mechanisms that promote stem cell maintenance throughout life. *Cell* 132, 598-611.

Muller-Rover, S., Handjiski, B., van der Veen, C., Eichmuller, S., Foitzik, K., McKay, I.A., Stenn, K.S., and Paus, R. (2001). A comprehensive guide for the accurate classification of murine hair follicles in distinct hair cycle stages. *J Invest Dermatol* 117, 3-15.

Nekrasova, O., and Green, K.J. (2013). Desmosome assembly and dynamics. *Trends Cell Biol* 23, 537-546.

Nguyen, H., Merrill, B., Polak, L., Nikolova, M., Rendl, M., Shaver, T., Pasoll, i.H., and Fuchs, E. (2009). Tcf3 and Tcf4 are essential for long-term homeostasis of skin epithelia. *Nature Genetics*.

Nguyen, H., Rendl, M., and Fuchs, E. (2006). Tcf3 governs stem cell features and represses cell fate determination in skin. *Cell* 127, 171-183.

Niessen, M.T., Scott, J., Zielinski, J.G., Vorhagen, S., Sotiropoulou, P.A., Blanpain, C., Leitges, M., and Niessen, C.M. (2013). aPKC $\lambda$  controls epidermal homeostasis and stem cell fate through regulation of division orientation. *J Cell Biol* 202, 887-900.

Nieto, M.A., Huang, R.Y., Jackson, R.A., and Thiery, J.P. (2016). Emt: 2016. *Cell* 166, 21-45.

Nishimura, E.K., Jordan, S.A., Oshima, H., Yoshida, H., Osawa, M., Moriyama, M., Jackson, I.J., Barrandon, Y., Miyachi, Y., and Nishikawa, S. (2002). Dominant role of the niche in melanocyte stem-cell fate determination. *Nature* 416, 854-860.

Nowak, J.A., Polak, L., Pasolli, H.A., and Fuchs, E. (2008). Hair follicle stem cells are specified and function in early skin morphogenesis. *Cell Stem Cell* 3, 33-43.

Oh, J., Lee, Y.D., and Wagers, A.J. (2014). Stem cell aging: mechanisms, regulators and therapeutic opportunities. *Nat Med* 20, 870-880.

Omatsu, Y., Seike, M., Sugiyama, T., Kume, T., and Nagasawa, T. (2014). Foxc1 is a critical regulator of haematopoietic stem/progenitor cell niche formation. *Nature* 508, 536-540.

Orford, K.W., and Scadden, D.T. (2008). Deconstructing stem cell self-renewal: genetic insights into cell-cycle regulation. *Nat Rev Genet* 9, 115-128.

Oshimori, N., and Fuchs, E. (2012). Paracrine TGF-beta signaling counterbalances BMP-mediated repression in hair follicle stem cell activation. *Cell Stem Cell* 10, 63-75.

Pan, Y., Lin, M.H., Tian, X., Cheng, H.T., Gridley, T., Shen, J., and Kopan, R. (2004). gamma-secretase functions through Notch signaling to maintain skin appendages but is not required for their patterning or initial morphogenesis. *Dev Cell* 7, 731-743.

Paredes, J., Figueiredo, J., Albergaria, A., Oliveira, P., Carvalho, J., Ribeiro, A.S., Caldeira, J., Costa, A.M., Simoes-Correia, J., Oliveira, M.J., *et al.* (2012). Epithelial E- and P-cadherins: role and clinical significance in cancer. *Biochim Biophys Acta* 1826, 297-311.

Perez-Moreno, M., Davis, M.A., Wong, E., Pasolli, H.A., Reynolds, A.B., and Fuchs, E. (2006). p120-catenin mediates inflammatory responses in the skin. *Cell* 124, 631-644.

Perrais, M., Chen, X., Perez-Moreno, M., and Gumbiner, B.M. (2007). E-cadherin homophilic ligation inhibits cell growth and epidermal growth factor receptor signaling independently of other cell interactions. *Mol Biol Cell* 18, 2013-2025.

Plikus, M.V., and Chuong, C.-M. (2008). Complex hair cycle domain patterns and regenerative hair waves in living rodents. *The Journal of investigative dermatology* 128, 1071-1080.

Plikus, M.V., Mayer, J.A., de la Cruz, D., Baker, R.E., Maini, P.K., Maxson, R., and Chuong, C.M. (2008). Cyclic dermal BMP signalling regulates stem cell activation during hair regeneration. *Nature* 451, 340-344.

Rabbani, P., Takeo, M., Chou, W., Myung, P., Bosenberg, M., Chin, L., Taketo, M.M., and Ito, M. (2011). Coordinated activation of Wnt in epithelial and melanocyte stem cells initiates pigmented hair regeneration. *Cell* 145, 941-955.

Rendl, M., Lewis, L., and Fuchs, E. (2005). Molecular dissection of mesenchymal-epithelial interactions in the hair follicle. *PLoS Biol* 3, 1910-1924.

Rhee, H., Polak, L., and Fuchs, E. (2006). Lhx2 maintains stem cells character in hair follicles. *Science* 312, 1946-1949.

Rice, R., Rice, D.P., Olsen, B.R., and Thesleff, I. (2003). Progression of calvarial bone development requires Foxc1 regulation of Msx2 and Alx4. *Dev Biol* 262, 75-87.

Rice, R., Rice, D.P., and Thesleff, I. (2005). *Foxc1* integrates Fgf and Bmp signalling independently of twist or noggin during calvarial bone development. *Dev Dyn* 233, 847-852.

Rosenquist, T.A., and Martin, G.R. (1996). Fibroblast growth factor signalling in the hair growth cycle: expression of the fibroblast growth factor receptor and ligand genes in the murine hair follicle. *Dev Dyn* 205, 379-386.

Rossi, D.J., Jamieson, C.H., and Weissman, I.L. (2008). Stems cells and the pathways to aging and cancer. *Cell* 132, 681-696.

Saleem, R.A., Banerjee-Basu, S., Murphy, T.C., Baxevanis, A., and Walter, M.A. (2004). Essential structural and functional determinants within the forkhead domain of FOXC1. *Nucleic Acids Res* 32, 4182-4193.

Samokhvalov, I.M., Samokhvalova, N.I., and Nishikawa, S. (2007). Cell tracing shows the contribution of the yolk sac to adult haematopoiesis. *Nature* 446, 1056-1061.

Sasman, A., Nassano-Miller, C., Shim, K.S., Koo, H.Y., Liu, T., Schultz, K.M., Millay, M., Nanano, A., Kang, M., Suzuki, T., *et al.* (2012). Generation of conditional alleles for *Foxc1* and *Foxc2* in mice. *Genesis* 50, 766-774.

Sato, T., and Clevers, H. (2015). SnapShot: Growing Organoids from Stem Cells. *Cell* 161, 1700-1700 e1701.

Sato, T., Vries, R.G., Snippert, H.J., van de Wetering, M., Barker, N., Stange, D.E., van Es, J.H., Abo, A., Kujala, P., Peters, P.J., *et al.* (2009). Single Lgr5 stem cells build crypt-villus structures in vitro without a mesenchymal niche. *Nature* 459, 262-265.

Schlegelmilch, K., Mohseni, M., Kirak, O., Pruszk, J., Rodriguez, J.R., Zhou, D., Kreger, B.T., Vasioukhin, V., Avruch, J., Brummelkamp, T.R., *et al.* (2011). Yap1 acts downstream of alpha-catenin to control epidermal proliferation. *Cell* 144, 782-795.

Seo, S., Fujita, H., Nakano, A., Kang, M., Duarte, A., and Kume, T. (2006). The forkhead transcription factors, Foxc1 and Foxc2, are required for arterial specification and lymphatic sprouting during vascular development. *Dev Biol* 294, 458-470.

Seo, S., and Kume, T. (2006). Forkhead transcription factors, Foxc1 and Foxc2, are required for the morphogenesis of the cardiac outflow tract. *Dev Biol* 296, 421-436.

Seo, S., Singh, H.P., Lacal, P.M., Sasman, A., Fatima, A., Liu, T., Schultz, K.M., Losordo, D.W., Lehmann, O.J., and Kume, T. (2012). Forkhead box transcription factor FoxC1 preserves corneal transparency by regulating vascular growth. *Proc Natl Acad Sci U S A* 109, 2015-2020.

Silvis, M.R., Kreger, B.T., Lien, W.H., Klezovitch, O., Rudakova, G.M., Camargo, F.D., Lantz, D.M., Seykora, J.T., and Vasioukhin, V. (2011). alpha-catenin is a

tumor suppressor that controls cell accumulation by regulating the localization and activity of the transcriptional coactivator Yap1. *Sci Signal* 4, ra33.

Smith, R.S., Zabaleta, A., Kume, T., Savinova, O.V., Kidson, S.H., Martin, J.E., Nishimura, D.Y., Alward, W.L., Hogan, B.L., and John, S.W. (2000). Haploinsufficiency of the transcription factors FOXC1 and FOXC2 results in aberrant ocular development. *Hum Mol Genet* 9, 1021-1032.

Soeda, T., Deng, J.M., de Crombrughe, B., Behringer, R.R., Nakamura, T., and Akiyama, H. (2010a). Sox9-expressing precursors are the cellular origin of the cruciate ligament of the knee joint and the limb tendons. *Genesis*.

Soeda, T., Deng, J.M., de Crombrughe, B., Behringer, R.R., Nakamura, T., and Akiyama, H. (2010b). Sox9-expressing precursors are the cellular origin of the cruciate ligament of the knee joint and the limb tendons. *Genesis* 48, 635-644.

Song, X., Zhu, C.-H., Doan, C., and Xie, T. (2002). Germline Stem Cells Anchored by Adherens Junctions in the Drosophila Ovary Niches. *Science* 296, 1855-1857.

Stewart, M.H., Bendall, S.C., and Bhatia, M. (2008). Deconstructing human embryonic stem cell cultures: niche regulation of self-renewal and pluripotency. *J Mol Med (Berl)* 86, 875-886.

Sun, J., Ramos, A., Chapman, B., Johnnidis, J.B., Le, L., Ho, Y.J., Klein, A., Hofmann, O., and Camargo, F.D. (2014). Clonal dynamics of native haematopoiesis. *Nature* 514, 322-327.

Takeichi, M. (2014). Dynamic contacts: rearranging adherens junctions to drive epithelial remodelling. *Nat Rev Mol Cell Biol* 15, 397-410.

Tinkle, C.L., and Fuchs, E. (2008). Loss of E-cadherin and P-cadherin expression in the skin: parallels and differences with  $\alpha$ -catenin loss of function mutations. *J Cell Biol*.

Tinkle, C.L., Lechler, T., Pasolli, H.A., and Fuchs, E. (2004). Conditional targeting of E-cadherin in skin: insights into hyperproliferative and degenerative responses. *Proc Natl Acad Sci U S A* 101, 552-557.

Trapnell, C., Roberts, A., Goff, L., Pertea, G., Kim, D., Kelley, D.R., Pimentel, H., Salzberg, S.L., Rinn, J.L., and Pachter, L. (2012). Differential gene and transcript expression analysis of RNA-seq experiments with TopHat and Cufflinks. *Nat Protoc* 7, 562-578.

Tumbar, T., Guasch, G., Greco, V., Blanpain, C., Lowry, W.E., Rendl, M., and Fuchs, E. (2004). Defining the epithelial stem cell niche in skin. *Science* 303, 359-363.

Tunggal, J.A., Helfrich, I., Schmitz, A., Schwarz, H., Gunzel, D., Fromm, M., Kemler, R., Krieg, T., and Niessen, C.M. (2005). E-cadherin is essential for in vivo epidermal barrier function by regulating tight junctions. *Embo J* 24, 1146-1156.

van Deursen, J.M. (2014). The role of senescent cells in ageing. *Nature* 509, 439-446.

Van Mater, D., Kolligs, F.T., Dlugosz, A.A., and Fearon, E.R. (2003). Transient activation of beta -catenin signaling in cutaneous keratinocytes is sufficient to trigger the active growth phase of the hair cycle in mice. *Genes Dev* 17, 1219-1224.

Vasioukhin, V., Bauer, C., Degenstein, L., Wise, B., and Fuchs, E. (2001). Hyperproliferation and defects in epithelial polarity upon conditional ablation of alpha-catenin in skin. *Cell* 104, 605-617.

Vasioukhin, V., Bauer, C., Yin, M., and Fuchs, E. (2000). Directed actin polymerization is the driving force for epithelial cell-cell adhesion. *Cell* 100, 209-219.

Vasioukhin, V., Degenstein, L., Wise, B., and Fuchs, E. (1999). The magical touch: genome targeting in epidermal stem cells induced by tamoxifen application to mouse skin. *Proc Natl Acad Sci U S A* 96, 8551-8556.

Vidal, V.P., Chaboissier, M.C., Lutzkendorf, S., Cotsarelis, G., Mill, P., Hui, C.C., Ortonne, N., Ortonne, J.P., and Schedl, A. (2005). Sox9 is essential for outer root sheath differentiation and the formation of the hair stem cell compartment. *Curr Biol* 15, 1340-1351.

Winograd-Katz, S.E., Fassler, R., Geiger, B., and Legate, K.R. (2014). The integrin adhesome: from genes and proteins to human disease. *Nat Rev Mol Cell Biol* 15, 273-288.

Woo, W.M., Zhen, H.H., and Oro, A.E. (2012). Shh maintains dermal papilla identity and hair morphogenesis via a Noggin-Shh regulatory loop. *Genes Dev* 26, 1235-1246.

Yamamoto, N., Tanigaki, K., Han, H., Hiai, H., and Honjo, T. (2003). Notch/RBP-J signaling regulates epidermis/hair fate determination of hair follicular stem cells. *Curr Biol* 13, 333-338.

Zarbalis, K., Siegenthaler, J.A., Choe, Y., May, S.R., Peterson, A.S., and Pleasure, S.J. (2007). Cortical dysplasia and skull defects in mice with a *Foxc1* allele reveal the role of meningeal differentiation in regulating cortical development. *Proc Natl Acad Sci U S A* 104, 14002-14007.

Zhang, J., He, X.C., Tong, W.G., Johnson, T., Wiedemann, L.M., Mishina, Y., Feng, J.Q., and Li, L. (2006). Bone morphogenetic protein signaling inhibits hair follicle anagen induction by restricting epithelial stem/progenitor cell activation and expansion. *Stem Cells* 24, 2826-2839.

Zihni, C., Mills, C., Matter, K., and Balda, M.S. (2016). Tight junctions: from simple barriers to multifunctional molecular gates. *Nat Rev Mol Cell Biol* 17, 564-580.